

# IN-PLANE VIBRATIONS OF LAYERED RINGS ON PERIODIC RADIAL SUPPORTS

By

EMANT SIVASANKARA REDDY

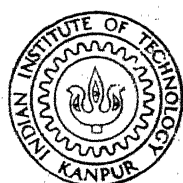
ME

1982

D  
RED

IN

TH  
ME/1982/D  
R 246



DEPARTMENT OF MECHANICAL ENGINEERING

INDIAN INSTITUTE OF TECHNOLOGY KANPUR

OCTOBER 1982

# IN-PLANE VIBRATIONS OF LAYERED RINGS ON PERIODIC RADIAL SUPPORTS

A Thesis Submitted  
in Partial Fulfilment of the Requirements  
for the Degree of  
**DOCTOR OF PHILOSOPHY**

16712

*By*  
**EMANI SIVASANKARA REDDY**

*to the*

**DEPARTMENT OF MECHANICAL ENGINEERING**  
**INDIAN INSTITUTE OF TECHNOLOGY KANPUR**  
**OCTOBER 1982**

## CERTIFICATE

This is to certify that the present work  
"IN-PLANE VIBRATIONS OF LAYERED RINGS ON PERIODIC RADIAL  
SUPPORTS" has been carried out under my supervision and  
has not been submitted elsewhere for the award of a degree.

*(Signature)*  
A.K. Mallik  
Professor  
Department of Mech. Engg.  
I.I.T. Kanpur  
INDIA

October, 1982

25/3/83

## CONTENTS

	Page
CERTIFICATE	ii
ACKNOWLEDGEMENT	iii
LIST OF FIGURES	vii
LIST OF TABLES	xi
LIST OF PRINCIPAL SYMBOLS	xii
SYNOPSIS	xvii
 CHAPTER 1 : INTRODUCTION	 1
1.1 : Introduction and Literature Review	1
1.2 : Objective and Scope of the Present Work	5
 CHAPTER 2 : FREE VIBRATION OF A TWO LAYERED RING	 9
2.1 : Introduction	9
2.2 : Equations of Motion	10
2.3 : Coupling Co-ordinates and Coupling Forces	16
2.4 : Natural Frequencies of an Elastic Ring	18
2.4.1 Theory of wave propagation and natural frequencies	18
2.4.2 Different support conditions	19
2.5 : Resonant Frequencies and Loss Factors of a Damped Ring	20
2.5.1 Different support conditions	22
2.5.2 Computational procedure	25
2.6 : Natural Modes of an Elastic Ring	27
2.7 : Results and Discussion	33

2.7.1	Outer layer elastic	33
2.7.2	Outer layer viscoelastic	44
CHAPTER 3	: FREE VIBRATION OF A THREE LAYERED RING	53
3.1	: Introduction	53
3.2	: Equations of Motion	54
3.3	: Natural Frequencies of an Elastic Ring	60
3.4	: Resonant Frequencies and Loss Factors of a Damped Ring	61
3.5	: Natural Modes of an Elastic Ring	66
3.6	: Results and Discussion	67
3.6.1	Elastic Core	67
3.6.2	Viscoelastic core	76
CHAPTER 4	: IN VACUO RESPONSE OF LAYERED RINGS	93
4.1	: Introduction	93
4.2	: Response Analysis for a Two Layered Ring	93
4.3	: Response Analysis for a Three Layered Ring	95
4.4	: Support Conditions	97
4.5	: Results and Discussion	98
4.5.1	Two layered ring	98
4.5.2	Three layered ring	107
CHAPTER 5	: RESPONSE AND SOUND TRANSMISSION CHARACTERISTICS IN AN ACOUSTIC FIELD	119
5.1	: Introduction	119
5.2	: Internal Acoustic Field	120
5.3	: Response Analysis for a Two Layered Ring	122

5.4	: Response Analysis for a Three Layered Ring	123
5.5	: Boundary Condition on Internal Pressure	124
5.6	: Response of a Single Layer Ring to a Plane Acoustic Wave	129
5.7	: Results and Discussion	134
	5.7.1 Two layered ring	134
	5.7.2 Three layered ring	140
CHAPTER 6	: CONCLUSIONS	148
REFERENCES		153
APPENDIX A	: STRAIN ENERGY OF A SINGLE LAYER RING ELEMENT	157
APPENDIX B	: RECEPANCE METHOD FOR A TWO LAYERED RING	159
B.1	: Mono-coupled system	159
B.2	: Bi-coupled system	160
B.3	: Tri-coupled system	161
APPENDIX C	: COEFFICIENTS OF THE AUXILIARY EQUATION (2.10) AND THE EXPRESSION FOR $T_j$	163
APPENDIX D	: RECEPANCE METHOD FOR A THREE LAYERED RING (TRI-COUPLED SYSTEM)	164
APPENDIX E	: CONSTANTS AND COEFFICIENTS USED IN CHAPTER 3	166

## LIST OF FIGURES

<u>Fig. No.</u>		<u>Page</u>
2.1	Two layered ring on equi-spaced radial supports	11
2.2	Periodic element of two layered ring	13
2.3	Variation of propagation constant with frequency: Mono-coupled system	34
2.4	Variation of propagation constant with frequency: Bi-coupled system	35
2.5	Variation of propagation constant with frequency: Tri-coupled system, $k_t = 180$	36
2.6	Mode shapes ( $U$ ) of two layered ring: Mono-coupled system, $\bar{k}_r = 0$	40
2.7	Mode shapes ( $V$ ) of two layered ring: Mono-coupled system, $\bar{k}_r = 0$	41
2.8	Mode shapes ( $U$ ) of two layered ring: Bi-coupled system, $\bar{k}_r = 0$	42
2.9	Mode shapes ( $V$ ) of two layered ring: Bi-coupled system, $\bar{k}_r = 0$	43
2.10	Variation of resonant frequency with thickness ratio: Mono-coupled system	45
2.11	Variation of modal loss factor with thickness ratio: Mono-coupled system	46
2.12	Variation of resonant frequency with thickness ratio: Bi-coupled system	48
2.13	Variation of modal loss factor with thickness ratio: Bi-coupled system	49
2.14	Variation of modal loss factor with thickness ratio: Bi-coupled system	50
2.15	Variation of modal loss factor with thickness ratio: Tri-coupled system, $k_t = 180$	52

3.1	Three layered ring on equi-spaced radial supports	55
3.2	Variation of propagation constant with frequency: Bi-coupled system, $k_r = 0$	68
3.3	Variation of propagation constant with frequency: Tri-coupled system, $k_r = 0$	69
3.4	Mode shapes ( $U$ ) of three layered ring: Bi-coupled system, $k_r = 0$	71
3.5	Mode shapes ( $V_1$ & $V_3$ ) of three layered ring: Bi -coupled system, $k_r = 0$	72
3.6	Mode shapes ( $U$ ) of three layered ring: Tri-coupled system, $k_r = 0$	73
3.7	Mode shapes ( $V_1$ & $V_3$ ) of three layered ring: Tri-coupled system, $k_r = 0$	74
3.8	Variation of resonant frequency with base layer thickness (mode 1): Bi-coupled system $k_r = 0$	78
3.9	Variation of resonant frequency with base layer thickness (mode 2): Bi-coupled system $k_r = 0$	79
3.10	Variation of resonant frequency with base layer thickness (mode 2): Tri-coupled system $k_r = 0$	80
3.11	Variation of resonant frequency with base layer thickness (mode 3): Tri-coupled system $k_r = 0$	81
3.12	Variation of modal loss factor with base layer thickness (mode 1): Bi-coupled system $k_r = 0$	82
3.13	Variation of modal loss factor with base layer thickness (mode 1): Bi-coupled system $k_r = 2$	83
3.14	Variation of modal loss factor with base layer thickness (mode 2): Bi-coupled system $k_r = 0$	84
3.15	Variation of modal loss factor with base layer thickness (mode 2): Tri-coupled system $k_r = 0$	85

3.16	Variation of modal loss factor and resonant frequency with core shear modulus: Bi-coupled system, $k_r = 0$	90
3.17	Variation of modal loss factor and resonant frequency with core shear modulus: Tri-coupled system, $k_r = 0$	91
4.1	Response of two layered ring: Mono-coupled system, $l = 1$	101
4.2	Response of two layered ring: Mono-coupled system, $l = 2$	102
4.3	Response of two layered ring: Mono-coupled system, $l = 3$	103
4.4	Response of two layered ring: Bi-coupled system, $l = 1$	104
4.5	Response of two layered ring: Bi-coupled system, $l = 2$	105
4.6	Response of two layered ring: Bi-coupled system, $l = 3$	106
4.7	Response of three layered ring: Bi-coupled system, $l = 1$	108
4.8	Response of three layered ring: Bi-coupled system, $l = 2$	109
4.9	Response of three layered ring: Bi-coupled system, $l = 3$	110
4.10	Response of three layered ring: Tri-coupled system, $l = 1$	111
4.11	Response of three layered ring: Tri-coupled system, $l = 2$	112
4.12	Response of three layered ring: Tri-coupled system, $l = 3$	113
4.13	Comparison of response for two (mono-coupled) and three (bi-coupled) layered rings, $l = 1$	116
4.14	Comparison of response for two (bi-coupled) and three (tri-coupled) layered rings, $l = 1$	117

5.1	Response of two layered ring, $l = 1$	135
5.2	Response of two layered ring, $l = 3$	136
5.3	Variation of sound power with frequency, two layered ring, $l = 1$	138
5.4	Variation of sound power with frequency, two layered ring, $l = 2$	139
5.5	Variation of sound power with frequency, two layered ring, $l = 3$	140
5.6	Response of three layered ring, $l = 1$	142
5.7	Response of three layered ring, $l = 3$	143
5.8	Variation of sound power with frequency, three layered ring, $l = 1$	144
5.9	Variation of sound power with frequency, three layered ring, $l = 2$	145
5.10	Variation of sound power with frequency, three layered ring, $l = 3$	146
5.11	Comparison of sound power in two (mono- coupled) and three (bi-coupled) layered rings, $l = 1$	147

## LIST OF TABLES

Table No.		Page
2.1	Natural Frequencies of Undamped Two Layered Ring on Three Supports	39
3.1	Natural Frequencies and Various Energies on an Elastic Three Layered Ring	77
3.2	Resonant Frequencies and Loss Factors of a Damped Three Layered Ring	89
4.1	Pressure Harmonics Exciting Various Modes of a Two Layered Ring: Mono-Coupled System	100
4.2	Pressure Harmonics Exciting Various Modes of a Two Layered Ring: Bi-Coupled System	100
4.3	Pressure Harmonics Exciting Various Modes of a Three Layered Ring: Bi-Coupled System	115
4.4	Pressure Harmonics Exciting Various Modes of a Three Layered Ring: Tri-Coupled System	115

## LIST OF PRINCIPAL SYMBOLS

A	area of cross section of a layer
$A_n^s$	constants in the series of scattered pressure
$A_n^t$	constants in the series of transmitted pressure
$B_j, \bar{B}_j$	constants in the tangential displacement solutions
b	width of the ring
$C_j$	constants in the radial displacement solution
$c_1$	sound velocity in the internal acoustic medium
$c_2$	sound velocity in the external acoustic medium
$\bar{c}_1, \bar{c}_2$	nondimensional sound velocities in the respective mediums
D	total bending stiffness
$D_j$	bending stiffness of the $j^{\text{th}}$ layer ( $= \frac{2}{3} E_j b \delta_j^3$ )
E	Young's modulus of a layer
$E_j$	Young's modulus of the $j^{\text{th}}$ layer
$F_j$	component of the $j^{\text{th}}$ coupling force due to stiffness at the supports
G	shear modulus of core
$H^{(1)}( )$	Hankel function of the first kind ( $= J + i Y$ )
$\underline{H}^{(1)}( )$	modified Hankel function of the first kind ( $= J + i \alpha Y$ )
$H^{(2)}( )$	Hankel function of the second kind ( $= J - i Y$ )
h	half thickness of a layer
$h_j$	half thickness of the $j^{\text{th}}$ layer
i	$\sqrt{-1}$ unit imaginary number

$J(\cdot)$	Bessel function of the first kind
$K_j$	extensional stiffness of the $j^{\text{th}}$ layer ( $= \frac{E_j A_j}{R_j}$ )
$k_r$	rotational stiffness at the supports
$\bar{k}_r$	nondimensional rotational stiffness at the supports
$k_t$	transverse stiffness at the supports
$\bar{k}_t$	nondimensional transverse stiffness at the supports
$k_1$	acoustic wave number in the internal medium
$k_2$	acoustic wave number in the external medium
$L_1, \dots, L_6$	differential operators
$l$	space harmonic number of the external pressure
$m$	mass of the ring per unit radian
$m_j$	mass of the $j^{\text{th}}$ layer per unit radian
$N$	Number of supports
$n_1$	total number of zero-displacement conditions
$n_2$	total number of support conditions
$P_i$	amplitude of the incident plane wave
$P_{il}$	amplitude of the $l^{\text{th}}$ space harmonic of the incident plane wave
$P_o$	amplitude of the exciting pressure harmonic
$\bar{P}_o$	nondimensional amplitude of the exciting pressure harmonic
$P_{sn}$	amplitude of the $n^{\text{th}}$ harmonic of the scattered pressure
$\bar{P}_{sn}$	nondimensional amplitude of the $n^{\text{th}}$ harmonic of the scattered pressure
$P_{tn}$	amplitude of the $n^{\text{th}}$ harmonic of the transmitted pressure

$\bar{P}_{tn}$	nondimensional amplitude of the $n^{\text{th}}$ harmonic of the transmitted pressure
$p_i$	pressure due to incident plane wave
$p_o$	exciting pressure
$p_s$	scattered pressure
$p_t$	transmitted pressure
$Q_j$	$j^{\text{th}}$ coupling force
$Q_{j0}, Q_{j\lambda}$	$j^{\text{th}}$ coupling force at $\theta = 0$ and at $\theta = \lambda$
$\{Q\}$	vector of coupling forces at $\theta = 0$ and at $\theta = \lambda$ $(= [Q_{10}, Q_{1\lambda}, Q_{20}, Q_{2\lambda}, \dots]^T)$
$\bar{Q}_j$	harmonic amplitude of $Q_j$
$Q_j$	coupling force at the $j^{\text{th}}$ support
$q_j$	$j^{\text{th}}$ coupling co-ordinate
$q_{j0}, q_{j\lambda}$	$j^{\text{th}}$ coupling co-ordinate at $\theta = 0$ and at $\theta = \lambda$
$\{q\}$	vector of coupling co-ordinate at $\theta = 0$ and at $\theta = \lambda$ ( $= [q_{10}, q_{1\lambda}, q_{20}, q_{2\lambda}, \dots]^T$ )
$R$	radius of mid-plane of a layer
$R_j$	radius of mid-plane of the $j^{\text{th}}$ layer
$R_b$	radius of mid-plane of the base layer
$r$	polar co-ordinate
$S_j$	component of the $j^{\text{th}}$ coupling force due to ring element
$s_j$	$j^{\text{th}}$ root of the auxiliary equation
$T_j, \bar{T}_j$	ratios of displacement amplitudes (tangential/ radial) for a solution $s = s_j$

$t, t_1, t_2$	time
$U$	harmonic amplitude of the radial displacement
$\bar{U}$	nondimensional amplitude of the radial displacement
$u$	radial displacement
$V_j$	harmonic amplitude of the tangential displacement ( $v_j$ ) of the $j^{\text{th}}$ layer
$\bar{V}_j$	nondimensional value of $V_j$
$v_j$	tangential displacement of mid-plane of the $j^{\text{th}}$ layer
$v_\theta$	tangential displacement
$W$	complex determinant
$w$	work done by non-conservative forces
$Y(\cdot)$	Bessel function of the second kind
$\alpha$	absorption coefficient
$\alpha_{ij}$	receptances
$\beta$	loss factor of the viscoelastic layer
$\delta_j$	nondimensional half thickness of the $j^{\text{th}}$ layer $(= h_j/R_j)$
$\epsilon_\theta$	circumferential strain
$\eta$	composite modal loss factor of the damped ring
$\theta$	polar co-ordinate
$\lambda$	angle subtended by a single bay at the ring centre
$\mu$	complex propagation constant
$\mu_r, \mu_i$	real and imaginary parts of $\mu$
$\mu_{rn}, \mu_{in}$	values of $\mu_r$ and $\mu_i$ at a natural frequency
$\Pi$	strain energy

$\rho_j$	density of the $j^{\text{th}}$ layer
$\rho_1^a$	density of the internal acoustic medium
$\rho_2^a$	density of the external acoustic medium
$\bar{\rho}_1^a, \bar{\rho}_2^a$	nondimensional values of $\rho_1^a$ and $\rho_2^a$
$\sigma_\theta$	circumferential stress
$\psi$	shear strain
$\Omega$	nondimensional frequency
$\Omega_n$	nondimensional natural/resonant frequency
$\Omega^*$	complex frequency ( $= \Omega\sqrt{1 + i\eta}$ )
$\omega$	frequency

## SYNOPSIS

### IN-PLANE VIBRATIONS OF LAYERED RINGS ON PERIODIC RADIAL SUPPORTS

A Thesis Submitted  
In Partial Fulfilment of the Requirements  
for the Degree of

DOCTOR OF PHILOSOPHY

by

EMANI SIVASANKARA REDDY

to the

DEPARTMENT OF MECHANICAL ENGINEERING  
INDIAN INSTITUTE OF TECHNOLOGY KANPUR

OCTOBER, 1982

The thesis presents a theoretical investigation of the in-plane vibration (free and forced) and sound transmission characteristics of layered rings on equi-spaced, identical radial supports. Differential equations and the generalized coupling forces are set up for a layered ring segment (comprising the periodic element) by using Hamilton's principle. The theory of wave propagation is used for both the free and forced vibration analyses.

For a two layered ring, three types of support conditions, viz., (i) supports preventing both the radial and tangential displacements, (ii) supports preventing only the radial displacement, and (iii) flexible radial supports, are considered. These conditions render the structure a mono-coupled, bi-coupled and tri-coupled system,

respectively. With the outer layer elastic, propagation constant curves are obtained by the receptance method. These curves are used to determine the natural frequencies of the structure. The mode shapes associated with the first few natural frequencies are also obtained. When the outer layer is viscoelastic, the problem is formulated using the theory of forced damped normal modes. An efficient algorithm based on a two dimensional Newton-Raphson method is used to compute the resonant frequencies and the associated modal loss factors. Results obtained earlier for the elastic case are found to be useful in this computation. Variations of resonant frequency and modal loss factor with the thickness ratio are presented. The effects of rotational and transverse stiffnesses at the supports are also studied.

A three layered ring is analysed, considering only the shear deformation in the middle layer. Again, following the receptance method, propagation constant curves are obtained for a purely elastic ring. These curves are used to determine the natural frequencies. A careful study of these curves reveals some possible characteristics of the modes. The mode shapes at these natural frequencies show that there exists predominantly tangential modes in addition to the flexural ones. This fact is verified by comparing various strain energies of the layers for different modes. Treating the middle layer to be

viscoelastic, resonant frequencies and modal loss factors are computed by a procedure similar to that used for a two layered ring. The variation of the loss factors in different modes is better understood through the study of the natural modes of the corresponding clastic ring. Only the first two types of support conditions (i.e., (i) and (ii) mentioned above), which makes the structure a bi-coupled and a tri-coupled system, respectively, are considered.

The response of a layered ring to any harmonic radial loading can be analysed by considering the load as a sum of infinite circumferential pressure waves of integer wave numbers. Hence, in the present work, analysis for the response is carried out for specific wave numbers. Responses are obtained as a function of frequency for different wave numbers. Results show the effect of the damping of the viscoelastic layer.

When a vibrating structure encloses a volume of fluid the acoustic effects within this volume modify the response characteristics considerably. Hence, the response due to radial loading and sound transmission characteristics of infinitely long, axially stiffened cylinder are investigated. This is carried out by neglecting any variation in the axial direction. Thus the problem is simplified to the two dimensional versions (i.e., layered rings) in presence of acoustic mediums.

Moreover, the interior can be totally resonant, totally absorbent or partially absorbent. For all these cases the response of the structure and the sound power radiated inside are computed considering a particular space harmonic of the external pressure and the associated transmitted pressure. The results are presented for two and three layered rings with and without damping.

Lastly, a more general problem involving a plane sound wave normally impinging upon the structure is considered. The mathematical model is presented for the response of a single layer ring which can readily be extended to include the multi-layered rings as well. The incident pressure is expressed as a sum of infinite cylindrical harmonics. For each of these components, the associated scattered and transmitted pressure fields are included in the model. The total response or the sound power transmitted inside can be obtained by summing up the individual contributions due to different harmonics in the series.

## CHAPTER 1

### INTRODUCTION

#### 1.1 INTRODUCTION AND LITERATURE REVIEW

The basic structural components commonly used in modern aircraft, missiles and other aerospace vehicles are stiffened cylindrical and conical shells. A convenient first step towards the understanding of vibration and sound transmission characteristics of such structures with axial stiffness may be provided by the study of the dynamic behaviour of rings on radial supports. As the stiffeners are often regularly spaced, the ring may be considered to be supported periodically. This periodicity can advantageously be used to simplify vibration and acoustic interaction studies.

For vibration analysis of infinite periodic structures (beams), the wave propagation theory has been developed by Heckl [1] and Mead [2]. Later, a generalized analysis has been presented by Mead [3 - 5] for any periodic structure. From the propagation characteristics of infinite beams, natural frequencies of a finite beam can be obtained by a simple graphical procedure [6]. Based on this procedure, a single layer ring on periodic radial supports has been analysed by Mallik and Mead [7]. The 'wave propagation approach' used in this work can be seen to be more efficient and

advantageous than the conventional method through differential equation formulation [8, 9]. It also provides a better physical picture as compared to the method using transfer matrices [10 - 12].

It is well known that considerable reduction in resonant vibration can be realized by using viscoelastic materials as both unconstrained and constrained layers. In the unconstrained and constrained treatments the high dissipation of energy is mainly due to extensional and shear deformations, respectively, of the viscoelastic material. Extensive work has been reported on free and forced vibration analysis of beams with damping layers. The study of the damping characteristics of a sandwich ring segment has been presented by Almy and Nelson [13]. They assumed the system to have very little damping and used Rayleigh's quotient for computing resonant frequencies. For a three layered ring with a viscoelastic core, Lu et al [14] have presented theoretical and experimental results in terms of the radial driving point mechanical impedance. This method has been extended to cover discontinuously constrained damped rings [15 - 17]. In these studies, a thin-walled ring, having a finite number of mass segments equally spaced and uniformly attached to its circumference by a thin viscoelastic layer, has been considered.

DiTaranto [18] has derived the governing differential equations of a three layered ring using variational approach. For the damping study, the core was assumed to be viscoelastic with a complex shear modulus and the resonant frequencies alongwith the associated modal loss factors were obtained. A similar analysis for a damped three layered ring has been carried out by Nelson and Sullivan [19]. The governing equations in this reference were obtained by the equilibrium approach. The condition of inextensibility was used in these equations. Considering the core to be elastic, Sagartz [20, 21], Forrestal and Overmier [22] have carried out theoretical and experimental studies for the transient response.

For vibration of a structure in a fluid environment, the acoustic effects such as scattered and transmitted pressures are strongly coupled with the motion of the structure. The effects of these pressures should be taken into consideration especially when the vibrations are infact induced by incident acoustic pressure waves or if the structure under consideration is very lightly damped. The different approaches to the problem can be found in works of Cremer et al [23], Junger and Feit [24], Lyon and Smith [25] and Lyon [26]. Here, only the literature which is directly relevant to the present work is referred to. A complete survey of the

works on noise and sound transmission through flexible structures can be found in reference [27].

Foxwell and Franklin [28] have studied a simple and relatively idealized problem in which a plane wave incidenting normally on an infinite stiffened cylindrical shell is considered. For simplicity, only the ring (frame) type stiffeners have been included in the model. Their results show additional resonant frequencies which are identified as 'cavity resonances'. These frequencies exist as the interior of the shell was assumed to be totally resonant, i.e., no energy is dissipated in the internal field. This shows that when a structure encloses a volume of fluid (a good example of this being an aircraft fuselage), internal pressure field alters the response characteristics considerably.

Smith [29] and Koval [30, 31], in their theoretical study of sound transmission through a cylindrical shell, have considered the case when the interior is totally absorbent, which implies that there exists only an inward - propagating waves. This was done because of the obvious analogy to the definition of transmission loss for a flat pannel. Koval [32, 33] has also studied the problem of axially stiffened cylinder by improving the smeared-stiffener theory. In actual practice, however, the interior region is neither totally resonant nor totally absorbent. The partially absorbing characteristic of the cavity has been included in a later work

by Koval [34] while studying the effect of cavity resonances on sound transmission. Shanbag [27] analysed the sound transmission characteristics of a layered cylindrical shell with simply supported ends. In this work only axisymmetric modes were considered.

Sound - structure interaction studies of periodic structures have been attempted by only a few investigators [2, 35, 36]. In the analysis of a periodic plate, Pujara [35], Mead and Pujara [37] have introduced a special series called 'space harmonic series' and obtained an exact solution for the response as well as for the sound power radiated. Later, an approximate 'assumed mode method' has been suggested by Mead and Mallik [36, 38]. In the references [35, 37], the number of equations to be solved for the response calculation depends on (equal to) the number of terms considered in the space harmonic series.

## 1.2 OBJECTIVE AND SCOPE OF THE PRESENT WORK

From the literature review presented in the previous section it can be seen that vibration of only an unsupported layered ring has been studied to a considerable depth. Radial supports being a better idealization of the axial stiffeners of a shell, the objective of the present work is to study the in-plane vibration (free and forced) of two and three layered rings on equi-spaced radial supports. The effect of

the solid-fluid interaction is also investigated. A 'wave propagation approach' is used for this study wherein the computational effort is independant of the number of supports. Numerical results are presented for rings on only three supports.

The work is broadly divided into four Chapters. The second and the third chapters are devoted to the study of free vibration characteristics of two and three layered rings. The fourth chapter deals with the in vacuo response of these structures to pressure loading. Lastly, the response and the sound transmission studies in the presence of acoustic fields are included in the fifth chapter.

In chapter 2, free vibration of a two layered ring on periodic radial supports is considered. The governing differential equations and the generalized coupling forces are set up for a single bay of the ring by using variational approach. Natural frequencies of a ring with elastic layers are obtained using the receptance method [7]. Using the theory of forced damped normal modes, resonant frequencies and the associated modal loss factors are computed for a damped ring (i.e., with the outer layer viscoelastic). Furthermore, the mode shapes of the elastic ring are also obtained as they are seen to provide better explanations for the behaviour of the damped ring. The effects of

various parameters, viz., thickness ratio, loss factor of the viscoelastic layer etc., are presented. Three types of support conditions viz., (1) supports preventing both the radial and tangential displacements, (ii) supports preventing only the radial displacement, and (iii) flexible radial supports are investigated.

Chapter 3 considers the free vibration analysis of a three layered ring on periodic radial supports. Natural frequencies of an elastic ring, resonant frequencies and the associated modal loss factors of a damped ring are obtained by methods similar to those used in Chapter 2. The variations of loss factors of the damped ring (i.e., core is viscoelastic) are explained with the aid of mode shapes of the corresponding elastic ring (i.e., core is elastic). The effects of thickness ratios of various layers are investigated. These results may help in the choice of thicknesses to be used for achieving the desired damping characteristics. Only the first two types of supports mentioned earlier are considered here.

In Chapter 4, the in vacuo response of both two and three layered rings to a pressure loading which is harmonic both in space and time is investigated. The governing differential equations presented in the previous chapters are modified to include the forcing function. Results are presented for different wave

numbers of the pressure loading with the first two types of support conditions. Any general loading can be expressed as a series of harmonics in the frequency-wave number domain. For such loading, this analysis can be extended to find the response.

In Chapter 5, the response due to radial loading and sound transmission characteristics of an infinitely long, axially stiffened layered cylinder are investigated. This is carried out by neglecting any variation in the axial direction. Thus the problem is simplified to the two dimensional versions (i.e., of layered rings) in presence of acoustic mediums. First, response to a particular space harmonic of the external pressure and the associated transmitted pressure is analysed. Different types of interior region, viz., totally resonant, totally absorbent and partially absorbent are investigated. Numerical results are presented with the first type of supports only. Secondly, an incident plane wave is expressed as a sum of infinite cylindrical harmonics. A particular component of this series, its associated scattered and transmitted pressure fields are included in the response analysis of a single layer ring. This analysis can, ofcourse be extended easily for multi-layered rings. No numerical results are presented for this case.

## CHAPTER 2

### FREE VIBRATION OF A TWO LAYERED RING

#### 2.1 INTRODUCTION

In the design of resonant system, vibration control can be achieved by increasing the damping capacity of the structure. One of the effective ways to enhance the damping capacity is to provide viscoelastic (damping) layers on the structure. Due to simplicity of implementation, unconstrained layer treatment is widely used. In this configuration, dissipation of energy is mainly due to extensional deformation of the viscoelastic layer. Hence, an in-depth study of both elastic and viscoelastic two layered ring is felt necessary.

In the present chapter, free vibration of a two layered ring on periodic radial supports is studied. The governing differential equations and the generalized coupling forces of the periodic element are set up by using Hamilton's principle. Natural frequencies of a purely elastic ring are obtained by wave propagation approach [2, 7 ]. Using the theory of forced damped normal modes [39, 40 ], resonant frequencies and the associated modal loss factors of the damped ring (outer layer viscoelastic) are obtained. The computation of the resonant frequencies of the damped ring is greatly facilitated by the knowledge of the natural frequencies of the corresponding elastic ring. Furthermore, the

mode shapes of the elastic ring are also obtained as they may provide better explanation of the behaviour of the damped ring. The effects of various parameters, viz., thickness ratio, loss factor of the viscoelastic layer etc., are presented. Three types of support conditions considered in the present work are as follows:

- i) supports preventing both the radial and tangential displacements;
- ii) supports preventing only the radial displacement;
- iii) flexible radial supports.

## 2.2 EQUATIONS OF MOTION

The following assumptions are made in deriving the differential equations and boundary conditions:

- i) radial displacement remains constant along a particular radial line;
- ii) a plane cross section of a layer remains plane after deformation;
- iii) there is no slip at the interface of the two layers.

Figure 2.1 shows a two layered ring on  $N$  equi-spaced supports, which offer rotational and transverse restraint at the mid-plane of the base layer (layer 2). The rotational and transverse (radial) stiffnesses at the supports are represented by  $k_r$  and  $k_t$  respectively.

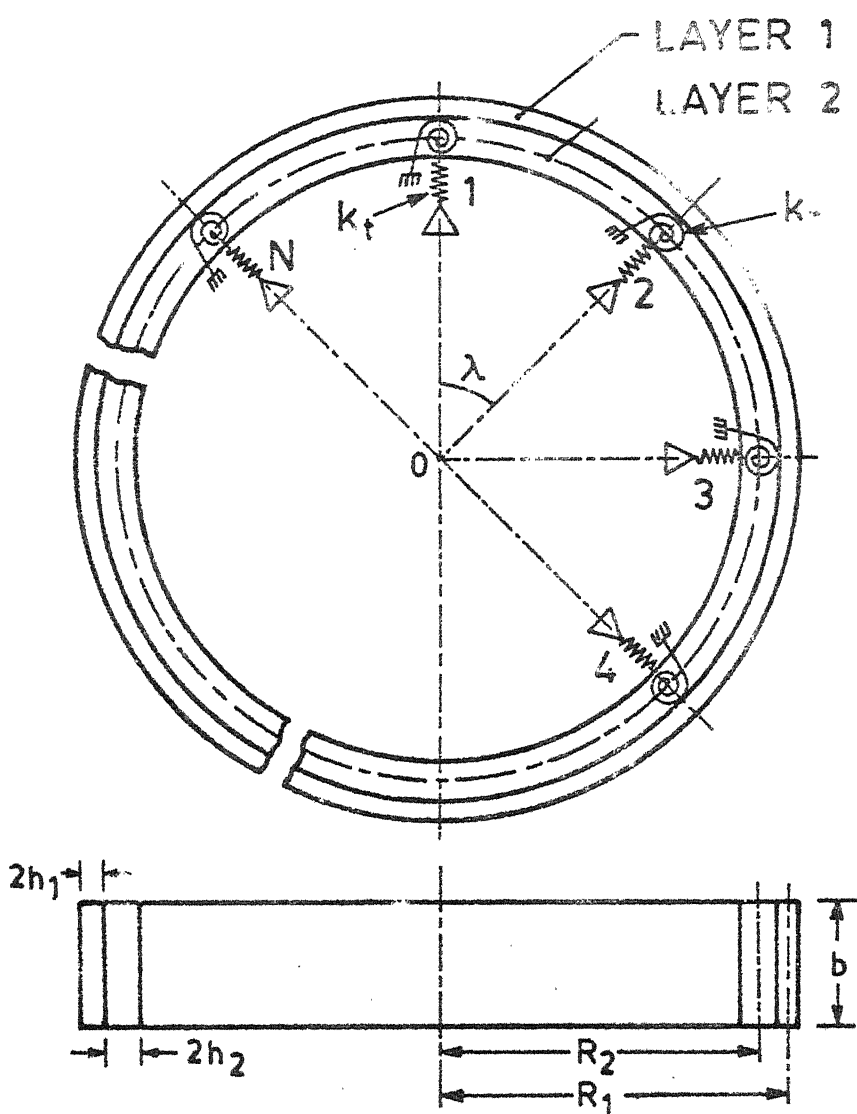


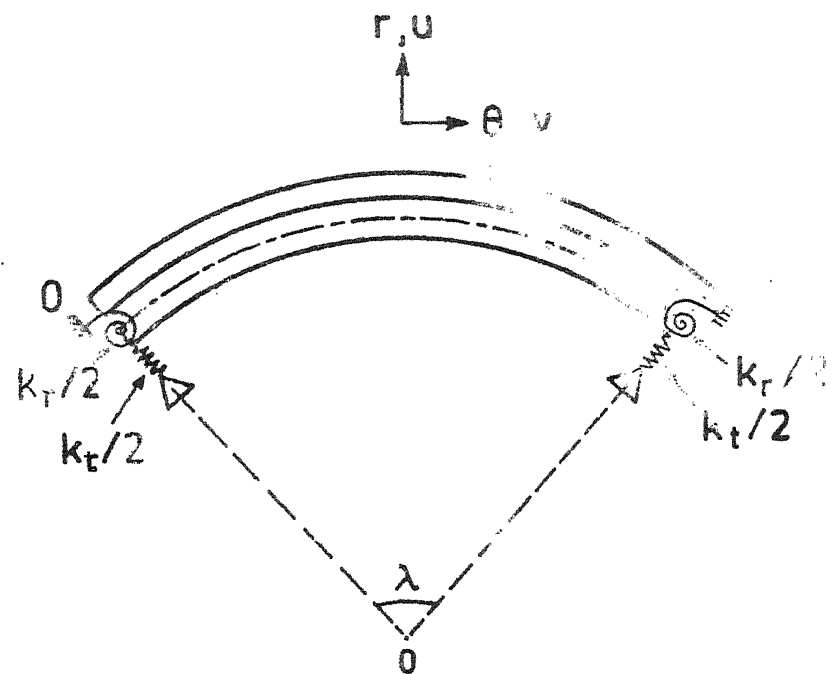
FIG. 2.1. TWO LAYERED RING ON EQUI-SPACED RADIAL SUPPORTS.

The total strain energy of a single bay (see Fig. 2.2 (a)) of the two layered ring consists of strain energies due to bending and extension of the individual layers 1 and 2 and that of the springs at the supports. Hence, by using the expression for strain energy of a single layer ring element given in Appendix A, the total strain energy ( $\Pi$ ) of a two layered ring bay subtending an angle  $\lambda$  at the ring centre can be written as

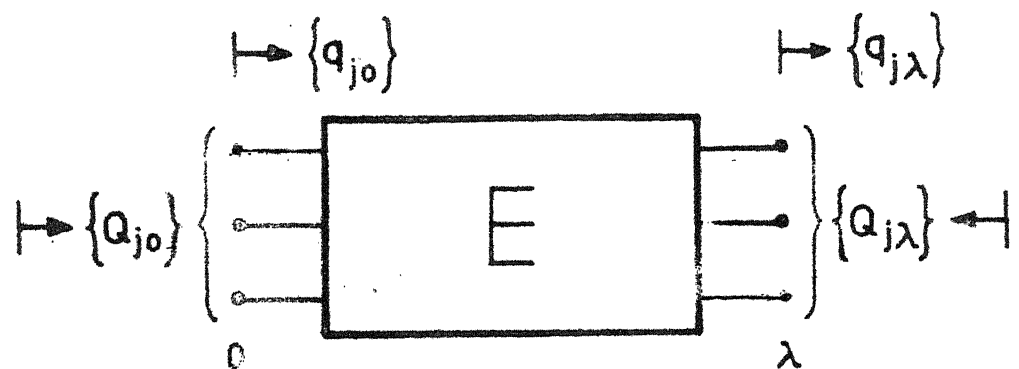
$$\begin{aligned} \Pi = & \frac{K_1}{2} \int_0^\lambda \left( u + \frac{\partial v_1}{\partial \theta} \right)^2 d\theta + \frac{K_2}{2} \int_0^\lambda \left( u + \frac{\partial v_2}{\partial \theta} \right)^2 d\theta \\ & + \frac{(D_1 + D_2)}{2} \int_0^\lambda \left( u + \frac{\partial^2 u}{\partial \theta^2} \right)^2 d\theta \\ & + \frac{1}{2} \frac{k_r}{2} \left[ \frac{1}{R_2} \left( \frac{\partial u}{\partial \theta} - v_2 \right) \right]_{\theta=0}^2 + \frac{1}{2} \frac{k_r}{2} \left[ \frac{1}{R_2} \left( \frac{\partial u}{\partial \theta} - v_2 \right) \right]_{\theta=\lambda}^2 \\ & + \frac{1}{2} \frac{k_t}{2} [u^2]_{\theta=0} + u^2]_{\theta=\lambda} \quad (2.1) \end{aligned}$$

where  $u$  is the radial displacement,  $v_i$  is the tangential displacement of the mid-plane,  $K_i$  ( $= \frac{E_i A_i}{R_i}$ ) is the extensional stiffness over a length  $R_i$ ,  $D_i$  ( $= \frac{2}{3} E_i b \delta_i^3$ ) is the bending stiffness,  $E_i$  is the Young's modulus,  $A_i$  is the area of cross section,  $R_i$  is the radius of the mid-plane,  $\delta_i$  ( $= \frac{h_i}{R_i}$ ) is the nondimensional half thickness,  $b$  is the width of the ring and  $h_i$  is the half thickness, with the subscript  $i$  referring to the  $i^{\text{th}}$  layer.

In (2.1) the quantity  $\frac{1}{R_2} (\frac{\partial u}{\partial \theta} - v_2)$  associated with the rotational stiffness  $k_r$ , is the local bending slope of the mid-plane of layer 2.



(a) ACTUAL



(b) SCHEMATIC

FIG. 2.2. PERIODIC ELEMENT OF TWO LAYERED RING.

The kinetic energy of a single bay, T, can be written as

$$T = \frac{(m_1 + m_2)}{2} \int_0^\lambda \left( \frac{\partial u}{\partial t} \right)^2 d\theta + \frac{m_1}{2} \int_0^\lambda \left( \frac{\partial v_1}{\partial t} \right)^2 d\theta + \frac{m_2}{2} \int_0^\lambda \left( \frac{\partial v_2}{\partial t} \right)^2 d\theta \quad (2.2)$$

where  $m_i (= 2b h_i \rho_i R_i)$  is the mass of the  $i^{\text{th}}$  layer over a length  $R_i$  with  $\rho_i$  as the density of the material of that layer.

By equating the tangential displacements of the interface as obtained from layers 1 and 2, no-slip condition can be expressed as

$$\frac{h_1}{R_1} \frac{\partial u}{\partial \theta} + \left( \frac{R_1 - h_1}{R_1} \right) v_1 = \left( \frac{R_2 + h_2}{R_2} \right) v_2 - \frac{h_2}{R_2} \frac{\partial u}{\partial \theta}$$

or

$$v_1 = \frac{d_3}{d_1} v_2 - \frac{d_2}{d_1} \frac{\partial u}{\partial \theta}, \quad (2.3)$$

where  $d_1 = 1 - \delta_1$ ,  $d_2 = \delta_1 + \delta_2$  and  $d_3 = 1 + \delta_2$ .

By substituting the above no-slip condition in (2.1) and (2.2), and setting the variation of Hamiltonian ( $T - \Pi$ ) equal to zero, the differential equations and boundary conditions are obtained as

$$\begin{aligned} D(u+2) \frac{\partial^2 u}{\partial \theta^2} + \frac{\partial^4 u}{\partial \theta^4} + K_1 (u-2) \frac{d_2}{d_1} \frac{\partial^2 u}{\partial \theta^2} + \frac{d_2^2}{d_1^2} \frac{\partial^4 u}{\partial \theta^4} + \frac{d_3}{d_1} \frac{\partial v_2}{\partial \theta} \\ - \frac{d_2 d_3}{d_1^2} \frac{\partial^3 v_2}{\partial \theta^3} + K_2 (u + \frac{\partial v_2}{\partial \theta}) + m \frac{\partial^2 u}{\partial t^2} \\ + m_1 \frac{d_2}{d_1} \left( \frac{d_3}{d_1} \frac{\partial^3 v_2}{\partial \theta \partial t^2} - \frac{d_2}{d_1} \frac{\partial^4 u}{\partial \theta^2 \partial t^2} \right) = 0; \end{aligned} \quad (2.4a)$$

$$K_1 \frac{d_3}{d_1} \left( \frac{\partial u}{\partial \theta} + \frac{d_3}{d_1} \frac{\partial^2 v_2}{\partial \theta^2} - \frac{d_2}{d_1} \frac{\partial^3 u}{\partial \theta^3} \right) + K_2 \left( \frac{\partial u}{\partial \theta} + \frac{\partial^2 v_2}{\partial \theta^2} \right) - m_2 \frac{\partial^2 v_2}{\partial t^2}$$

$$- m_1 \frac{d_3}{d_1} \left( \frac{d_3}{d_1} \frac{\partial^2 v_2}{\partial t^2} - \frac{d_2}{d_1} \frac{\partial^3 u}{\partial \theta \partial t^2} \right) = 0 \quad (2.4b)$$

$$- [D(u + \frac{\partial^2 u}{\partial \theta^2}) - K_1 \frac{d_2}{d_1} (u + \frac{d_3}{d_1} \frac{\partial v_2}{\partial \theta} - \frac{d_2}{d_1} \frac{\partial^2 u}{\partial \theta^2})] \delta(\frac{\partial u}{\partial \theta}) \Big|_0$$

$$- \frac{k_r}{2R_2^2} [( \frac{\partial u}{\partial \theta} - v_2 ) \delta(\frac{\partial u}{\partial \theta}) \Big|_{\theta=0} + (\frac{\partial u}{\partial \theta} - v_2) \delta(\frac{\partial u}{\partial \theta}) \Big|_{\theta=\lambda}] = 0 \quad (2.5a)$$

$$- [K_1 \frac{d_3}{d_1} (u + \frac{d_3}{d_1} \frac{\partial v_2}{\partial \theta} - \frac{d_2}{d_1} \frac{\partial^2 u}{\partial \theta^2}) + K_2 (u + \frac{\partial v_2}{\partial \theta})] \delta(v_2) \Big|_0$$

$$+ \frac{k_r}{2R_2^2} [(\frac{\partial u}{\partial \theta} - v_2) \delta(v_2) \Big|_{\theta=0} + (\frac{\partial u}{\partial \theta} - v_2) \delta(v_2) \Big|_{\theta=\lambda}] = 0 \quad (2.5b)$$

and

$$[m_1 \frac{d_2}{d_1} \left( \frac{d_3}{d_1} \frac{\partial^2 v_2}{\partial t^2} - \frac{d_2}{d_1} \frac{\partial^3 u}{\partial \theta \partial t^2} \right) + D \left( \frac{\partial u}{\partial \theta} + \frac{\partial^3 u}{\partial \theta^3} \right)$$

$$- K_1 \frac{d_2}{d_1} \left( \frac{\partial u}{\partial \theta} + \frac{d_3}{d_1} \frac{\partial^2 v_2}{\partial \theta^2} - \frac{d_2}{d_1} \frac{\partial^3 u}{\partial \theta^3} \right)] \delta(u) \Big|_0$$

$$- \frac{k_t}{2} [u \delta(u) \Big|_{\theta=0} + u \delta(u) \Big|_{\theta=\lambda}] = 0. \quad (2.5c)$$

Here  $D = D_1 + D_2$  and  $m = m_1 + m_2$ .

It should be noted that by letting  $\delta_1 = 0$  in (2.4) and (2.5), the governing differential equations and the boundary conditions for a single layer ring can be obtained. The equations so derived are more accurate

than the extensional equation given by Lang [41]. He made the assumption that the extensional strain ( $\epsilon_\theta$ ) has little effect on the moment and used the condition that  $\epsilon_\theta = 0$  in deriving the moment displacement relation.

### 2.3 COUPLING CO-ORDINATES AND COUPLING FORCES

The boundary conditions given by (2.5a) - (2.5c) are of the form

$$[-F_j + S_j] \delta(q_j) \Big|_{\theta=0} = 0 \text{ and } [F_j + S_j] \delta(q_j) \Big|_{\theta=\lambda} = 0, \\ j = 1, 2, 3$$

where  $q_j$ 's are a set of generalized coupling coordinates, namely,  $q_1 = \frac{\partial u}{\partial \theta}$ ,  $q_2 = v_2$  and  $q_3 = u$ ,  $F_j$ 's represents the associated generalized force due to the ring element and  $S_j$ 's that due to the support.

The periodic element of the ring (Fig. 2.2(a)) can be schematically represented by a block diagram as shown in Fig. 2.2(b). For this element the maximum number of coupling co-ordinates is three. The associated coupling forces at the ends 0 and  $\lambda$  are  $Q_{j0}$  ( $= -F_j - S_j$ , at  $\theta = 0$ ) and  $Q_{j\lambda}$  ( $= F_j + S_j$ , at  $\theta = \lambda$ ), respectively. The directions of these coordinates and the forces with respect to the element are also indicated in Fig. 2.2(b). The harmonic amplitudes of these forces are given by

$$\bar{Q}_{10} = - [D(U + \frac{d^2U}{d\theta^2}) - K_1 \frac{d_2}{d_1} (U + \frac{d_3}{d_1} \frac{dV_2}{d\theta} - \frac{d_2}{d_1} \frac{d^2U}{d\theta^2}) - \frac{k_r}{2R_2^2} (\frac{dU}{d\theta} - V_2)]_{\theta=0} \quad (2.6a)$$

$$\bar{Q}_{1\lambda} = - [D(U + \frac{d^2U}{d\theta^2}) - K_1 \frac{d_2}{d_1} (U + \frac{d_3}{d_1} \frac{dV_2}{d\theta} - \frac{d_2}{d_1} \frac{d^2U}{d\theta^2}) + \frac{k_r}{2R_2^2} (\frac{dU}{d\theta} - V_2)]_{\theta=\lambda} \quad (2.6b)$$

$$\bar{Q}_{20} = - [K_1 \frac{d_3}{d_1} (U + \frac{d_3}{d_1} \frac{dV_2}{d\theta} - \frac{d_2}{d_1} \frac{d^2U}{d\theta^2}) + K_2 (U + \frac{dV_2}{d\theta}) + \frac{k_r}{2R_2^2} (\frac{dU}{d\theta} - V_2)]_{\theta=0} \quad (2.6c)$$

$$\bar{Q}_{2\lambda} = - [K_1 \frac{d_3}{d_1} (U + \frac{d_3}{d_1} \frac{dV_2}{d\theta} - \frac{d_2}{d_1} \frac{d^2U}{d\theta^2}) + K_2 (U + \frac{dV_2}{d\theta}) - \frac{k_r}{2R_2^2} (\frac{dU}{d\theta} - V_2)]_{\theta=\lambda} \quad (2.6d)$$

$$\bar{Q}_{30} = [D(\frac{dU}{d\theta} + \frac{d^3U}{d\theta^3}) - K_1 \frac{d_2}{d_1} (\frac{dU}{d\theta} + \frac{d_3}{d_1} \frac{d^2V_2}{d\theta^2} - \frac{d_2}{d_1} \frac{d^3U}{d\theta^3}) - m_1 \omega^2 \frac{d_2}{d_1} (\frac{d_3}{d_1} V_2 - \frac{d_2}{d_1} \frac{dU}{d\theta}) + \frac{k_t}{2} U]_{\theta=0} \quad (2.6e)$$

$$\bar{Q}_{3\lambda} = [D(\frac{dU}{d\theta} + \frac{d^3U}{d\theta^3}) - K_1 \frac{d_2}{d_1} (\frac{dU}{d\theta} + \frac{d_3}{d_1} \frac{d^2V_2}{d\theta^2} - \frac{d_2}{d_1} \frac{d^3U}{d\theta^3}) - m_1 \omega^2 \frac{d_2}{d_1} (\frac{d_3}{d_1} V_2 - \frac{d_2}{d_1} \frac{dU}{d\theta}) - k_t U]_{\theta=\lambda} \quad (2.6f)$$

where  $u = U e^{i\omega t}$ ,  $v_2 = V_2 e^{i\omega t}$ ,  $Q_{j0} = \bar{Q}_{j0} e^{i\omega t}$  and  
 $Q_{j\lambda} = \bar{Q}_{j\lambda} e^{i\omega t}$  ( $j = 1, 2, 3$ ).

## 2.4 NATURAL FREQUENCIES OF AN ELASTIC RING

### 2.4.1 Theory of Wave Propagation and Natural Frequencies

Free harmonic vibration of an infinite periodic, undamped structures can be analysed into a special type of wave motion [2]. These free waves can propagate through the structure without decaying only in certain frequency zones called 'propagation bands'. Outside these bands, the waves decay as they spread outwards. This motion is characterized by complex constants,  $\mu$ , called the propagation constants. The real ( $\mu_r$ ) and imaginary ( $\mu_i$ ) parts of these constants are the measures of the rate of decay and the change of phase, respectively, over the distance between the adjacent supports. This implies that

$$e^{\mu} q_j \Big|_{\theta=0} = q_j \Big|_{\theta=\lambda} \text{ and } e^{\mu} Q_j \Big|_{\theta=0} = Q_j \Big|_{\theta=\lambda}, \quad (j=1,2,3)$$

in the present case. The propagation constants always occur in pairs (positive and negative) and the number of pairs are equal to the minimum number of coupling coordinates between the adjacent periodic elements [3].

For the ring under consideration, the special type of harmonic waves propagate without any reflection as the structure does not have any ends. Hence, the ring can be considered as an infinite periodic structure except that the propagating waves should have the same phase and magnitude after travelling once around the complete ring.

Consequently, frequencies (natural) at which harmonic waves can propagate are not given by the entire propagation band but are limited to a discrete set [7], given by

$$\mu_{rn} = 0, \quad \text{and} \quad \mu_{in} = \pm 2j\pi/N \quad (j=0, 1, 2\dots N) \quad (2.7)$$

where  $N$  is the number of bays in the ring and the subscript  $n$  refers to the value at a natural frequency.

#### 2.4.2 Different Support Conditions

In the first type of support conditions, radial supports are assumed to prevent not only the radial displacement but also the mid-plane tangential displacement of the base layer (layer 2). Consequently the only non-zero coupling co-ordinate is  $q_1 = \partial u / \partial \theta$  and the system becomes mono-coupled [4]. As mentioned in the previous section, only one pair of opposite going free waves exist in the system. Amplitudes of the associated harmonic coupling forces ( $Q_{10}$  and  $Q_{1\lambda}$ ) are given by (2.6a) and (2.6b).

By following the receptance method [7], propagation constant ( $\mu$ ) versus frequency ( $\Omega$ ) curves are obtained for a given number of bays ( $N$ ). The receptance method and the necessary equations are given in Appendix B.1. Here, the non-dimensional frequency  $\Omega$  is defined as  $\Omega = \omega \sqrt{m_2/D_2}$ . The natural frequencies of the ring can be determined from these curves by using (2.7).

With the second type of support conditions, the ring becomes a bi-coupled system having coupling co-ordinates  $q_1 = \partial u / \partial \theta$  and  $q_2 = v_2$ . As a result, two pairs of opposite going waves exist in the structure and the amplitudes of the associated harmonic forces ( $Q_{10}$ ,  $Q_{1\lambda}$ ,  $Q_{20}$  and  $Q_{2\lambda}$ ) are given by (2.6a) - (2.6d). Then, the propagation constant versus frequency curves and the natural frequencies are obtained by the same procedure outlined earlier. The equations necessary for evaluating the receptances are included in Appendix B.2.

When the supports are considered to be radially flexible (third type of support conditions), all the three coupling co-ordinates ( $q_1 = \partial u / \partial \theta$ ,  $q_2 = v_2$  and  $q_3 = u$ ) are non-zero rendering the structure tri-coupled. By using the amplitudes of the associated harmonic forces given by (2.6a) - (2.6f), the propagation constant curves and the natural frequencies can be obtained. For this type of supports also, necessary equations for the receptance method are given in Appendix B.3.

## 2.5 RESONANT FREQUENCIES AND LOSS FACTORS OF A DAMPED RING

When the outer layer is considered to be visco-elastic with a loss factor,  $\beta$ , its complex Young's modulus can be written as  $E_1^* = E_1 (1 + i \beta)$ . Then, the composite ring becomes a damped structure and the free waves can no longer propagate without decay at any frequency. To find the resonant frequencies and the associated loss factors

of such damped structures, a theory of 'forced damped normal modes' is used [39, 40]. These forced damped normal modes are obtained by exciting the structure with a loading which is harmonic and is in phase with the local velocity but proportional in amplitude to the local inertia. This is achieved by replacing  $\omega^2$  by  $\omega^{*2} = \omega^2 (1 + i n)$ , in (2.4) and (2.5).

For harmonic variation of the displacements  $u$  and  $v_2$ , (2.4a) and (2.4b) become, respectively,

$$L_1 U + L_2 V_2 = 0 \quad (2.8a)$$

$$\text{and } L_2 U + L_3 V_2 = 0 \quad (2.8b)$$

where differential operators

$$L_1 = (D^* + K_1^* \frac{d^2}{d\theta^2}) \frac{d^4}{d\theta^4} + (2 D^* - 2K_1^* \frac{d^2}{d\theta^2} + m_1 \omega^{*2} \frac{d^2}{d\theta^2}) \frac{d^2}{d\theta^2}$$

$$+ (D^* + K_1^* + K_2 - m_1 \omega^{*2})$$

$$L_2 = -K_1^* \frac{d_2 d_3}{d_1^2} \frac{d^3}{d\theta^3} + (K_1^* \frac{d_3}{d_1} + K_2 - m_1 \omega^{*2} \frac{d_2 d_3}{d_1^2}) \frac{d}{d\theta}$$

$$\text{and } L_3 = (K_1^* \frac{d_3^2}{d_1^2} + K_2) \frac{d^2}{d\theta^2} + (m_1 \frac{d_3^2}{d_1^2} + m_2) \omega^{*2},$$

$$\text{with } D_1^* = D_1 (1 + i \beta), K_1^* = K_1 (1 + i \beta) \text{ and } D^* = D_1^* + D_2$$

To solve for the resonant frequencies and the associated modal loss factors, the general solution of (2.8) can be written in the form

$$U(\theta) = \sum_{j=1}^6 C_j e^{s_j \theta} \text{ and } V_2(\theta) = \sum_{j=1}^6 B_j e^{s_j \theta} \quad (2.9)$$

The  $s_j$ 's are the six roots of the auxilary equation

$$s^6 + a_1 s^4 + a_2 s^2 + a_3 = 0 \quad (2.10)$$

where  $a_1$ ,  $a_2$  and  $a_3$  are defined in Appendix C.

### 2.5.1 Different Support Conditions

For the first type of supports, the following conditions are to be satisfied.

- i) The radial displacement,  $u$ , is zero at  $\theta = 0$  and at  $\theta = \lambda$ : i.e.,

$$\sum_{j=1}^6 c_j = 0 \quad (2.11a)$$

and

$$\sum_{j=1}^6 c_j e^{s_j \lambda} = 0 \quad (2.11b)$$

- ii) The tangential displacement of base layer,  $v_2$ , is zero at  $\theta = 0$  and at  $\theta = \lambda$ : i.e.,

$$\sum_{j=1}^6 c_j T_j = 0 \quad (2.11c)$$

and

$$\sum_{j=1}^6 c_j T_j e^{s_j \lambda} = 0 \quad (2.11d)$$

where  $T_j = B_j/C_j$  and the expression for it is given in Appendix C.

- iii) The coupling co-ordinate,  $\partial u / \partial \theta$ , and the associated coupling force,  $Q_1$  must satisfy the wave condition, i.e.,

$$e^{i\mu_{in}} \frac{\partial u}{\partial \theta} \Big|_{\theta=0} = \frac{\partial u}{\partial \theta} \Big|_{\theta=\lambda}, \text{ or } \sum_{j=1}^6 C_j s_j (e^{i\mu_{in}} - e^{s_j \lambda}) = 0 \quad (2.11e)$$

and  $e^{i\mu_{in}} Q_{10} = Q_1 \lambda$ , or

$$\sum_{j=1}^6 C_j [s_j \left\{ \left( \frac{D_1^*}{D_2} + \frac{K_1^*}{D_2} \frac{d_2^2}{d_1^2} \right) s_j - \frac{K_1^*}{D_2} \frac{d_2 d_3}{d_1^2} T_j \right\} (e^{i\mu_{in}} - e^{s_j \lambda}) - \bar{k}_r s_j e^{s_j \lambda}] = 0 \quad (2.11f)$$

where  $\mu_{in}$  is given by (2.7) and  $\bar{k}_r (= k_r / D_2 R_2^2)$  is the non-dimensional rotational stiffness.

Equations (2.11a) - (2.11f) constitute a set of six homogeneous equations in six unknown coefficients  $C_j$ . For non-trivial solution of these unknowns, the coefficient determinant should vanish. Equation (2.10) along with this condition can be used to determine the resonant frequencies and the loss factors of the damped ring on different number of radial supports. The computational procedure is described in the following section.

Similarly, for the second type of supports also, the conditions to be satisfied can be written as

- i) The radial displacement,  $u$  is zero at  $\theta = 0$   
and at  $\theta = \lambda$  : i.e.,

$$\sum_{j=1}^6 C_j = 0 \quad (2.12a)$$

and

$$\sum_{j=1}^6 C_j e^{s_j \lambda} = 0 \quad (2.12b)$$

ii) The coupling co-ordinate,  $\partial u / \partial \theta$ , and the associated force must satisfy the wave condition: i.e.,

$$\sum_{j=1}^6 C_j s_j (e^{i\mu_{in}} - e^{s_j \lambda}) = 0 \quad (2.12c)$$

and

$$\begin{aligned} & \sum_{j=1}^6 C_j [s_j \{ \left( \frac{D_1^*}{D_2} + \frac{K_1^* d_2^2}{D_2 d_1^2} \right) s_j \right. \\ & \left. - \frac{K_1^*}{D_2} \frac{d_2 d_3}{d_1^2} T_j \} (e^{i\mu_{in}} - e^{s_j \lambda}) \\ & - \bar{k}_r (s_j - T_j) e^{s_j \lambda}] = 0 \end{aligned} \quad (2.12d)$$

iii) The coupling co-ordinate,  $v_2$ , and the associated force must satisfy the wave condition: i.e.,

$$e^{i\mu_{in}} v_2 (0) = v_2 (\lambda), \text{ or}$$

$$\sum_{j=1}^6 C_j T_j (e^{i\mu_{in}} - e^{s_j \lambda}) = 0 \quad (2.12e)$$

$$\text{and } e^{i\mu_{in}} Q_{20} = Q_2 \lambda, \text{ or}$$

$$\begin{aligned} & \sum_{j=1}^6 C_j [s_j \{ \frac{K_1^* d_3}{D_2 d_1} (\frac{d_3}{d_1} T_j - \frac{d_2}{d_1} s_j) \\ & + \frac{K_2}{D_2} T_j \} (e^{i\mu_{in}} - e^{s_j \lambda}) + \bar{k}_r (s_j - T_j) e^{s_j \lambda}] = 0 \end{aligned} \quad (2.12f)$$

When flexible radial supports (third type) are considered, equations (2.12c) - (2.12f) remain same and the zero displacement conditions given by (2.12a) and

(2.12b) are to be replaced by wave conditions as explained below.

The coupling co-ordinate,  $u$ , and the associated force must satisfy the wave condition: i.e.,

$$e^{i\mu_{in}} u(0) = u(\lambda), \text{ or } \sum_{j=1}^6 c_j (e^{i\mu_{in}} - e^{s_j \lambda}) = 0 \quad (2.13a)$$

and  $e^{i\mu_{in}} Q_{30} = Q_3 \lambda$ , or

$$\sum_{j=1}^6 c_j [s_j \left\{ \frac{D^*}{D_2} s_j^2 - \frac{k_1^*}{D_2} \frac{d_2}{d_1} \left( \frac{d_3}{d_1} s_j T_j - \frac{d_2}{d_1} s_j^2 \right) \right\} (e^{i\mu_{in}} - e^{s_j \lambda}) + \bar{k}_t e^{s_j \lambda}] = 0 \quad (2.13b)$$

where  $\bar{k}_t (= k_t/D_2)$  is the non-dimensional transverse stiffness.

Resonant frequencies and modal loss factors can be computed for the second and third type of supports using (2.12) and (2.13), respectively.

### 2.5.2 Computational Procedure

For beams and plates, it is known that if the structure is purely elastic, one root of the auxiliary equation (corresponding to (2.10)) is real and lies within finite bounds. In the first mode, these bounds are given by 3.14 and 4.73. This fact has been made use of in the interpolation method adapted by Mead [40, 42] while investigating damped beams and plates. For the present problem, this method is found to be unsuitable because no knowledge about such bounds of a root is available.

In order to compute the resonant frequencies and the associated modal loss factors of the damped ring, an algorithm based on a two-dimensional Newton-Raphson method [43] is used. The iterative scheme of this method is as follows.

Let  $W$  be the determinant of the coefficient matrix described in the previous section. As  $W$  is a function of complex frequency  $\Omega^*$  ( $= \Omega\sqrt{1+i\eta}$ ), the condition that the determinant should vanish at the correct resonant frequency and correct loss factor implies

$$W_R(x, y) = 0 \quad (2.14a)$$

$$\text{and } W_I(x, y) = 0 \quad (2.14b)$$

where  $W_R$  and  $W_I$  are real and imaginary parts of  $W$ , with  $x = \Omega^2$  and  $y = \Omega^2 \eta$ .

Since  $W_R$  and  $W_I$  are two functions in two unknowns  $x$  and  $y$ , roots of (2.14a) and (2.14b) can be computed by the two-dimensional Newton - Raphson iterative procedure given by

$$x_{j+1} = x_j + \left( \frac{\frac{W_I}{W_R} \frac{W_R}{y} - \frac{W_R}{W_I} \frac{W_I}{y}}{\frac{W_I}{W_R} \frac{y}{x} - \frac{W_R}{W_I} \frac{y}{x}} \right)_j \quad (2.15a)$$

$$\text{and } y_{j+1} = y_j + \left( \frac{\frac{W_R}{W_I} \frac{W_I}{x} - \frac{W_I}{W_R} \frac{W_R}{x}}{\frac{W_R}{W_I} \frac{x}{y} - \frac{W_I}{W_R} \frac{x}{y}} \right)_j \quad (2.15b)$$

where suffixes  $x$  and  $y$  indicate partial derivatives of  $W_R$  or  $W_I$ . The required partial derivatives in the iterations

are computed by a central difference scheme. The iterative process is terminated when the absolute value of the normalized (with respect to the starting value) determinant is less than a prescribed small number.

In the present work, convergence of this method is found to be very sensitive to the perturbation chosen for computing the partial derivatives. In some cases, the perturbation is as small as 0.1%. The first choice of frequency required for the iteration is guided by the corresponding elastic analysis (i.e., with  $\beta = 0$  and other parameters remaining same) outlined in section 2.4. It is taken some what higher ( $\approx 10 - 15\%$ ) than the natural frequencies obtained for the corresponding elastic structure. With such starting values, the desired convergence is achieved within 5-8 iterations. Hence, the analysis for the elastic case, using the receptance method, should precede that for the viscoelastic case.

## 2.6 NATURAL MODES OF AN ELASTIC RING

The mode shapes of a periodic structure can be thought of a group of freely propagating waves travelling in positive and negative directions. For the ring under consideration, natural frequencies are the frequencies at which propagation constant satisfies (2.7). Mode shapes at these natural frequencies are formed by the superposition of positive and negative going propagating waves (i.e.,  $\mu_{rn} = 0$ ) with this propagation constant.

Here, in the case of bi-coupled and tri-coupled systems, it is to be noted that there exists a possibility for two or more propagating waves to have the same phase constant ( $\mu_{in}$ ) at a natural frequency. Then, superposition of all (two or three) these waves are to be considered for obtaining the mode shape. However, in the frequency range considered (for bi-coupled and tri-coupled systems), only one propagating wave is found to exist at all the natural frequencies. Based on this fact, the following analysis for the mode shapes is carried out.

Let  $\underline{Q}$  be harmonic amplitude of any generalized coupling force of the periodic element.

At the supports, this force can be written as follows:

$$\begin{aligned}
 \text{at support No. 1: } \underline{Q}_1 &= \underline{Q}_1^+ + \underline{Q}_1^- \\
 \text{at support No. 2: } \underline{Q}_2 &= \underline{Q}_1^+ e^{-i\mu_{in}} + \underline{Q}_1^- e^{+i\mu_{in}} \\
 \text{Or } \underline{Q}_2 &= (\underline{Q}_1^+ + \underline{Q}_1^-) \cos \mu_{in} - i(\underline{Q}_1^+ - \underline{Q}_1^-) \sin \mu_{in} \\
 \text{at support No. 3: } \underline{Q}_3 &= (\underline{Q}_1^+ + \underline{Q}_1^-) \cos 2\mu_{in} - i(\underline{Q}_1^+ - \underline{Q}_1^-) \sin 2\mu_{in} \\
 \text{at support No. j: } \underline{Q}_j &= (\underline{Q}_1^+ + \underline{Q}_1^-) \cos (j-1)\mu_{in} \\
 &\quad - (\underline{Q}_1^+ - \underline{Q}_1^-) \sin (j-1)\mu_{in}
 \end{aligned}$$

(2.16)

where the superscripts + and - refer to positive and negative going waves, respectively.

$$\begin{aligned}
 \text{Let } Q_1^+ + Q_1^- &= B_R + i B_I \\
 \text{and } Q_1^+ - Q_1^- &= C_R + i C_I \\
 \text{then, } Q_1 &= B_R + i B_I \\
 Q_2 &= (B_R \cos \mu_{in} + C_I \sin \mu_{in}) \\
 &\quad + i (B_I \cos \mu_{in} - C_R \sin \mu_{in}) \\
 &\quad \vdots \\
 &\quad \vdots \\
 Q_j &= B_R \cos (j-1) \mu_{in} + C_I \sin (j-1) \mu_{in} \\
 &\quad + i [B_I \cos (j-1) \mu_{in} - C_R \sin (j-1) \mu_{in}]
 \end{aligned} \tag{2.17}$$

At a natural frequency, all these forces must be exactly in phase or in counter phase: i.e., they should all be real or imaginary.

Without loss of generality, the force at support 1 can be assumed to be real or imaginary (say real),

$$\begin{aligned}
 \text{then } Q_1 &= B_R \quad (\text{i.e., } B_I = 0) \\
 Q_2 &= (B_R \cos \mu_{in} + C_I \sin \mu_{in}) - i C_R \sin \mu_{in} \\
 Q_j &= B_R \cos (j-1) \mu_{in} + C_I \sin (j-1) \mu_{in} \\
 &\quad - i C_R \sin (j-1) \mu_{in}
 \end{aligned} \tag{2.18}$$

Using the fact that for a standing mode to exist all forces should be real (since  $B_I = 0$ ): i.e.,  $C_R$  must be equal to zero. Still the forces at the supports are not uniquely defined for  $\mu_{in} \neq 0$ , implying that the corresponding modes have a degeneracy. Any arbitrary

value for  $B_R$  and  $C_I$  gives rise to a mode shape. For simplicity, taking  $B_R = 0$  and  $C_I = 2$ ,  $Q$ 's can be written as follows:

$$\begin{aligned} \underline{Q}_1 &= 0 ; \quad \underline{Q}_1^+ = +i ; \quad \underline{Q}_1^- = -i \\ \underline{Q}_2 &= 2 \sin \mu_{in} ; \quad \underline{Q}_2^+ = i e^{-i\mu_{in}} ; \quad \underline{Q}_2^- = -i e^{+i\mu_{in}} \\ &\vdots \\ &\vdots \\ \underline{Q}_j &= 2 \sin (j-1) \mu_{in} ; \quad \underline{Q}_j^+ = i e^{-i(j-1)\mu_{in}} ; \quad (2.19) \\ \underline{Q}_j^- &= -i e^{+i(j-1)\mu_{in}} \end{aligned}$$

Similarly taking  $B_R = 2$  and  $C_I = 0$ , one gets

$$\begin{aligned} \underline{Q}_1 &= 2 ; \quad \underline{Q}_1^+ = 1 ; \quad \underline{Q}_1^- = 1 \\ \underline{Q}_2 &= 2 \cos \mu_{in} ; \quad \underline{Q}_2^+ = e^{-i\mu_{in}} ; \quad \underline{Q}_2^- = e^{+i\mu_{in}} \quad (2.20) \\ &\vdots \\ &\vdots \\ \underline{Q}_j &= 2 \cos(j-1) \mu_{in} ; \quad \underline{Q}_j^+ = e^{-i(j-1)\mu_{in}} ; \quad \underline{Q}_j^- = e^{+i(j-1)\mu_{in}} \end{aligned}$$

The forces given by (2.19) and (2.20) lead to anti-symmetric and symmetric modes with respect to a diameter passing through a support [7]. Using (2.19) (or (2.20)) along with the support conditions modes can be computed. It is to be noted that even for bi-coupled and tri-coupled systems, any one coupling force may be prescribed according to (2.19) or (2.20).

Forces at all the supports are equal (either real or imaginary) with  $\mu_{in} = 0$ , i.e. they can either

be equal to zero or have a finite value. In general, the values of the force can not be preassigned and it depends on the mode. So, the following eigenvalue problem is formulated for this case.

Depending upon the type of supports, the zero displacement conditions at the supports can be expressed in the matrix form as

$$[H] \{C\} = \{0\} \quad (2.21)$$

where  $[H]$  is  $(n_1 \times n_2)$  matrix with  $n_1 (< n_2)$  as the number of zero displacement conditions,  $n_2$  as the total number of conditions and  $\{C\}$  is a vector of unknown constants ( $= n_2$ ) in the series given by (2.9). For a two layered ring,  $n_2$  is equal to six.

Choosing first  $n_1$  elements of the vector  $\{C\}$  as dependent, they can be written from (2.21) as

$$\{C'\} = - [H']^{-1} [H''] \{C''\} \quad (2.22)$$

where  $\{C'\}$  is the vector of first  $n_1$  elements of  $\{C\}$  and  $\{C''\}$  is vector of last  $(n_2 - n_1)$  elements of  $\{C\}$  such that  $[H] \{C\} = [H'] \{C'\} + [H''] \{C''\}$

The remaining  $n_2 - n_1$  wave conditions to be satisfied by coupling co-ordinates and coupling forces can be written in the matrix form as

$$[\Phi] \{C\} = e^{i\mu_{in}} [M] \{C\} \quad (2.23)$$

where  $[\Phi]$  and  $[M]$  are  $(n_2 - n_1) \times n_2$  matrices.

Partitioning the matrices  $[\Phi]$  and  $[M]$  similar to  $[H]$ , (2.23) can be rewritten in the following form:

$$\text{i.e., } [\Phi']\{C'\} + [\Phi'']\{C''\} = e^{i\mu_{in}} \left[ [M']\{C'\} + [M'']\{C''\} \right] \quad (2.24)$$

Eliminating  $\{C'\}$  from (2.24) with the help of (2.22),  $(n_2 - n_1)^{\text{th}}$  order eigenvalue problem with  $e^{i\mu_{in}}$  as the eigenvalue, can be obtained.

$$\text{i.e., } [[\chi] - e^{i\mu_{in}} [I]]\{C''\} = \{0\} \quad (2.25)$$

where

$$[\chi] = [[M''] - [M']] [H']^{-1} [H'']^{-1} [[\Phi''] - [\Phi']] [H']^{-1} [H'']]$$

and  $[I]$  is the identity matrix.

Here, all the matrices are functions of frequency,  $\Omega$ . To solve the eigenvalue problem, the exact value of  $\Omega_n$  corresponding to  $\mu_{rn} = 0$  and  $\mu_{in} = 0$  has to be used. Since the exact value is difficult to read from the propagation constant curves, an iterative scheme which requires only an approximate eigenvalue, is used. The approximate eigenvalue corresponding to  $\mu_{rn} = 0$  and  $\mu_{in} = 0$  is 1. The steps involved in the iterative scheme are as follows:

- i) Choose any vector  $\{\epsilon\}$  of size  $(n_2 - n_1)$
- ii) Compute the solution vector  $\{C''\}$  such that  

$$[[\chi] - e^{i\mu_{in}} [I]]\{C''\} = \{\epsilon\}$$
- iii) Normalize the vector  $\{C''\}$

iv) Improve the approximate eigenvalues using Rayleigh quotient formula given by

$$e^{i\tilde{\mu}_{in}} = \frac{\{C''\}^T \{x\} \{C''\}}{\{C''\}^T \{C''\}}$$

where  $e^{i\tilde{\mu}_{in}}$  is the improved eigenvalue.

v) Take  $\{\epsilon\} = \{C''\}$  and repeat steps (ii) to (v) till the specified convergence is achieved.

## 2.7 RESULTS AND DISCUSSION

Numerical results are presented for the following data:

$$\delta_2 = 0.02, \quad E_1/E_2 = 0.001, \quad \rho_1/\rho_2 = 0.2,$$

$$N = 3 \text{ (i.e., } \lambda = 2\pi/3), \quad \beta = 0.2, 0.6 \text{ and } 1.0,$$

$$\bar{k}_r = 0 \text{ and } 2, \quad \bar{k}_t = 180$$

### 2.7.1 Outer Layer Elastic

Propagation constant ( $\mu$ ) versus frequency ( $\Omega$ ) curves are presented in Figs. (2.3) - (2.5) for thickness ratio,  $\delta_1/\delta_2 = 2.0$ . For the mono-coupled system, only the imaginary part ( $\mu_i$ ) is plotted in Fig. 2.3 whereas for the bi-coupled and tri-coupled systems both the real and imaginary parts are shown in Figs. 2.4 and 2.5.

The curves shown in Fig. 2.3 are very similar to those reported in reference [7] for a single layer ring. When  $\bar{k}_r = 2.0$ , the starting points of the propagation bands shift to higher frequencies. This indicates an

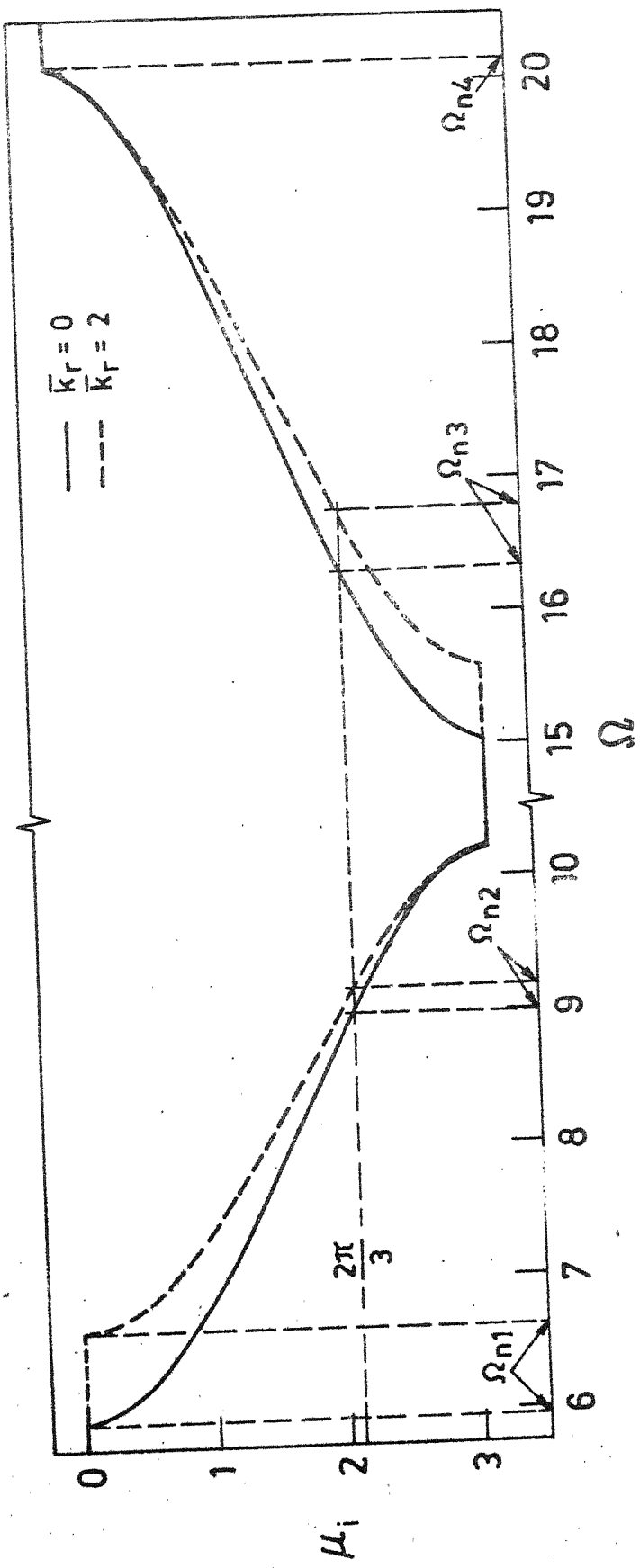


FIG. 2.3. VARIATION OF PROPAGATION CONSTANT WITH FREQUENCY : MONO-COUPLED SYSTEM.

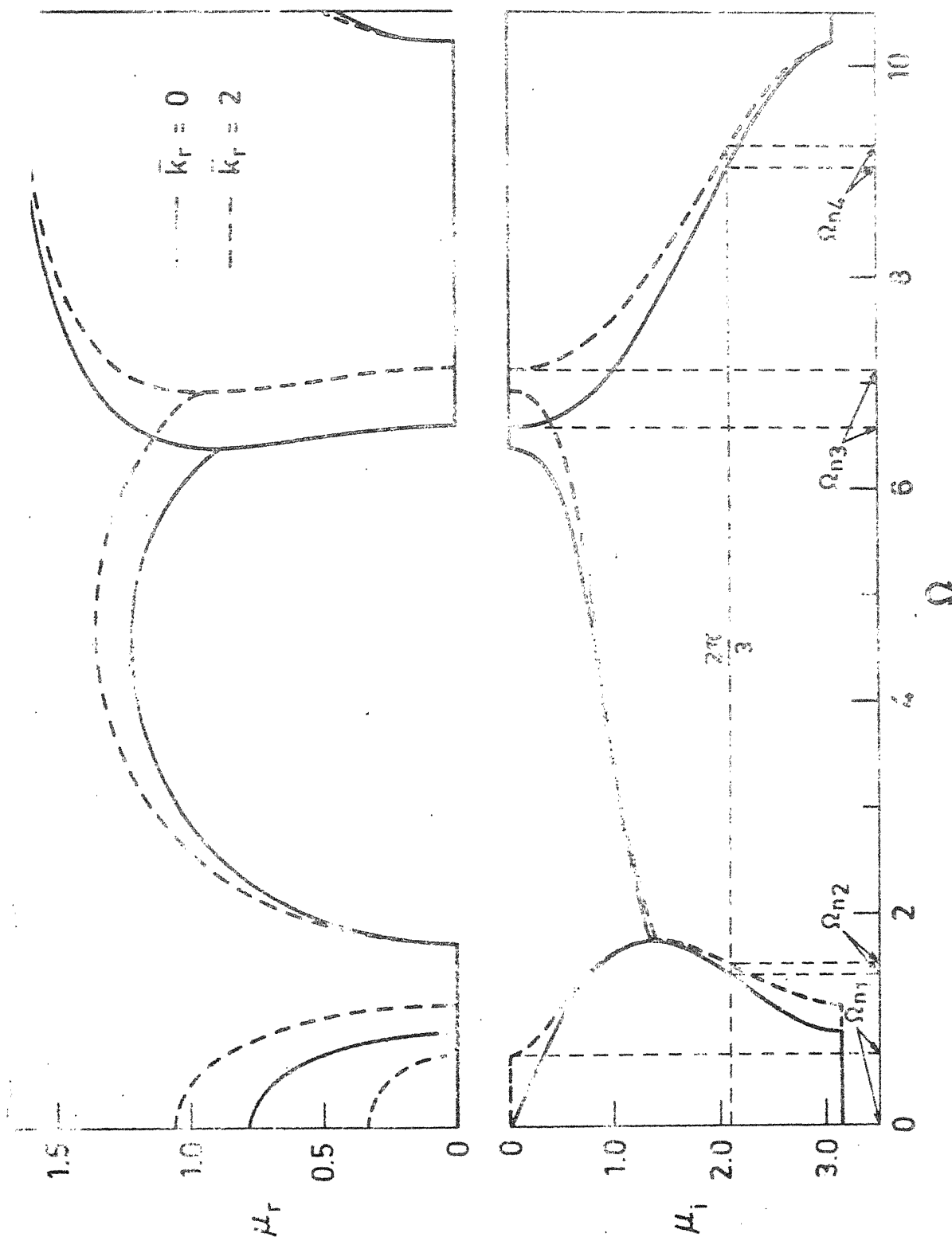


FIG. 2.4. VARIATION OF PROPAGATION CONSTANT WITH FREQUENCY  
2D COUPLED SYSTEM

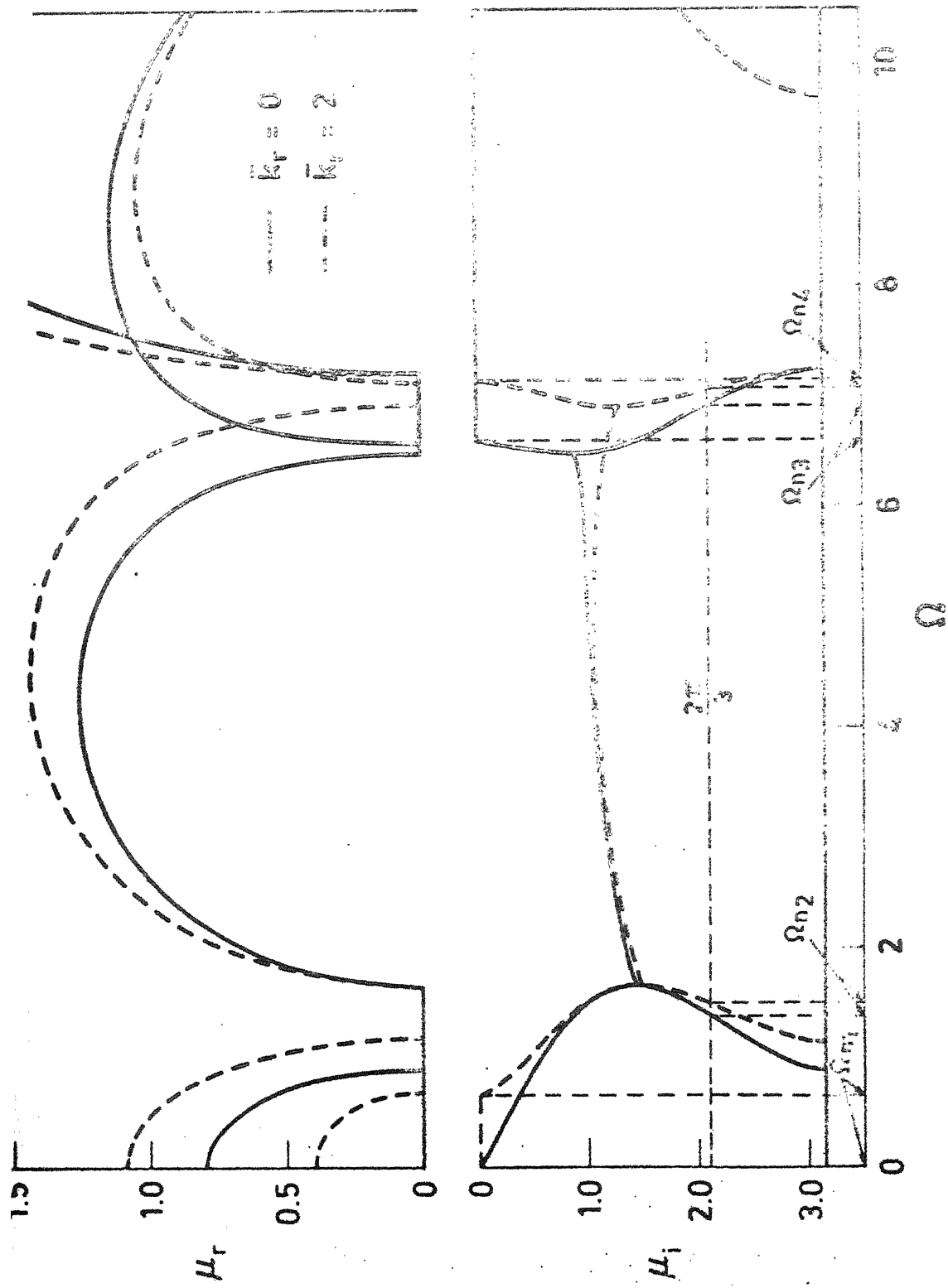


Fig. 2.5. VARIATION OF PROPAGATION CONSTANT WITH FREQUENCY FOR TRI-COUPLED SYSTEMS,  $K_c = 100$ .

increase in the natural frequencies due to increased stiffness of the ring as a whole. The addition of rotational stiffness ( $k_r$ ) at the supports does not alter the ends of the propagation bands because these upper bounding frequencies correspond to the natural frequencies of a periodic element with its coupling coordinates being locked [4].

When the supports prevent only the radial displacement, the propagation band starts from zero frequency only if  $\bar{k}_r = 0$  (see Fig. 2.4), indicating the existence of a rigid body motion. As the tangential displacement,  $v_2$ , is not prevented by the supports, a rigid body motion of the ring in the form of rotation about its centre is possible. However, when  $\bar{k}_r \neq 0$ , the propagation band starts from a frequency greater than zero, i.e., the rigid body motion is prevented as  $v_2$  is restrained by the rotational stiffness.

With the introduction of radial flexibility at the supports ( $\bar{k}_t = 180$ ), the propagation constant curves (Fig. 2.5) do not deviate much from the ones obtained for the bi-coupled system (Fig. 2.4) in the frequency range 0 to 6. Beyond this value, the propagation band narrows down considerably irrespective of the value of  $\bar{k}_r$ . This indicates that the natural frequencies of ring lying in this band decreases due to increase in the flexibility of the structure.

The first four natural frequencies ( $\omega_n$ ) for the above three cases are given in Table 2.1. Comparing the natural frequencies for different types of supports, it can be seen that the third natural frequency with second and third type of supports are comparable to the first one with the first type of supports. The first and second ones with the second and third type of supports are due to relaxation of the displacement,  $v_2$ , at the supports. This indicates that tangential displacements at the supports in the corresponding modes are predominant compared to others. The fourth frequency with the third type of supports is somewhat less compared to the corresponding ones with the first two types. This obviously implies that mode at this frequency has radial displacements at the supports.

Figures 2.6 - 2.9 show the mode shapes for  $\bar{k}_r = 0$  at the first two non-zero natural frequencies for mono-coupled and bi-coupled systems. For tri-coupled system, the mode shapes (first two) are nearly same as for bi-coupled and hence are not shown. The radial displacements of the modes (Figs. 2.6 and 2.8) are found to be very much similar to the ones presented for a single layer ring [7]. Comparing Figs. 2.7 and 2.8, it can be observed that the tangential displacement ( $v_2$ ) of the modes at the supports has a large (maximum) value only in the case of bi-coupled system.

TABLE 2.1

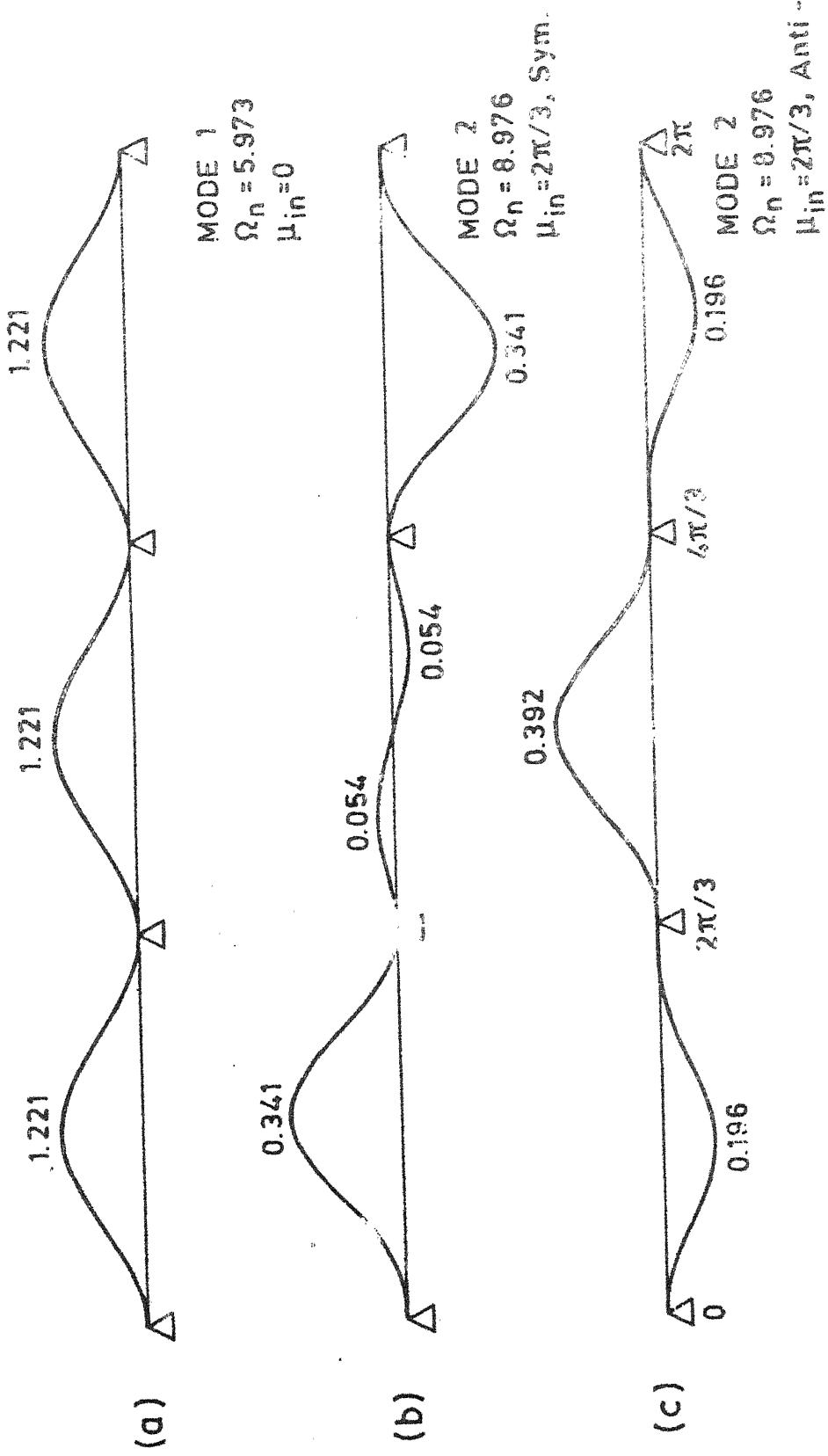
NATURAL FREQUENCIES OF UNDAMPED TWO LAYERED RING ON THREE SUPPORTS

$$\rho_1/\rho_2 = 0.2, \quad E_1/E_2 = 0.001, \quad \delta_2 = 0.02,$$

$$\delta_1/\delta_2 = 2, \quad N = 3$$

Mode No	$\mu_{in}$	$\Omega_n$					
		Mono-coupled System		Ei-coupled System		Tri-coupled system ( $k_t=18$ )	
		$\bar{k}_r = 0$	$\bar{k}_r = 2$	$\bar{k}_r = 0$	$\bar{k}_r = 2$	$\bar{k}_r = 0$	$\bar{k}_r = 2$
1	0	5.973	6.619	0.0	0.677	0.0	0.689
2	$2\pi/3$	8.976	9.179	1.414	1.527	1.384	1.489
	$2\pi/3$	16.381	16.750	-	-	-	-
3	0	-	-	6.581	7.143	6.582	7.142
	$2\pi/3$	-	-	9.031	9.235	6.922	7.056
4	0	20.130	20.130	-	-	-	-

FIG. 2.7. MODE SHAPES ( $V_2$ ) OF TWO LAYERED RING : MONO-COUPLED SYSTEM,  $\bar{k}_r = 0$



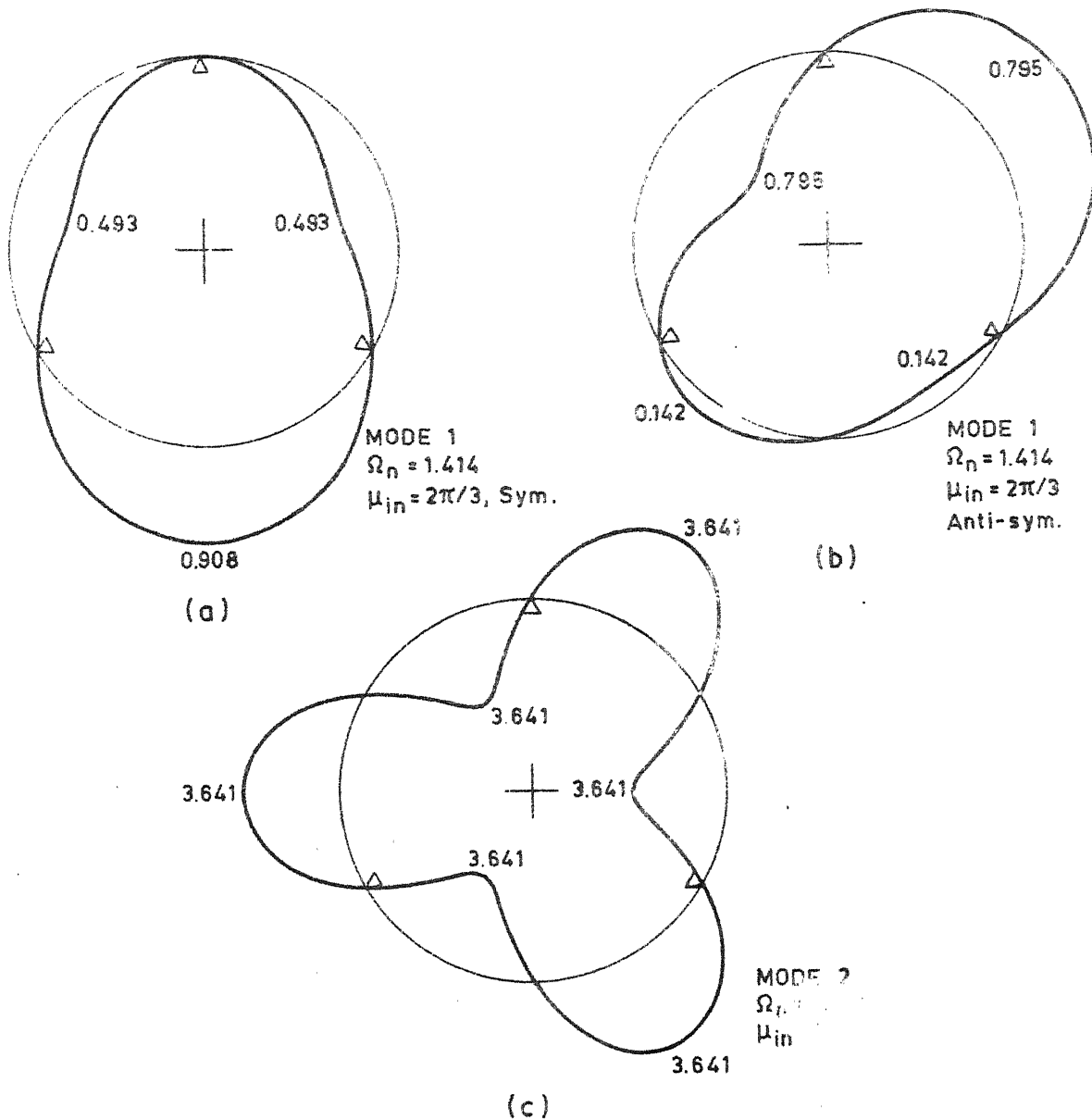


FIG. 2.8. MODE SHAPES ( $U$ ) OF TWO LAYERED RING : BI-COUPLED SYSTEM,  $\bar{k}_r = 0$ .

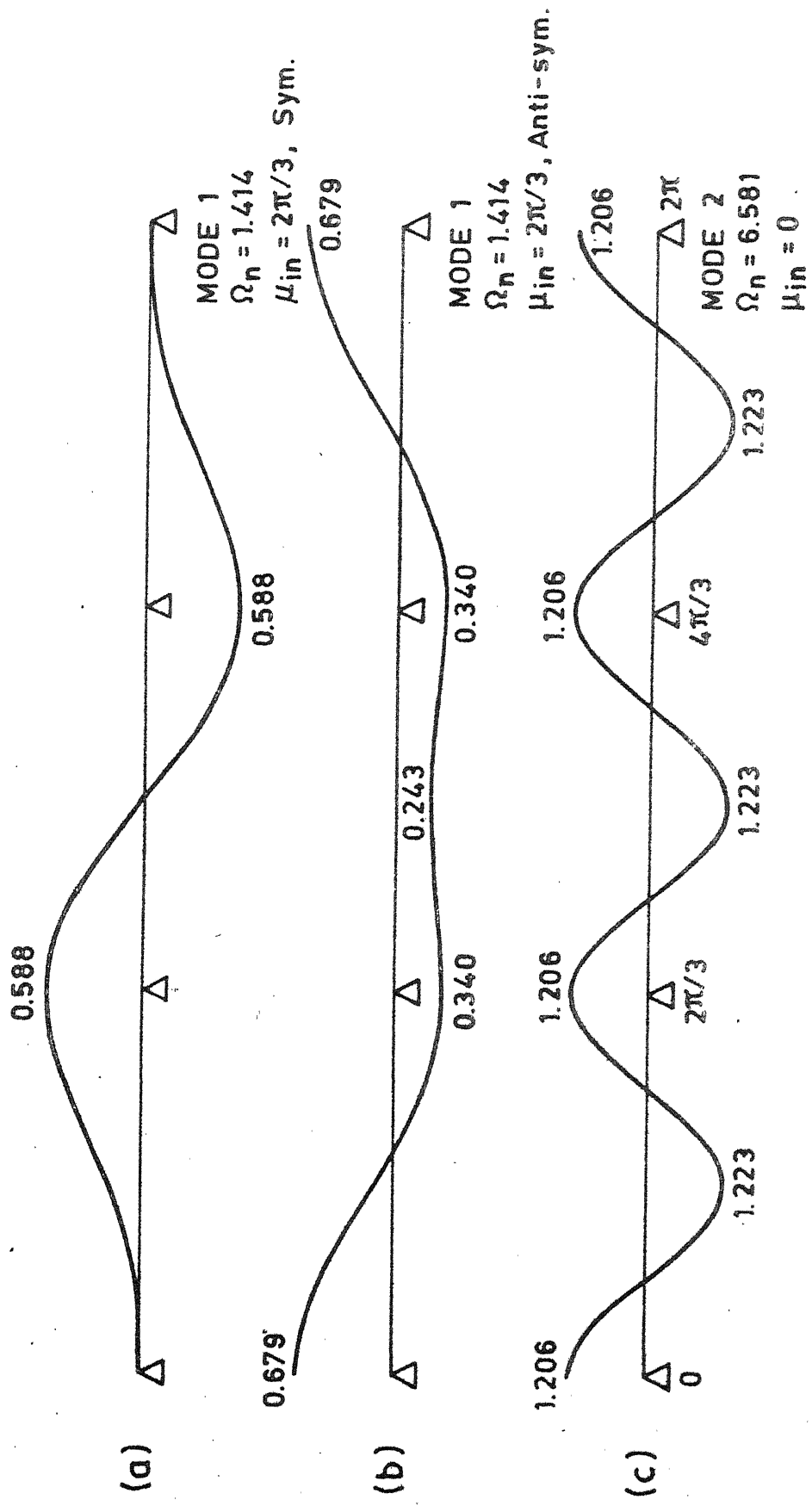


FIG. 2.9. MODE SHAPE ( $V_2$ ) OF TWO LAYERED, BI-COUPLED SYSTEM,  
 $k_r = 0$ .

This is expected as  $v_2$  at the supports is relaxed. A mode is referred to as 'symmetric' or 'anti-symmetric' about a diameter passing through a support depending on the pattern of its radial displacement. It can be seen that such symmetric and anti-symmetric modes (Figs. 2.6 and 2.8) are associated with anti-symmetric and symmetric tangential displacement pattern (Figs. 2.7 and 2.9), respectively, about the same diameter.

### 2.7.2 Outer Layer Viscoelastic

Variations of the resonant frequencies ( $\Omega_n$ ) and the composite loss factors ( $\eta$ ) with nondimensional thickness ratio ( $\delta_1/\delta_2$ ) are presented for different loss factors ( $\beta = 0.2, 0.6$  and  $1.0$ ) of the viscoelastic layer. For simplicity, the loss factor,  $\beta$  is assumed to be frequency independent. However, the variation of  $\beta$  with frequency can easily be incorporated in the computational procedure.

Figures 2.10 and 2.11 show the variation of  $\Omega_n$  and  $\eta$  for the first two modes with supports preventing both the displacements  $u$  and  $v_2$ . In both the modes, it is found that  $\Omega_n$  is nearly independent of  $\beta$  and decreases with  $\delta_1/\delta_2$ . This decreasing effect is due to the fact that for the data considered, mass of the structure increases with increasing  $\delta_1/\delta_2$  more rapidly than the stiffness. It can also be noted that for the limiting case of a single layer (i.e.,  $\delta_1/\delta_2 \rightarrow 0$ ),  $\Omega_n$

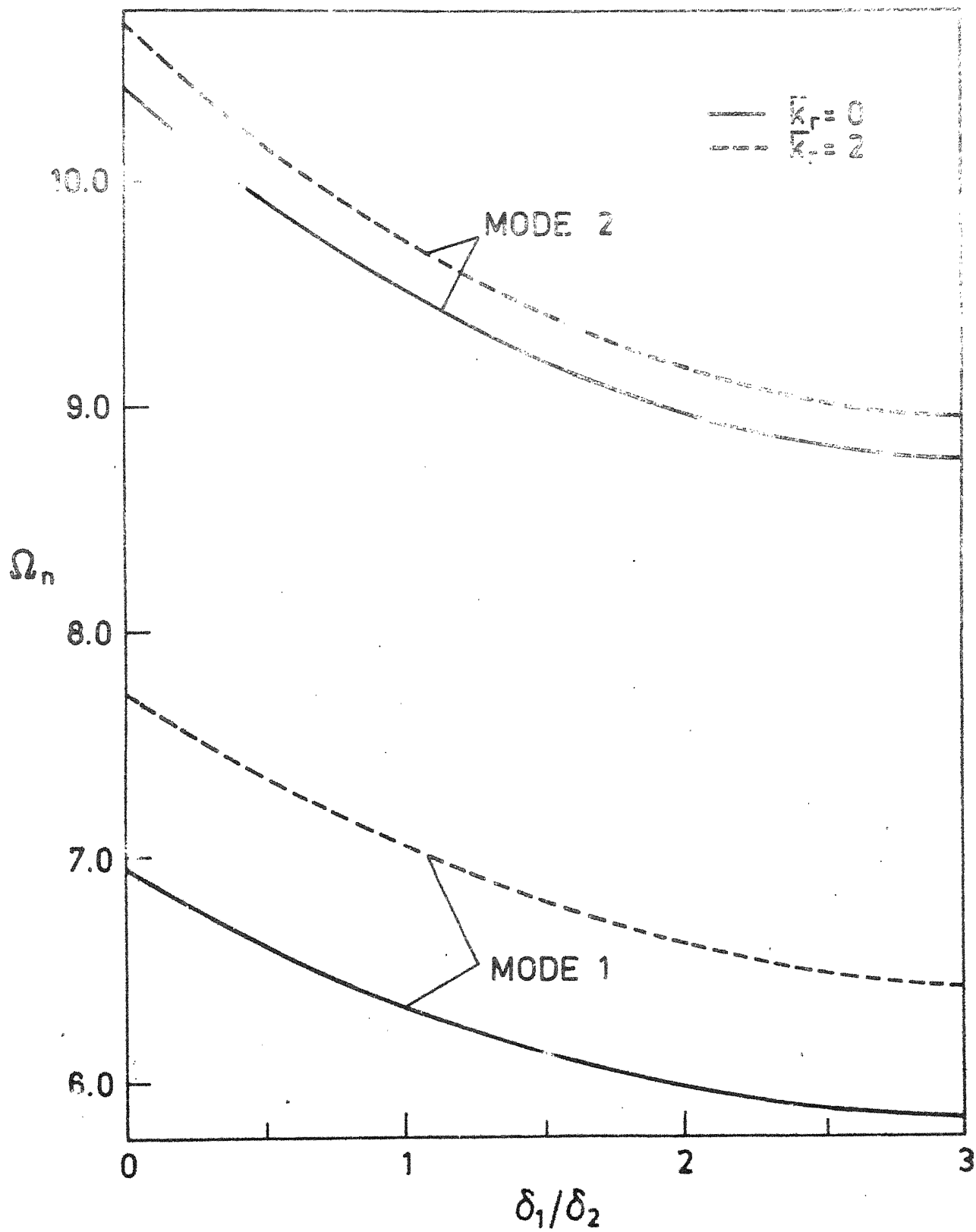


FIG. 2.10. VARIATION OF RESONANT FREQUENCY WITH THICKNESS RATIO: MONO-COUPLED SYSTEM.

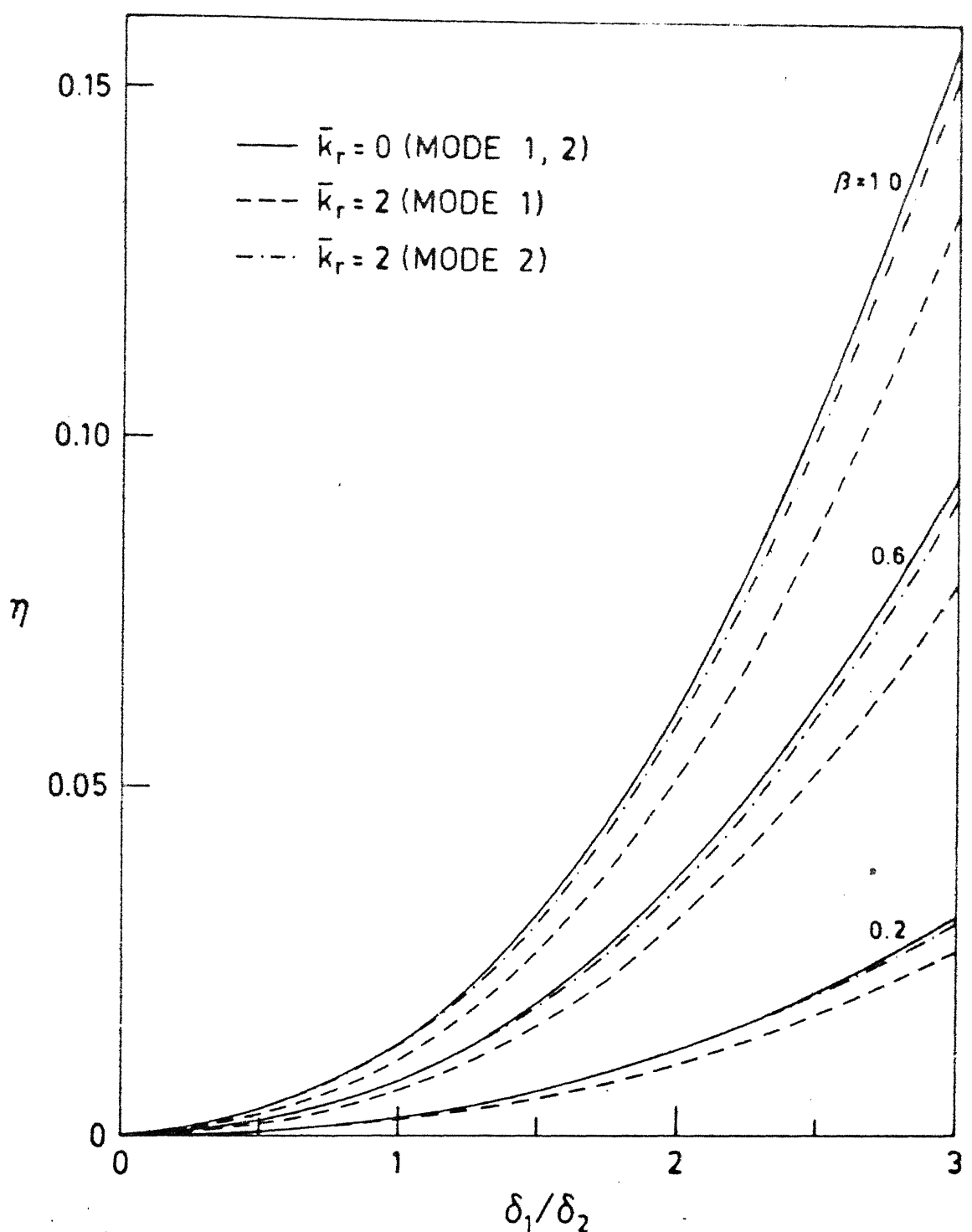


FIG. 2.11. VARIATION OF MODAL LOSS FACTOR WITH THICKNESS RATIO: MONO-COUPLED SYSTEM.

compares with the results given in the references [7, 12]. The rotational stiffness at the supports increases  $\Omega_n$ , and this effect can be seen to be more in the first mode than in the second.

With  $\bar{k}_r = 0$ , the composite modal loss factor,  $\eta$  is observed to be independent of the mode as in the case of a beam [43]. But this is not so when  $\bar{k}_r \neq 0$ . Figure 2.11 shows that  $\eta$  increases nonlinearly with  $\delta_1/\delta_2$  and the rate of increase is very sharp for  $\delta_1/\delta_2 > 1$ . For a given value of  $\delta_1/\delta_2$ ,  $\eta$  is less with  $\bar{k}_r = 2$  than that with  $\bar{k}_r = 0$  in both the modes. However, this difference is significant only in the first mode.

Figures 2.12 - 2.14 show the results when supports prevent only the radial displacement. In such cases with  $\bar{k}_r = 0$ , the first mode is a rigid body rotation with both frequency and the loss factor as zero. For a given value of  $\delta_1/\delta_2$ , the computed results show very little effect of  $\beta$  on  $\Omega_n$ . Figure 2.12 indicates that  $\Omega_n$  decreases (essentially for all values of  $\beta$ ) with  $\delta_1/\delta_2$ . Unlike in the third mode, the decrease is nearly linear in the first two modes. The effect of  $k_r$  is seen to be more in the first and the third modes as compared to that in the second.

Variations of  $\eta$  in the first mode are shown in Figure 2.13, and for the second and third in Figure 2.14. In all the three modes  $\eta$  steadily increases with

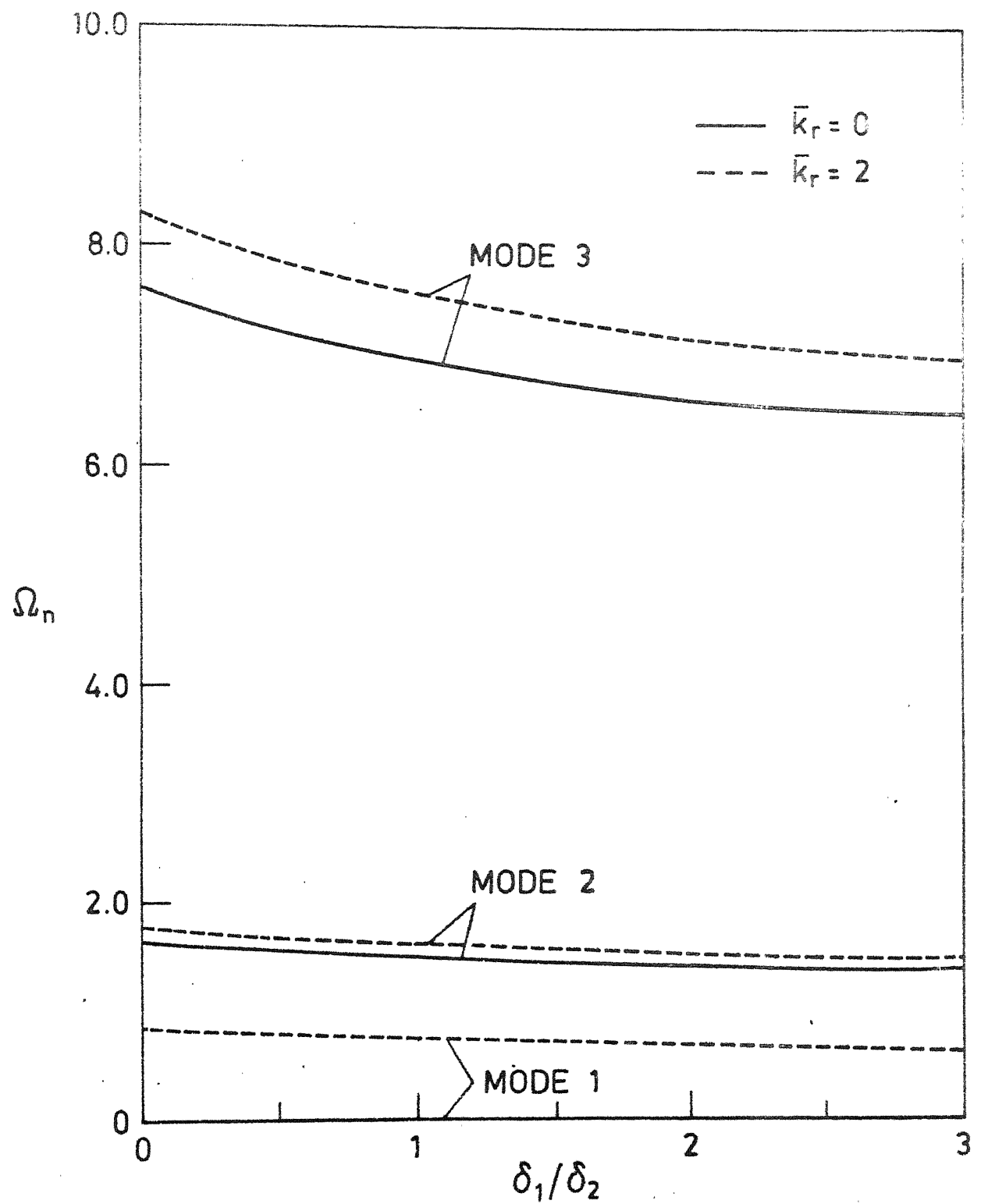


FIG. 2.12. VARIATION OF RESONANT FREQUENCY WITH THICKNESS RATIO: BI-COUPLED SYSTEM.

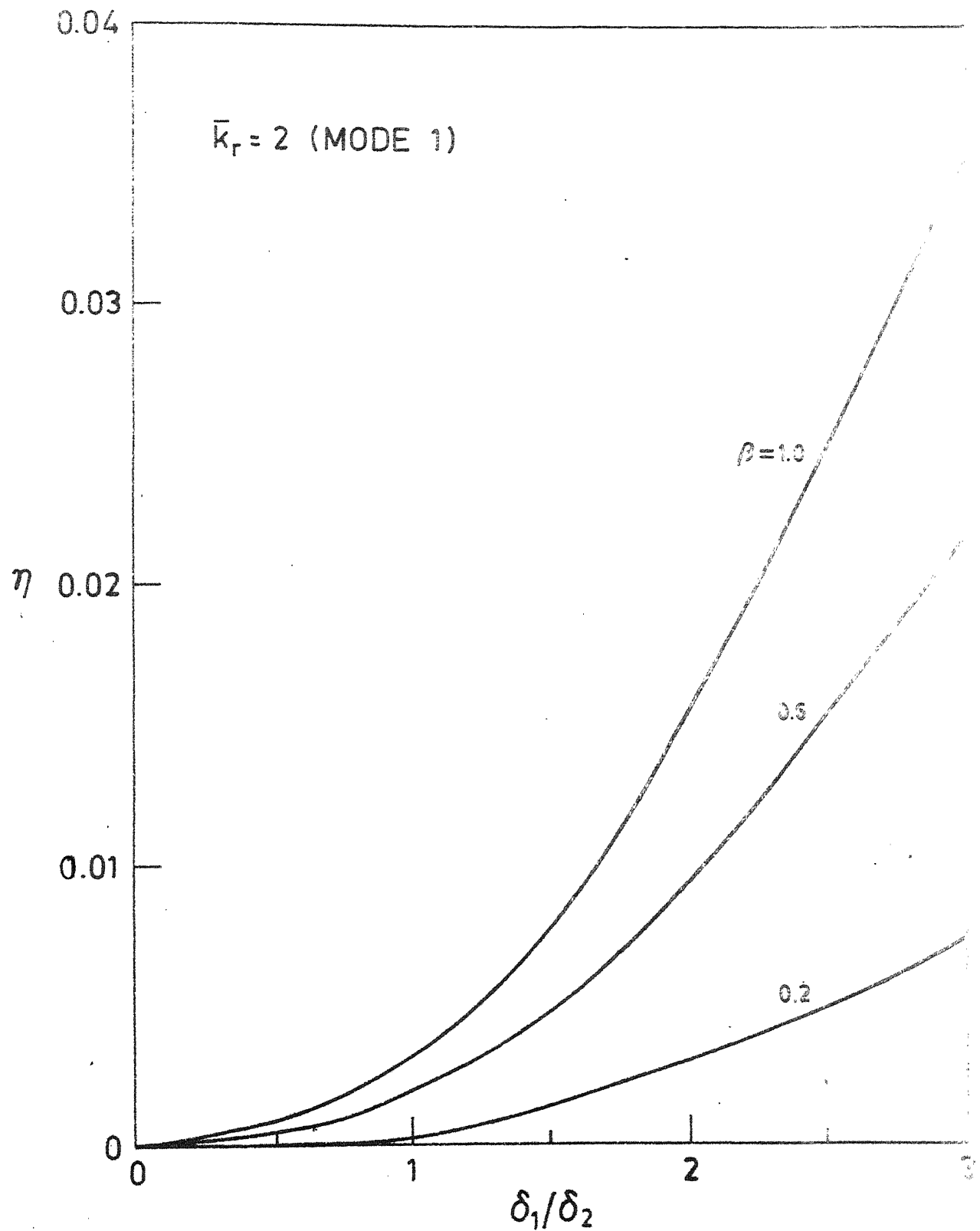


FIG. 2.13. VARIATION OF MODAL LOSS FACTOR WITH THICKNESS RATIO: BI-COUPLED SYSTEM.

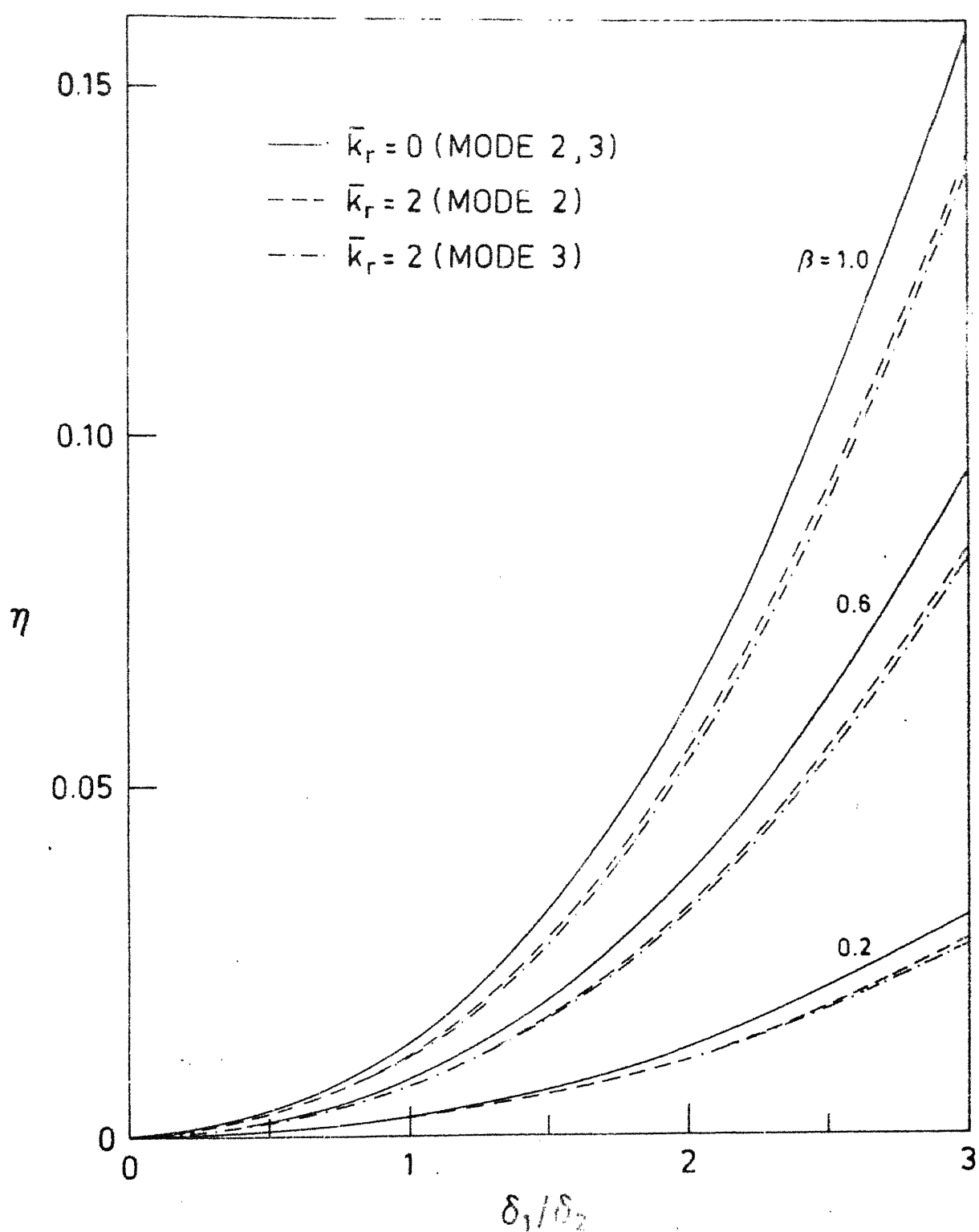


FIG. 2.14. VARIATION OF MODAL LOSS FACTOR WITH THICKNESS RATIO : BI-COUPLED SYSTEM .

$\delta_1/\delta_2$  and the rate of increase is very high for  $\delta_1/\delta_2 > 1$ . Loss factors in the first mode (with  $\bar{k}_r = 2$ ) are seen to be rather low. This is because in this mode the bending deformation in the ring is caused only by the presence of rotational constraint at the supports. When  $\bar{k}_r = 0$ ,  $\eta$  remains same in the second and third mode, whereas with  $\bar{k}_r = 2$ , it is less in the third mode as compared to that in the second mode. Comparing Figs. 2.11 and 2.14, it may be noted that with  $\bar{k}_r = 0$ , the modal loss factor in flexure is same with the first two types of support conditions.

Effects of  $\delta_1/\delta_2$  on the resonant frequencies ( $\Omega_n$ ) with the third type of supports are not shown. It was observed that upto the third mode, the natures of variation remained same as that for radially rigid supports (Fig. 2.12). Figure 2.15 shows that, unlike in the earlier cases with  $\bar{k}_r = 0$ ,  $\eta$  is not independent of mode if the supports have radial flexibility. It is more in the third mode than in the second. The presence of rotational stiffness at the supports decreases the loss factor marginally in both the modes for this case as well. With  $\bar{k}_r = 2$ , the loss factor is very small in the first mode for the reasons already explained in connection with bi-coupled system.

CENTRAL LIBRARY

Acc. No. A.....82705

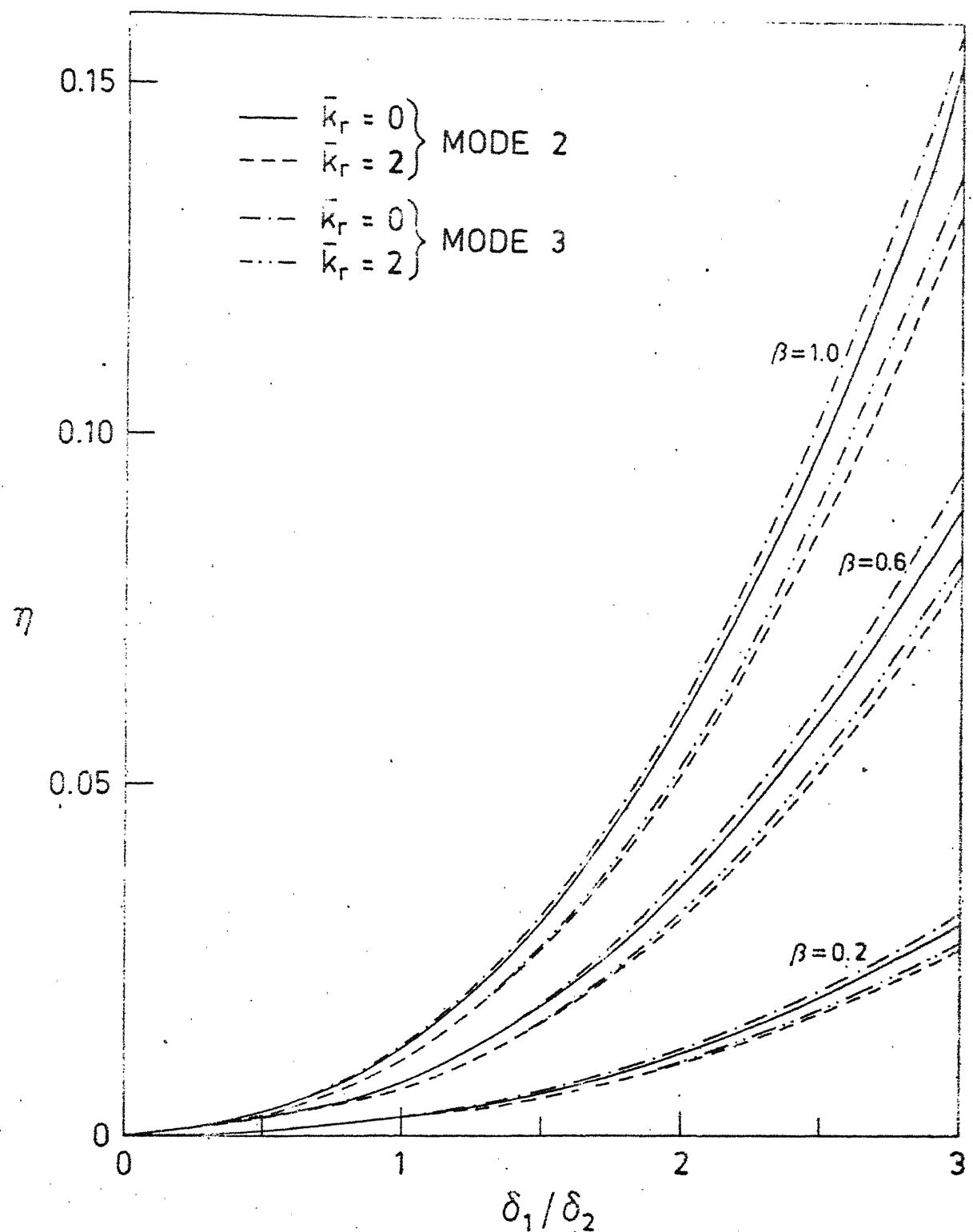


FIG. 2.15. VARIATION OF MODAL LOSS FACTOR WITH THICKNESS RATIO : TRI-COUPLED SYSTEM,  
 $\bar{k}_t = 180$ .

## CHAPTER 3

### FREE VIBRATION OF A THREE LAYERED RING

#### 3.1 INTRODUCTION

With the increased need of highly damped structures, it became necessary to augment the damping capacity of the structure with the addition of viscoelastic layers. In particular, a constrained damping layer is effective for this purpose. A constrained layer is one in which viscoelastic material adhering to the vibrating surface has a stiff elastic layer on the top. This configuration with a soft damping core is also referred to as a sandwich structure. The dissipation of energy in these structures is primarily due to the shear strain in the core.

In this chapter, free vibration of a three layered ring on periodic radial supports is investigated. The methodology, presentation and the parametric study follow similar lines as those presented in the previous chapter. The following two types of support conditions are considered in the case of a three layered ring.

- i) Supports preventing both the radial and tangential displacements.
- ii) Supports preventing only the radial displacement.

### 3.2 EQUATIONS OF MOTION

The following assumptions are made in deriving the differential equations and boundary conditions:

- i) radial displacement remains constant along a particular radial line;
- ii) a plane cross section remains plane after deformation;
- iii) there is no slip at the interfaces of the layers;
- iv) extensional deformation in the middle layer is negligible compared to those in the other layers.

Figure 3.1a shows a three layered ring on  $N$  equi-spaced radial supports which offer rotational restraint at the mid-plane of the base layer (layer 3). The rotational stiffness at the supports is represented by  $k_r$ .

The total strain energy,  $\Pi$ , of a single bay (Fig. 3.1b) of a three layered ring consists of individual bending and extensional strain energies of layers 1 and 3, shear strain energy of layer 2 and the strain energy of the springs at the supports. Using strain energy expression for a single layer ring element (see equation (A.6)),  $\Pi$ , can be written as

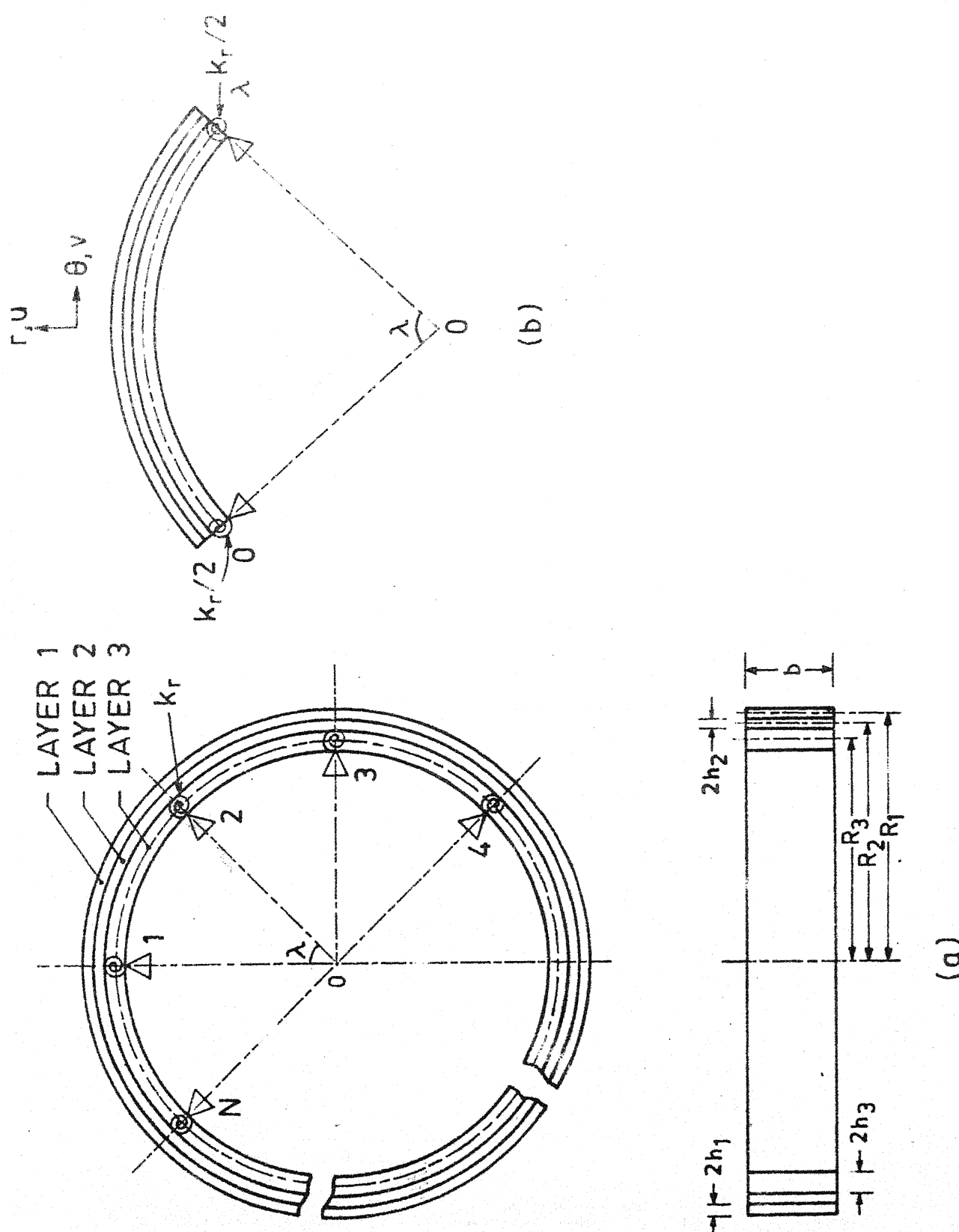


FIG. 3.1. THREE LAYERED RING ON EQUI-SPACED RADIAL SUPPORTS.

$$\begin{aligned}
 W = & \frac{K_1}{2} \int_0^\lambda (u + \frac{\partial v_1}{\partial \theta})^2 d\theta + \frac{K_3}{2} \int_0^\lambda (u + \frac{\partial v_3}{\partial \theta})^2 d\theta \\
 & + \frac{(D_1 + D_3)}{2} \int_0^\lambda (u + \frac{\partial^2 u}{\partial \theta^2})^2 d\theta + \frac{G_2 H_2 R_2 b}{2} \int_0^\lambda \psi^2 d\theta \\
 & + \frac{1}{2} \frac{k_r}{R_3} \left[ \frac{1}{R_3} \left( \frac{\partial u}{\partial \theta} - v_3 \right) \right]_0^2 \\
 & + \frac{1}{2} \frac{k_r}{R_3} \left[ \frac{1}{R_3} \left( \frac{\partial u}{\partial \theta} - v_3 \right) \right]_{\theta=\lambda}^2 \quad (3.1)
 \end{aligned}$$

where  $u$  is the radial displacement,  $v_j$  is the tangential displacement of the mid-plane,  $K_j$  ( $= \frac{E_j A_j}{R_j}$ ) is the extensional stiffness over a length  $R_j$ ,  $D_j$  ( $= \frac{2}{3} E_j b \delta_j^3$ ) is the bending stiffness.  $E_j$  is the Young's modulus,  $A_j$  is the area of cross section,  $R_j$  is the radius of the midplane,  $\delta_j$  ( $= \frac{h_j}{R_j}$ ) is the non-dimensional half thickness,  $b$  is the width of the ring,  $h_j$  is the half thickness,  $G$  is the shear modulus of layer 2 and  $\psi$  is the shear strain in layer 2 with subscript  $j$  referring to the  $j^{th}$  layer.

Using the assumption (iii), shear strain,  $\psi$  can be expressed in terms of displacements as follows:

$$2 h_2 \psi = v_1 d_1 - v_3 d_3 + \frac{\partial u}{\partial \theta} d_2 \quad (3.2)$$

where  $d_1 = 1 - \delta_1$ ,  $d_2 = \delta_1 + 2 \delta_2 + \delta_3$  and  
 $d_3 = 1 + \delta_3$ .

The kinetic energy of a single bay,  $T$ , can be written as

$$T = \frac{(m_1 + m_2 + m_3)}{2} \int_0^\lambda \left( \frac{\partial u}{\partial t} \right)^2 d\theta + \frac{m_1}{2} \int_0^\lambda \left( \frac{\partial v_1}{\partial t} \right)^2 d\theta \\ + \frac{m_2}{2} \int_0^\lambda \left( \frac{\partial v_2}{\partial t} \right)^2 d\theta + \frac{m_3}{2} \int_0^\lambda \left( \frac{\partial v_3}{\partial t} \right)^2 d\theta \quad (3.3)$$

where  $m_j = (2 b h_j \rho_j R_j)$  is the mass of the  $j^{\text{th}}$  layer over a length  $R_j$  with  $\rho_j$  as the density of the material of that layer.

The mid-plane tangential displacement of layer 2,  $v_2$ , can be expressed in terms of  $u$ ,  $v_1$  and  $v_3$  as

$$v_2 = \frac{1}{2} [v_1 d_1 + v_3 d_3 + \frac{\partial u}{\partial \theta} d_4] \text{ where } d_4 = \delta_1 - \delta_3 \quad (3.4)$$

By substituting (3.2) and (3.4) in (3.1) and (3.3), and setting the variation of Hamiltonian ( $T - H$ ) equal to zero, the differential equations and the boundary conditions are obtained as

$$D(u + 2 \frac{\partial^2 u}{\partial \theta^2} + \frac{\partial^4 u}{\partial \theta^4}) + K_1(u + \frac{\partial v_1}{\partial \theta}) + K_3(u + \frac{\partial v_3}{\partial \theta}) \\ - g d_2 (\frac{\partial v_1}{\partial \theta} d_1 - \frac{\partial v_3}{\partial \theta} d_3 + \frac{\partial^2 u}{\partial \theta^2} d_2) + m \frac{\partial^2 u}{\partial t^2} \\ - \frac{m_2 d_4}{2} (\frac{\partial^3 v_1}{\partial \theta \partial t^2} d_1 + \frac{\partial^3 v_3}{\partial \theta \partial t^2} d_3 + \frac{\partial^4 u}{\partial \theta^2 \partial t^2} d_4) = 0 \quad (3.5a)$$

$$K_1 (\frac{\partial u}{\partial \theta} + \frac{\partial^2 v_1}{\partial \theta^2}) - g d_1 (v_1 d_1 - v_3 d_3 + \frac{\partial u}{\partial \theta} d_2) \\ - m_1 \frac{\partial^2 v_1}{\partial t^2} - \frac{m_2}{2} d_1 (\frac{\partial^2 v_1}{\partial t^2} d_1 + \frac{\partial^2 v_3}{\partial t^2} d_3 + \frac{\partial^3 u}{\partial \theta \partial t^2} d_4) = 0 \quad (3.5b)$$

$$\begin{aligned} K_3 \left( \frac{\partial u}{\partial \theta} + \frac{\partial^2 v_3}{\partial \theta^2} \right) + g d_3 (v_1 d_1 - v_3 d_3 + \frac{\partial u}{\partial \theta} d_2) \\ - m_3 \frac{\partial^2 v_3}{\partial t^2} - \frac{m_2}{2} d_3 \left( \frac{\partial^2 v_1}{\partial t^2} d_1 + \frac{\partial^2 v_3}{\partial t^2} d_3 + \frac{\partial^3 u}{\partial \theta \partial t^2} d_4 \right) = 0 \end{aligned} \quad (3.5c)$$

$$- [D (u + \frac{\partial^2 u}{\partial \theta^2})] \delta(\frac{\partial u}{\partial \theta}) \Big|_{\theta=0} - \frac{1}{2} \frac{k_r}{R_3^2} \{ [(\frac{\partial u}{\partial \theta} - v_3) \delta(\frac{\partial u}{\partial \theta})] \Big|_{\theta=\lambda}$$

$$+ [(\frac{\partial u}{\partial \theta} - v_3) \delta(\frac{\partial u}{\partial \theta})] \Big|_{\theta=\lambda} = 0 \quad (3.6a)$$

$$- K_1 [ (u + \frac{\partial v_1}{\partial \theta}) \delta(v_1) ] \Big|_{\theta=0} = 0 \quad (3.6b)$$

$$- K_3 [ (u + \frac{\partial v_3}{\partial \theta}) \delta(v_3) ] \Big|_{\theta=0} + \frac{1}{2} \frac{k_r}{R_3^2} \{ [(\frac{\partial u}{\partial \theta} - v_3) \delta(v_3)] \Big|_{\theta=0} = 0$$

$$+ [(\frac{\partial u}{\partial \theta} - v_3) \delta(v_3)] \Big|_{\theta=\lambda} = 0 \quad (3.6c)$$

$$\{ [D (\frac{\partial u}{\partial \theta} + \frac{\partial^3 u}{\partial \theta^3}) - g d_2 (v_1 d_1 - v_3 d_3 + \frac{\partial u}{\partial \theta} d_2) \\ - \frac{m_2}{2} d_4 (\frac{\partial^2 v_1}{\partial t^2} d_1 + \frac{\partial^2 v_3}{\partial t^2} d_3 + \frac{\partial^3 u}{\partial \theta \partial t^2} d_4)] \delta(u) \} \Big|_{\theta=0} = 0$$

(3.6d)

$$\text{where } m = m_1 + m_2 + m_3 \text{ and } g = \frac{G b}{2 \delta_2}.$$

The differential equations (3.5) are different from the ones given in reference [18], as the tangential inertia of the core is also included in the present work.

From the boundary conditions (3.6a) - (3.6d), harmonic amplitudes of the generalized coupling forces (at either ends of a bay) of the periodic element corresponding to the coupling co-ordinates  $\frac{\partial u}{\partial \theta}$ ,  $v_1$ ,  $v_3$  and  $u$

can be identified as

$$\bar{Q}_{10} = [ - D (U + \frac{d^2 U}{d\theta^2}) + \frac{k_r}{2 R_3^2} (\frac{dU}{d\theta} - V_3) ] \Big|_{\theta=0} \quad (3.7a)$$

$$\bar{Q}_{1\lambda} = [ - D (U + \frac{d^2 U}{d\theta^2}) - \frac{k_r}{2 R_3^2} (\frac{dU}{d\theta} - V_3) ] \Big|_{\theta=\lambda} \quad (3.7b)$$

$$\bar{Q}_{20} = [ - K_1 (U + \frac{d V_1}{d\theta}) ] \Big|_{\theta=0} \quad (3.7c)$$

$$\bar{Q}_{2\lambda} = [ - K_1 (U + \frac{d V_1}{d\theta}) ] \Big|_{\theta=\lambda} \quad (3.7d)$$

$$\bar{Q}_{30} = [ - K_3 (U + \frac{d V_3}{d\theta}) - \frac{k_r}{2 R_3^2} (\frac{dU}{d\theta} - V_3) ] \Big|_{\theta=0} \quad (3.7e)$$

$$\bar{Q}_{3\lambda} = [ - K_3 (U + \frac{d V_3}{d\theta}) + \frac{k_r}{2 R_3^2} (\frac{dU}{d\theta} - V_3) ] \Big|_{\theta=\lambda} \quad (3.7f)$$

$$\begin{aligned} \bar{Q}_{40} = & [ D (\frac{dU}{d\theta} + \frac{d^3 U}{d\theta^3}) - g d_2 (V_1 d_1 - V_3 d_3 + \frac{dU}{d\theta} d_2) \\ & + \frac{m_2}{2} \omega^2 d_4 (V_1 d_1 + V_3 d_3 + \frac{dU}{d\theta} d_4) ] \Big|_{\theta=0} \end{aligned} \quad (3.7g)$$

$$\begin{aligned} \bar{Q}_{4\lambda} = & [ D (\frac{dU}{d\theta} + \frac{d^3 U}{d\theta^3}) - g d_2 (V_1 d_1 - V_3 d_3 + \frac{dU}{d\theta} d_2) \\ & + \frac{m_2}{2} \omega^2 d_4 (V_1 d_1 + V_3 d_3 + \frac{dU}{d\theta} d_4) ] \Big|_{\theta=\lambda} \end{aligned} \quad (3.7h)$$

where  $Q_{j0} = \bar{Q}_{j0} e^{i\omega t}$ ,  $Q_{j\lambda} = \bar{Q}_{j\lambda} e^{i\omega t}$ , ( $j = 1, 2, 3, 4$ ),

$$u = U e^{i\omega t}, \quad v_1 = V_1 e^{i\omega t} \text{ and } v_3 = V_3 e^{i\omega t}$$

It may be noted that the maximum number of coupling co-ordinates for the three layered ring is four.

### 3.3 NATURAL FREQUENCIES OF AN ELASTIC RING

Considering all the three layers of the ring to be elastic, the theory of wave propagation described in section 2.4.1 is used to find the natural frequencies of the structure on different types of supports.

For the first type of support conditions, unlike in the two layered ring, the coupling co-ordinates at the supports are two (i.e.,  $q_1 = \partial u / \partial \theta$ ;  $q_2 = v_1$ ) and the system is bi-coupled. The amplitudes of the associated harmonic coupling forces are given by (3.7a) - (3.7d). The propagation constant curves for this system are obtained by the receptance method discussed in Chapter 2. The receptance relations are also same as the ones given for the bi-coupled system in Appendix B (see equation B.2). Hence, equations (B.10) and (B.11) can be used to compute the propagation constant ( $\mu$ ) for a given number of bays ( $N$ ). From the propagation constant curves,  $\Omega_n (= \omega_n \sqrt{m_3/D_3})$ , natural frequencies, can be obtained by using (2.7).

When the supports are considered to prevent only the radial displacement, the ring becomes a tri-coupled system with coupling co-ordinates  $q_1 = \partial u / \partial \theta$ ,  $q_2 = v_1$  and  $q_3 = v_3$ . For this system, the amplitudes of the associated harmonic coupling forces are given by (3.7a) - (3.7f). Then, the natural frequencies can be obtained by the same procedure used for the bi-coupled system. The equations necessary for the receptance method are

different from the ones given for the tri-coupled system of two layer ring and these are given separately in Appendix D.

### 3.4 RESONANT FREQUENCIES AND LOSS FACTORS OF A DAMPED RING

Unlike in section 3.3, here, the core (middle layer) is considered to be viscoelastic with a loss factor,  $\beta$  : i.e., its shear modulus becomes complex, and is of the form  $G^* = G(1 + i\beta)$ . Then, the ring becomes a damped structure. To find the resonant frequencies ( $\Omega_n$ ) and loss factors ( $\eta$ ) of the composite structure, the theory of forced damped normal modes explained in section 2.5, is used.

Assuming harmonic variation for the displacements,  $u$ ,  $v_1$  and  $v_3$ , and replacing  $\omega^2$  by  $\omega^{*2}$  ( $= \omega^2(1 + i\eta)$ ), (3.5) can be rewritten for the damped ring as follows:

$$L_1 U + L_2 V_1 + L_3 V_3 = 0 \quad (3.8a)$$

$$L_2 U + L_4 V_1 + L_5 V_3 = 0 \quad (3.8b)$$

$$L_3 U + L_5 V_1 + L_6 V_3 = 0 \quad (3.8c)$$

In the above equations,

$$L_1 = I_1 \frac{d^4}{d\theta^4} + I_2 \frac{d^2}{d\theta^2} + I_3$$

$$L_2 = I_4 \frac{d}{d\theta}$$

$$L_3 = I_5 \frac{d}{d\theta}$$

$$L_4 = I_6 \frac{d^2}{d\theta^2} + I_7$$

$$L_5 = I_8$$

$$L_6 = I_9 \frac{d^2}{d\theta^2} + I_{10}$$

where  $I$ 's are defined by (E.1) in Appendix E.

To compute the resonant frequencies and the associated modal loss factors, the general solution of (3.8) can be written in the form

$$\bar{U}(\theta) = \sum_{j=1}^8 C_j e^{s_j \theta}; \quad \bar{V}_1(\theta) = \sum_{j=1}^8 B_j e^{s_j \theta};$$

$$\bar{V}_3(\theta) = \sum_{j=1}^8 \bar{B}_j e^{s_j \theta} \quad (3.9)$$

The  $s_j$ 's are the eight roots of the auxiliary equation

$$s^8 + a_1 s^6 + a_2 s^4 + a_3 s^2 + a_4 = 0 \quad (3.10)$$

where  $a_1, a_2, a_3$  and  $a_4$  are defined by (E.2) in Appendix E.

### 3.4.1 Different Support Conditions

For the first type of supports (bi-coupled system), the following conditions are to be satisfied.

- i) The radial displacement,  $u$  is zero at  $\theta = 0$   
and at  $\theta = \lambda$  : i.e.,

$$\sum_{j=1}^8 C_j = 0 \quad (3.11a)$$

$$\text{and } \sum_{j=1}^8 C_j e^{s_j \lambda} = 0 \quad (3.11b)$$

- ii) The tangential displacement of base layer (layer 3),  $v_3$ , is zero at  $\theta = 0$  and at  $\theta = \lambda$ : i.e.,

$$\sum_{j=1}^8 C_j \bar{T}_j = 0 \quad (3.11c)$$

$$\text{and } \sum_{j=1}^8 C_j \bar{T}_j e^{s_j \lambda} = 0 \quad (3.11d)$$

where  $\bar{T}_j = \bar{B}_j/C_j$  and the expression for it is given by (E.3).

- iii) The coupling co-ordinate,  $\partial u/\partial\theta$ , and the associated coupling force,  $Q_1$ , must satisfy the wave condition: i.e.,

$$e^{i\mu_{in}} \left. \frac{\partial u}{\partial \theta} \right|_{\theta=0} = \left. \frac{\partial u}{\partial \theta} \right|_{\theta=\lambda}, \text{ or } \sum_{j=1}^8 C_j s_j (e^{i\mu_{in}} - e^{s_j \lambda}) = 0 \quad (3.11e)$$

and

$$\begin{aligned} e^{i\mu_{in}} Q_{10} &= Q_{1\lambda}, \text{ or } \sum_{j=1}^8 C_j \\ &\quad \left[ -\frac{D}{D_3} s_j^2 (e^{i\mu_{in}} - e^{s_j \lambda}) \right. \\ &\quad \left. + \bar{k}_r s_j e^{s_j \lambda} \right] = 0 \end{aligned} \quad (3.11f)$$

where  $\bar{k}_r = k_r/D_3 R_3^2$ .

iv) The coupling co-ordinate,  $v_1$ , and the associated coupling force,  $Q_2$ , must satisfy the wave condition: i.e.,

$$e^{i\mu_{in}} v_1(0) = v_1(\lambda), \text{ or } \sum_{j=1}^8 C_j T_j (e^{i\mu_{in}} - e^{s_j \lambda}) = 0 \quad (3.11g)$$

and

$$e^{i\mu_{in}} Q_{20} = Q_2 \lambda, \text{ or } \sum_{j=1}^8 C_j T_j s_j (e^{i\mu_{in}} - e^{s_j \lambda}) = 0 \quad (3.11h)$$

where  $T_j = B_j/C_j$  and the expression for it is given by (E.4).

Equation (3.11a) - (3.11h) are eight homogeneous equations in eight unknowns ( $C_j$ 's). For non-trivial solution of these unknowns, the coefficient determinant should vanish. Using (3.10) along with this condition, the resonant frequencies ( $\Omega_n$ ) and the associated modal loss factors ( $n$ ) of the composite structure can be determined. The computational procedure for this purpose is given in section 2.5.2 in connection with a damped two layered ring.

When the ring is considered to be tri-coupled, the conditions to be satisfied are as follows:

- i) The radial displacement,  $u$ , is zero at  $\theta = 0$  and at  $\theta = \lambda$ : i.e.,

$$\sum_{j=1}^8 c_j = 0 \quad (3.12a)$$

and

$$\sum_{j=1}^8 c_j e^{s_j \lambda} = 0 \quad (3.12b)$$

- ii) The coupling co-ordinate,  $\partial u / \partial \theta$ , and the coupling force,  $Q_1$ , must satisfy the wave condition, i.e.,

$$\sum_{j=1}^8 c_j s_j (e^{i\mu_{in}} - e^{s_j \lambda}) = 0 \quad (3.12c)$$

and

$$\sum_{j=1}^8 c_j \left[ -\frac{D}{D_3} s_j^2 (e^{i\mu_{in}} - e^{s_j \lambda}) + \bar{k}_r (s_j - \bar{T}_j) e^{s_j \lambda} \right] = 0 \quad (3.12d)$$

- iii) The coupling co-ordinate,  $v_1$ , and the coupling force,  $Q_2$ , must satisfy the wave condition: i.e.,

$$\sum_{j=1}^8 c_j T_j (e^{i\mu_{in}} - e^{s_j \lambda}) = 0 \quad (3.12e)$$

and

$$\sum_{j=1}^8 c_j T_j s_j (e^{i\mu_{in}} - e^{s_j \lambda}) = 0 \quad (3.12f)$$

- iv) The coupling co-ordinate,  $v_3$ , and the coupling force,  $Q_3$ , must satisfy the wave condition: i.e.,

$$e^{i\mu_{in}} v_3(0) = v_3(\lambda), \text{ or}$$

$$\sum_{j=1}^8 c_j \bar{T}_j (e^{i\mu_{in}} - e^{s_j \lambda}) = 0 \quad (3.12g)$$

and

$$e^{i\mu_{in}} Q_{30} = Q_3 \lambda, \text{ or}$$

$$\sum_{j=1}^8 c_j \left[ -\frac{K_3}{D_3} s_j \bar{T}_j (e^{i\mu_{in}} - e^{s_j \lambda}) - \bar{k}_r (s_j - \bar{T}_j) e^{s_j \lambda} \right] = 0 \quad (3.12h)$$

Again, equations (3.12a) - (3.12h) constitute a set of eight homogeneous equations for the tri-coupled system and hence, the resonant frequencies and the loss factors can be computed for this type of supports as well.

### 3.5 NATURAL MODES OF AN ELASTIC RING

With the numerical data considered for propagation curves, the number of pairs of propagating waves which give rise to natural modes is found to be only one. Hence, based on the analysis presented in section 2.6, natural modes of the composite elastic ring can be computed. Similar to the case of a two layered ring, the cases for which  $\mu_{in} \neq 0$  and  $\mu_{in} = 0$  are treated separately as the former leads to degenerate modes whereas the later gives rise to unique modes.

For  $\mu_{in} \neq 0$ , two modes (anti-symmetric and symmetric with respect to a diameter passing through a support) are obtained by prescribing a coupling force at the supports given by (2.19) and (2.20). With  $\mu_{in} = 0$ , an eigenvalue problem is considered which can

again be expressed finally in the form (2.25). The same iterative scheme described in section 2.6 is used to find the natural mode. Here, it is to be noted that the total number of support conditions ( $n_2$ ) are eight and {C} represents the vector of unknown constants given by the series (3.9).

### 3.6 RESULTS AND DISCUSSION

Numerical results are presented for the following data:

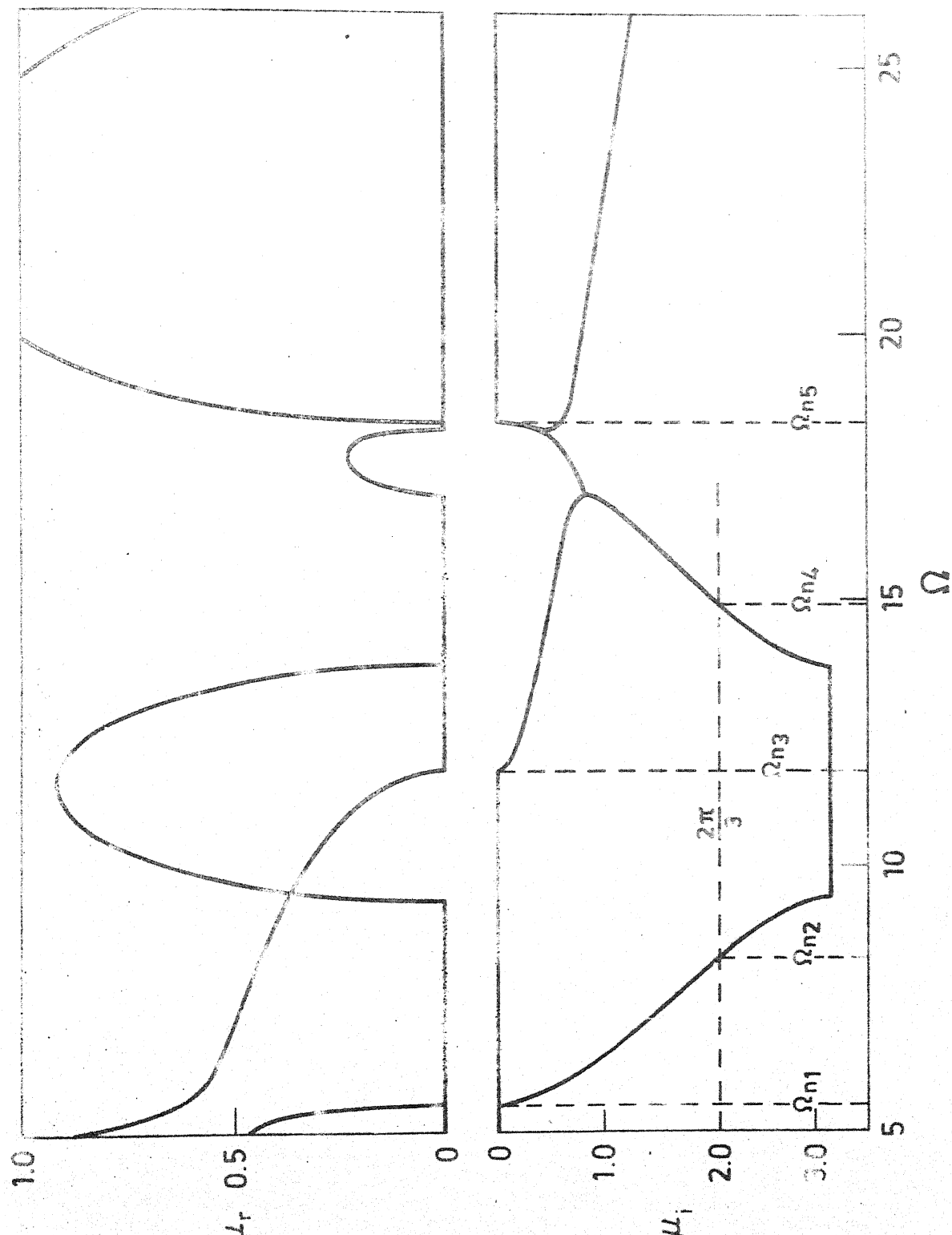
$$\rho_1/\rho_3 = 1.0, \quad \rho_2/\rho_3 = 0.2, \quad E_1/E_3 = 1.0,$$

$$\bar{k}_r = 0 \text{ and } 2, \quad G/E_3 = 0.0001, \quad N = 3 \text{ (i.e., } \lambda = 2\pi/3), \\ \beta = 1.0$$

#### 3.6.1 Elastic Core

Figures 3.2 and 3.3 show the propagation constant curves for the bi-coupled and the tri-coupled systems, respectively, with  $\delta_1 = 0.015$ ,  $\delta_2 = 0.03$  and  $\delta_3 = 0.03$ . Comparing Fig. 3.2 with 2.3, it can be immediately seen that natures of the curves are somewhat different. This difference arises due to the additional propagation constant. This propagation constant may be associated with the extra degree of freedom: i.e., the tangential displacement of the outer layer, (layer 1),  $v_1$ . By reducing the thickness of the core ( $\delta_2$ ) and consequently curtailing the degree of freedom  $v_1$ , it was found that this difference appears only at higher frequencies.

FIG. 3.2. VARIATION OF PROPAGATION CONSTANT WITH FREQUENCY  
BI-COUPLED SYSTEM,  $\bar{k}_r = 0$ .



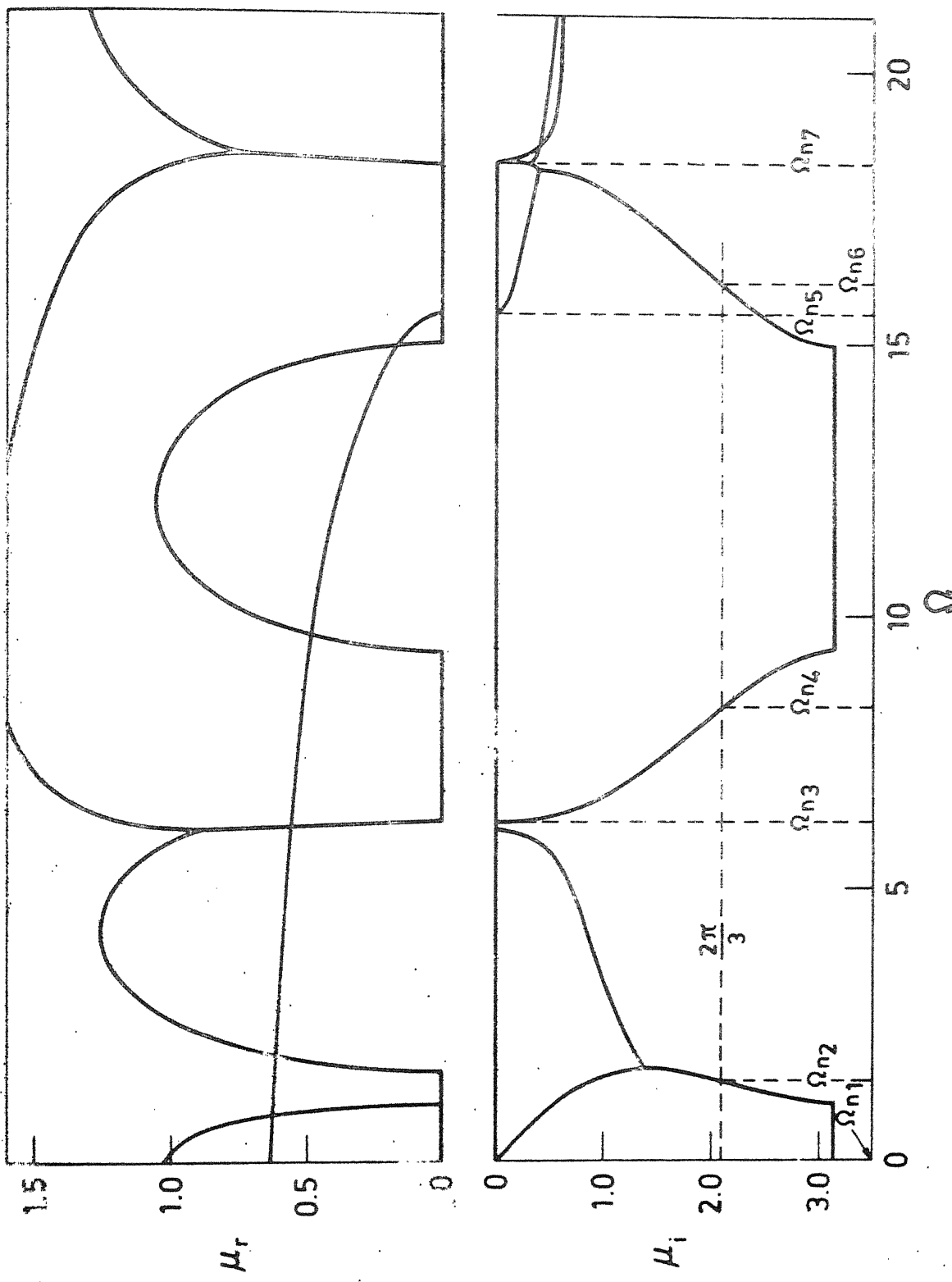


FIG. 3.3. VARIATION OF PROPAGATION CONSTANT WITH FREQUENCY  
TRI-COUPLED SYSTEM.  $\bar{k}_r = 0$ .

The data for Fig. 3.2 indicates a rather thick core and a low value of the shear modulus parameter ( $G/E_3$ ). Hence, under such conditions, a predominant tangential motion of the outer layer is expected. Thus the natural frequency obtained ( $\Omega_n = 11.768$ , third one in Fig. 3.2) due to the additional propagation constant is expected to be associated with the tangential motion. A confirmation to this effect can be had from the mode shapes or from comparison of various energies at this frequency, which are discussed later. However, the other natural frequencies (1, 2 and 4) do not exhibit any such characteristic. In Fig. 3.3 also, a similar argument applies and the mode at the fifth natural frequency,  $\Omega_n = 15.550$  can be said to be associated with predominant tangential motion of the outer layer. Hereafter, these modes are referred to as 'tangential' modes whereas the others are called 'flexural' modes.

The first two flexural and the first 'tangential' modes obtained at the frequencies indicated in Figs. 3.2 and 3.3 are shown in Figs. 3.4 - 3.7. Both the radial and the tangential displacements are included in these figures. Just as in the case of a two layered ring, here also if the radial displacement pattern in a mode is symmetric about a diameter passing through a support then the corresponding tangential displacement pattern is anti-symmetric about the same diameter and vice versa. Various strain energies of different layers

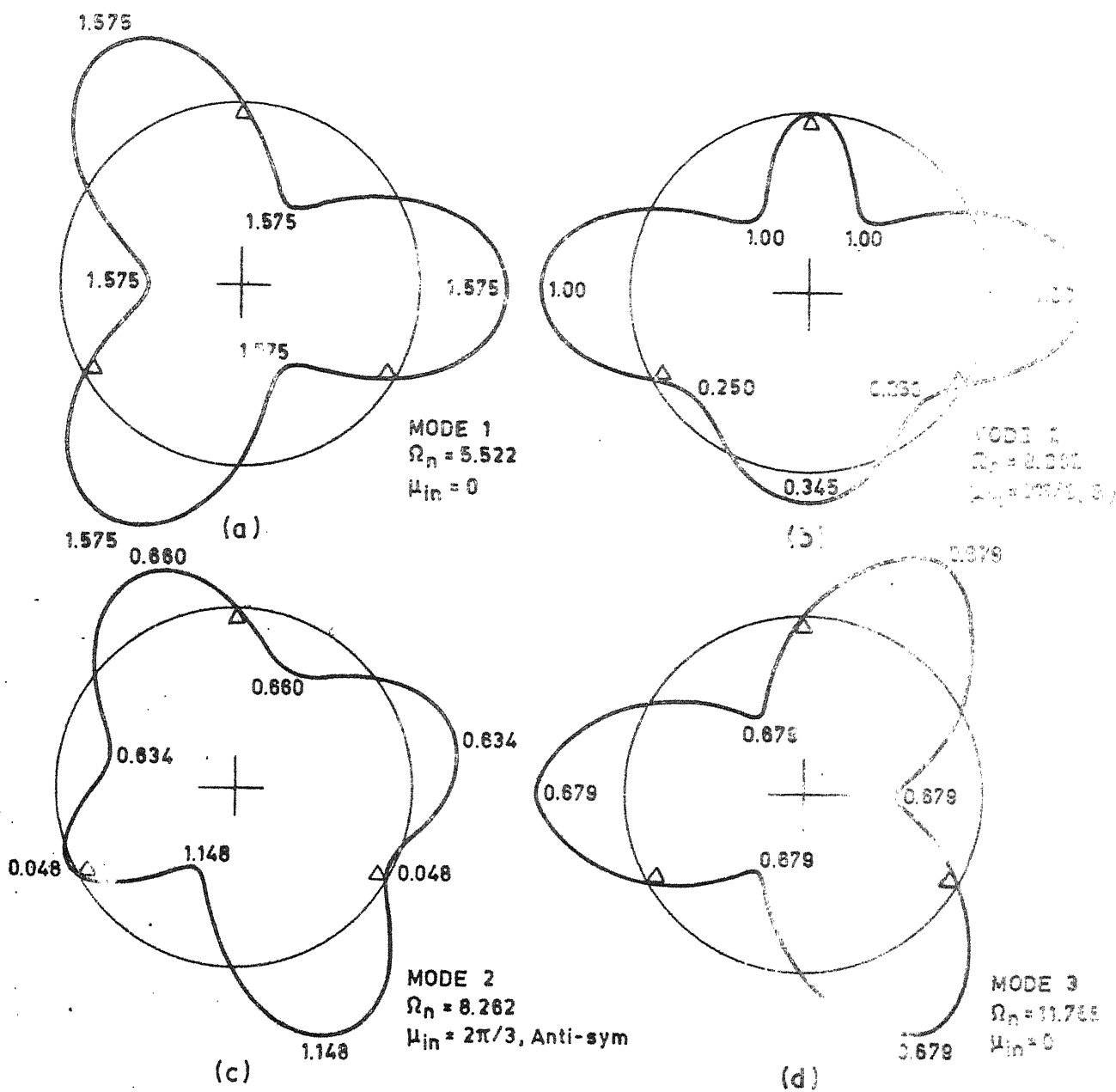


FIG. 3.4. MODE SHAPES ( $U$ ) OF THREE LAYERED RING: BI-COUPLED SYSTEM,  $k_r = 0$ .

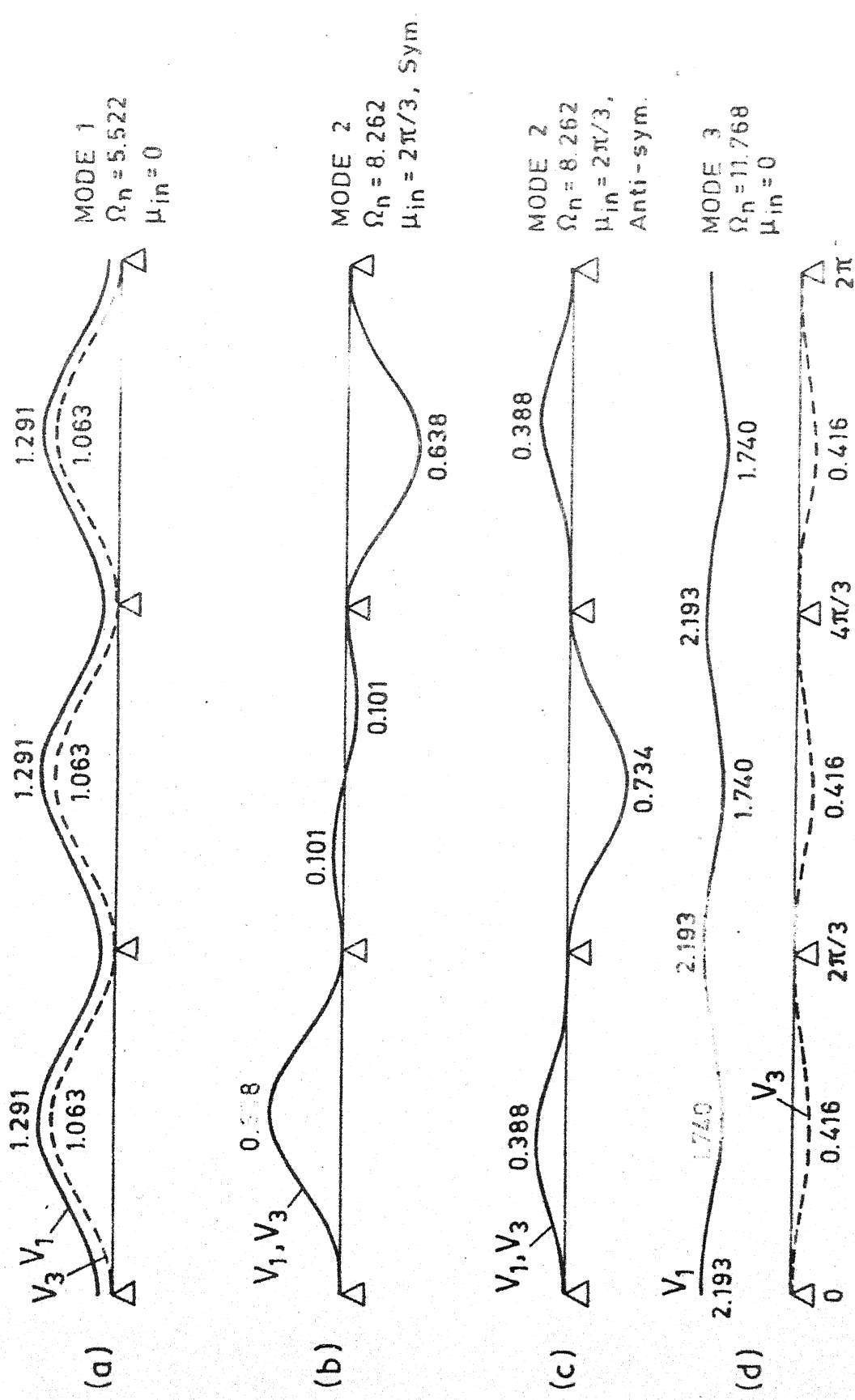


FIG. 3.5. MODE SHAPES ( $V_1$  &  $V_3$ ) OF THREE LAYERED RING : BI-COUPLED SYSTEM.  $\bar{k}_r = 0$ .

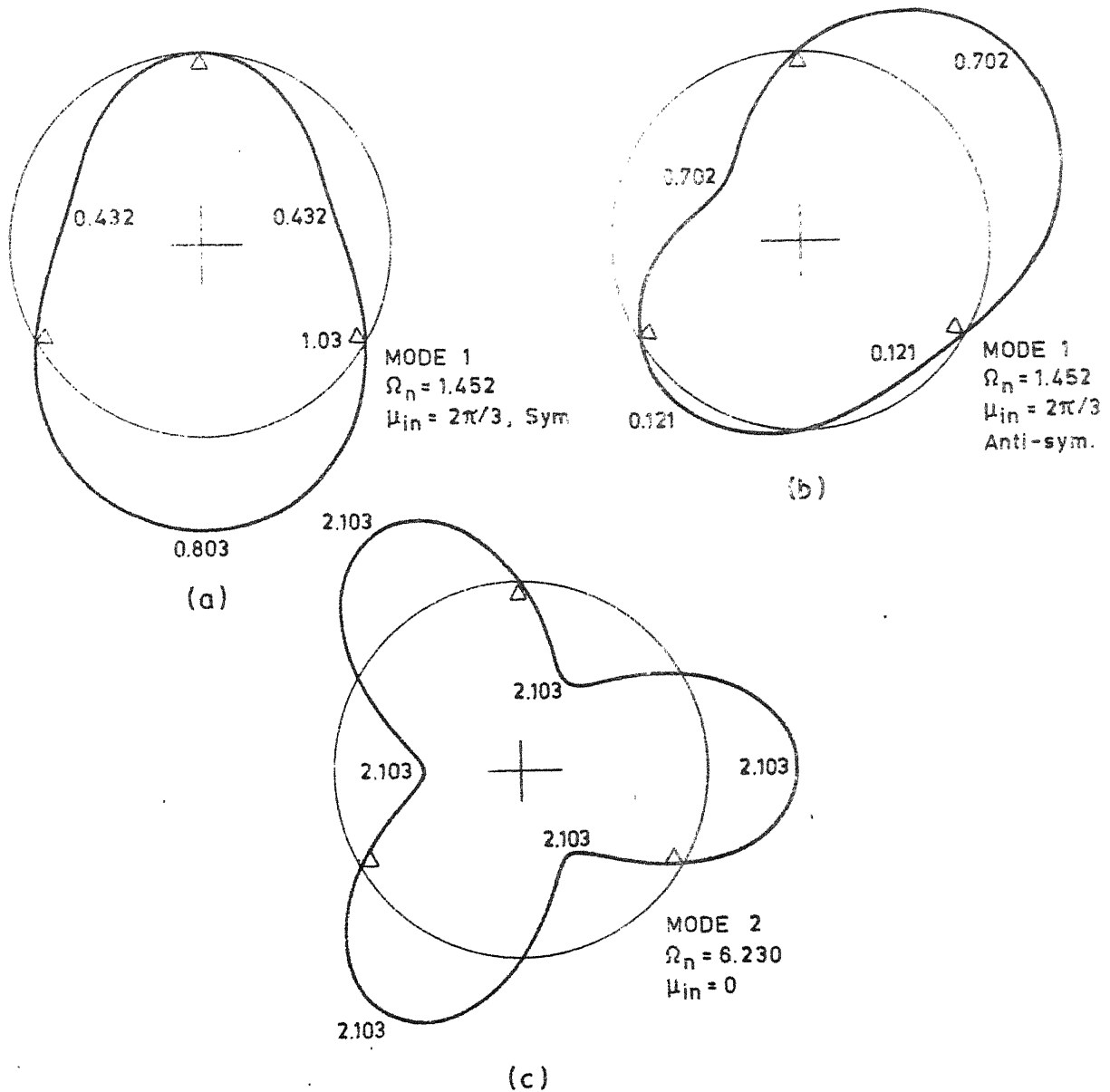
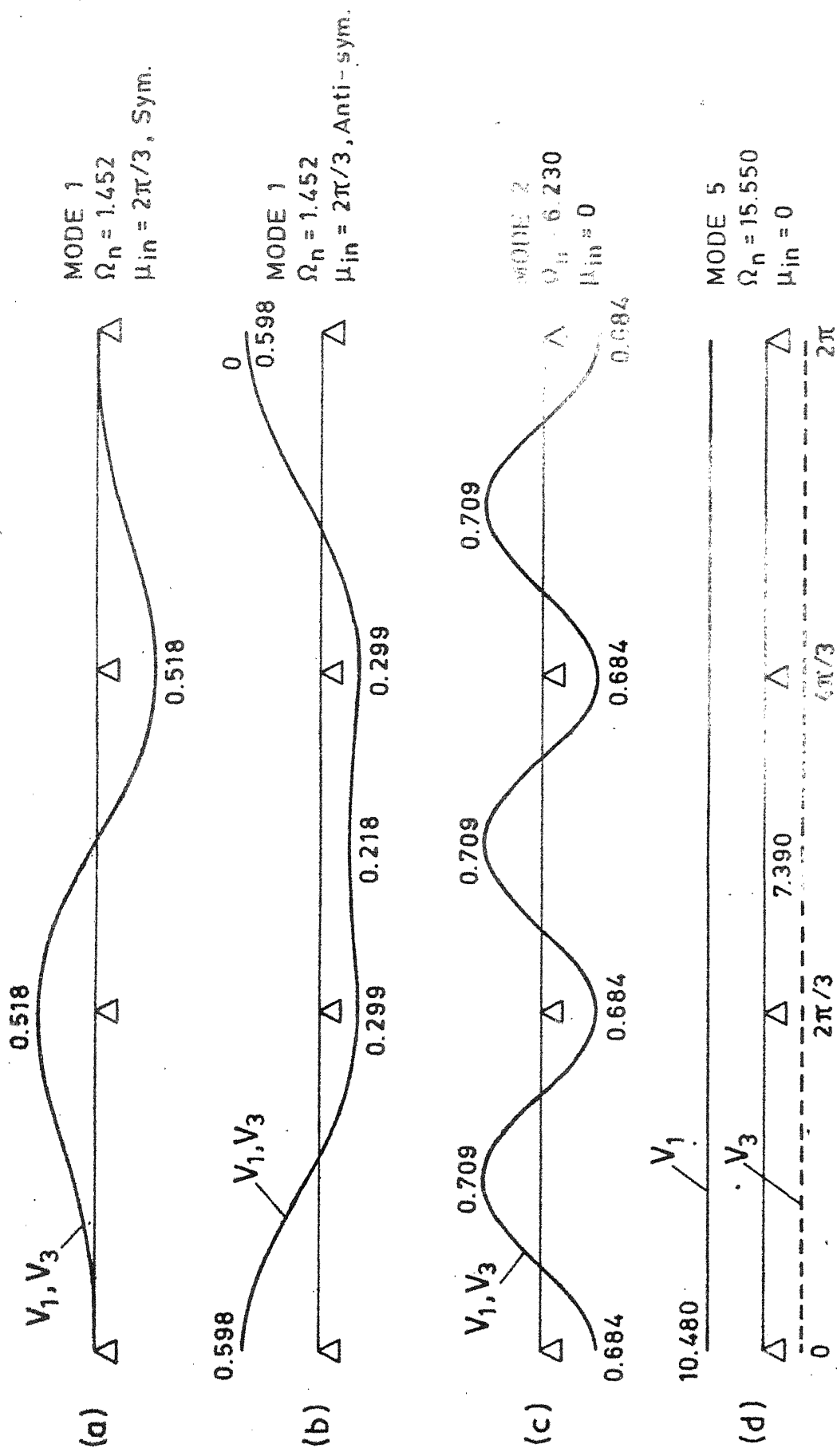


FIG. 3.6. MODE SHAPES ( $U$ ) OF THREE LAYERED RING, TRI-COUPLE SYSTEM,  $k_r = 0$

FIG. 3.7. MODE SHAPES ( $V_1$  &  $V_3$ ) OF THREE LAYERED RING: TRI-COUPLED SYSTEM,  $\bar{k}_r = 0$



in these modes are also computed. Ratios of these to the total bending strain energy are presented in Table 3.1. The flexural mode shapes are very similar to the corresponding ones obtained for a single layer ring in reference [7] and presented for a two layered ring in Figs. 2.6 - 2.9.

Comparing the relative magnitudes of the displacements, it is observed that the ratios of (radial/tangential) displacements in the flexural modes are of the order of 1.1 - 1.5. This is true for both bi-coupled and tri-coupled systems. On the other hand, these ratios in the tangential modes are approximately 0.3 for the bi-coupled system and exactly zero for the tri-coupled system. Further discussion on these tangential modes is presented for the two systems, separately.

For the bi-coupled system, the tangential mode is associated with small radial displacements. Moreover, this radial displacement pattern (Fig. 3.4d) is very similar to that of the nearest flexural mode having  $\mu_{in} = 0$  as the tangential mode also corresponds to zero phase difference. From Fig. 3.5d, it can be seen that the difference in tangential displacements ( $V_1 - V_3$ ) of this mode is independent of  $\theta$ .

For the tri-coupled system, however, the tangential mode is not associated with any radial displacement and both the displacements  $V_1$  and  $V_3$  remain

TABLE 3.1

NATURAL FREQUENCIES AND VARIOUS ENERGIES OF AN ELASTIC  
THREE LAYERED RING

$$\delta_1 = 0.015, \quad \delta_2 = \delta_3 = 0.03, \quad \bar{k}_r = 0,$$

$$G/E_3 = 0.0001, \quad \rho_1/\rho_3 = 1, \quad \rho_2/\rho_3 = 0.2, \quad N = 3$$

Mode No	Phase constant ( $\mu_{in}$ )	Natural frequency ( $\Omega_n$ )	Strain Energy/Total Bending Strain Energy		
			Extensional (Layer 1)	(Layer 3)	Shear (Layer 2)

(i) Bi-coupled system:

1	0	5.522	$3.36 \times 10^{-4}$	$4.74 \times 10^{-3}$	$1.57 \times 10^{-1}$
2	$2\pi/3$	8.262	$1.92 \times 10^{-3}$	$2.57 \times 10^{-3}$	$6.09 \times 10^{-2}$
3	0	11.768	$1.07 \times 10^{-3}$	$2.09 \times 10^{-1}$	$2.26 \times 10^{-1}$
4	$2\pi/3$	14.920	$7.02 \times 10^{-4}$	$3.91 \times 10^{-2}$	$4.26 \times 10^{-2}$

(ii) Tri-coupled system:

2	$2\pi/3$	1.452	$4.29 \times 10^{-3}$	$4.50 \times 10^{-3}$	$3.29 \times 10^{-1}$
3	0	6.230	$2.68 \times 10^{-4}$	$9.14 \times 10^{-4}$	$1.14 \times 10^{-1}$
4	$2\pi/3$	8.325	$1.42 \times 10^{-3}$	$2.84 \times 10^{-3}$	$6.19 \times 10^{-2}$
5	0	15.550	$\infty$	$\infty$	$\infty$

independent of  $\theta$  (Fig. 3.7d). It may be noted that the natural frequency and the relative magnitudes of  $V_1$  and  $V_3$  (i.e.,  $V_1/V_3$ ) of this mode can be verified by substituting the solution  $U = 0$ ,  $V_1 = B$  and  $V_3 = \bar{B}$ , ( $B$  and  $\bar{B}$  are constants) in the differential equations (3.8). Hence, this mode is nothing but a torsional oscillations of the ring about its centre in which layers 1 and 3 move in counterphase without any radial deformation anywhere. In other words, at this mode the system behaves like a torsional system consisting of two discs connected by a shaft.

For both the systems,  $v_1$  and  $v_3$  are out of phase giving rise to a large shear deformation in the core. As mentioned earlier, it can be seen from Table 3.1 that the shear strain energies in these modes are large compared to bending and extensional strain energies. Moreover, the table indicates that the third and the fourth natural frequencies in the tri-coupled system are comparable to the first and the second ones, respectively, in the bi-coupled system. The deformation pattern and the values of strain energies at the corresponding frequencies are also seen to be similar.

### 3.5.2 Viscoelastic Core

Figures 3.8 - 3.15 show the variations of resonant frequencies ( $\Omega_n$ ) and loss factors ( $\eta$ ) with base layer thickness ( $\delta_3$ ) for both the systems in the first

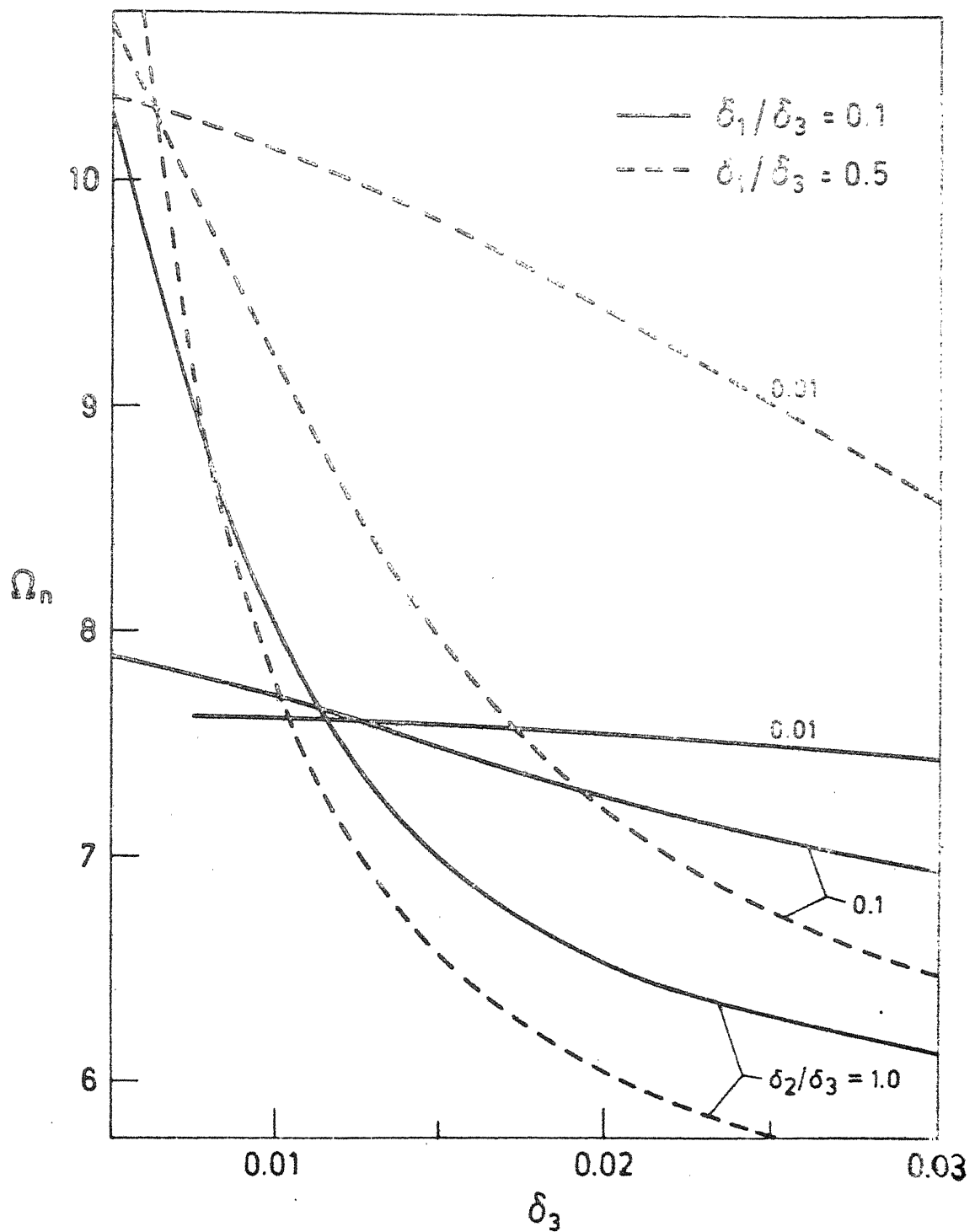


FIG. 3.8. VARIATION OF RESONANT FREQUENCY WITH BASE LAYER THICKNESS (MODE 1):  
BI-COUPLED SYSTEM,  $k_r = 0$ .

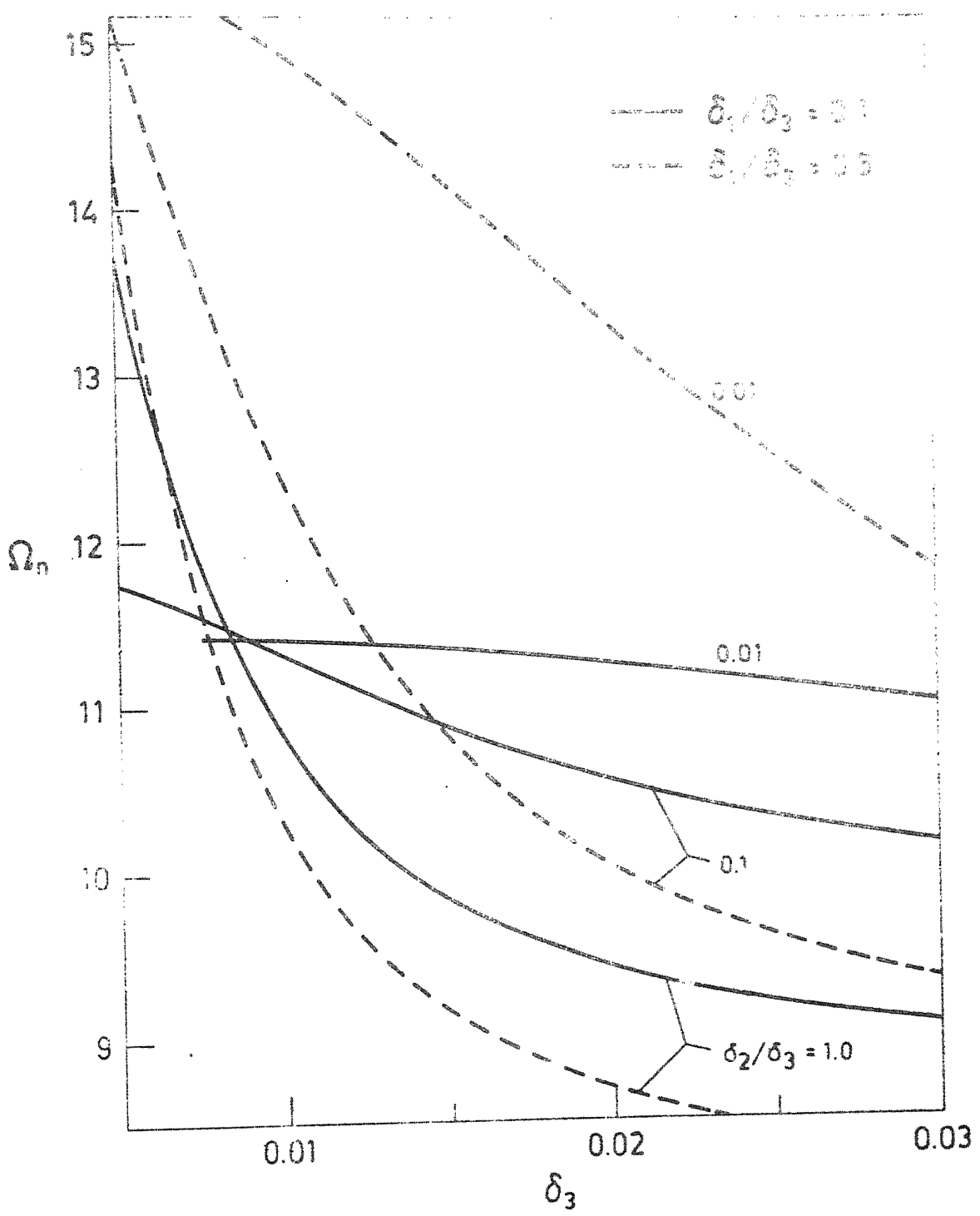


FIG. 3.9. VARIATION OF RESONANT FREQUENCY WITH BASE LAYER THICKNESS (MODE 2): BI-COUPLED SYSTEM,  
 $\bar{k}_r = 0$

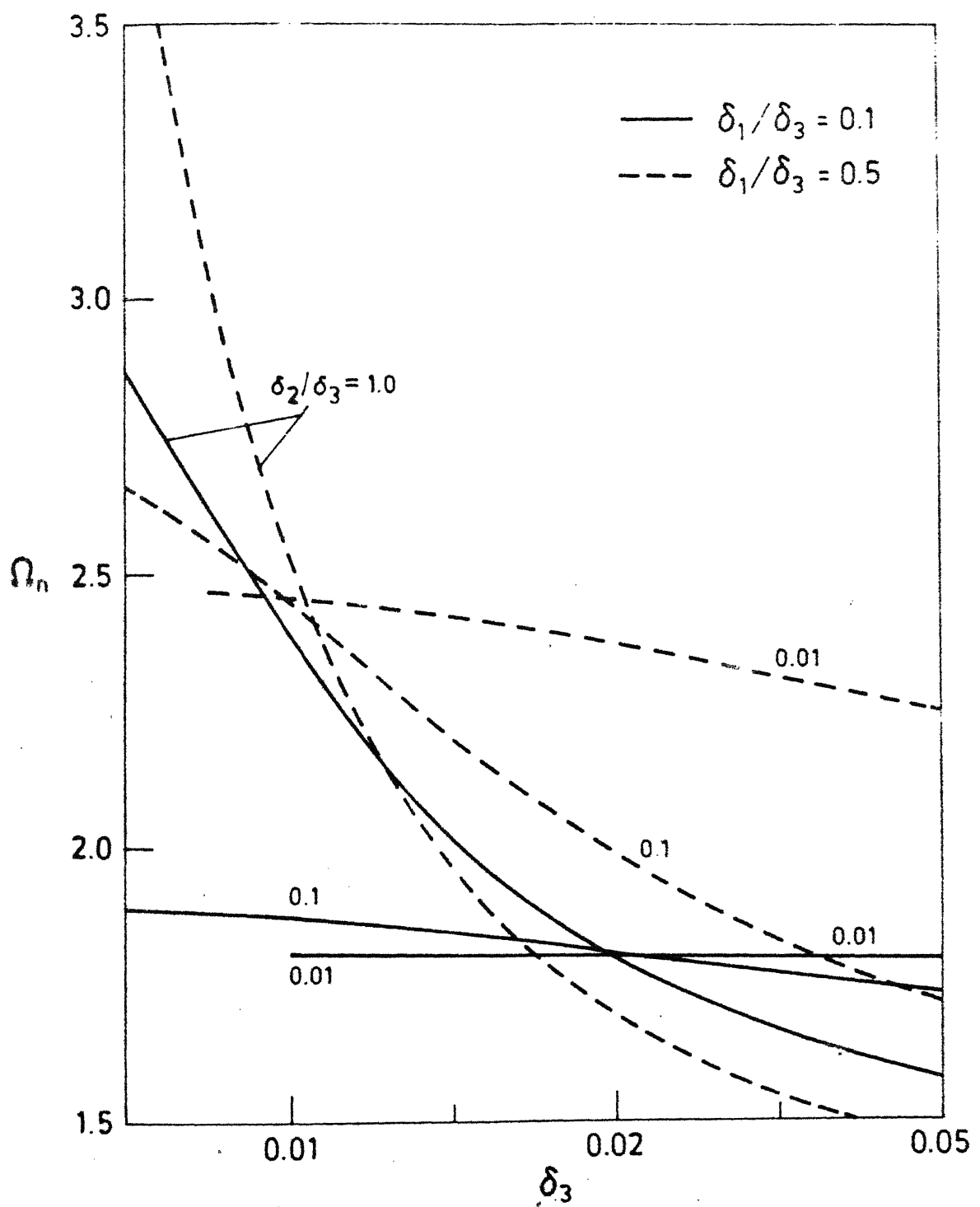


FIG. 3.10. VARIATION OF RESONANT FREQUENCY WITH BASE LAYER THICKNESS (MODE 2): TRI-COUPLED SYSTEM,  $\bar{k}_r = 0$ .

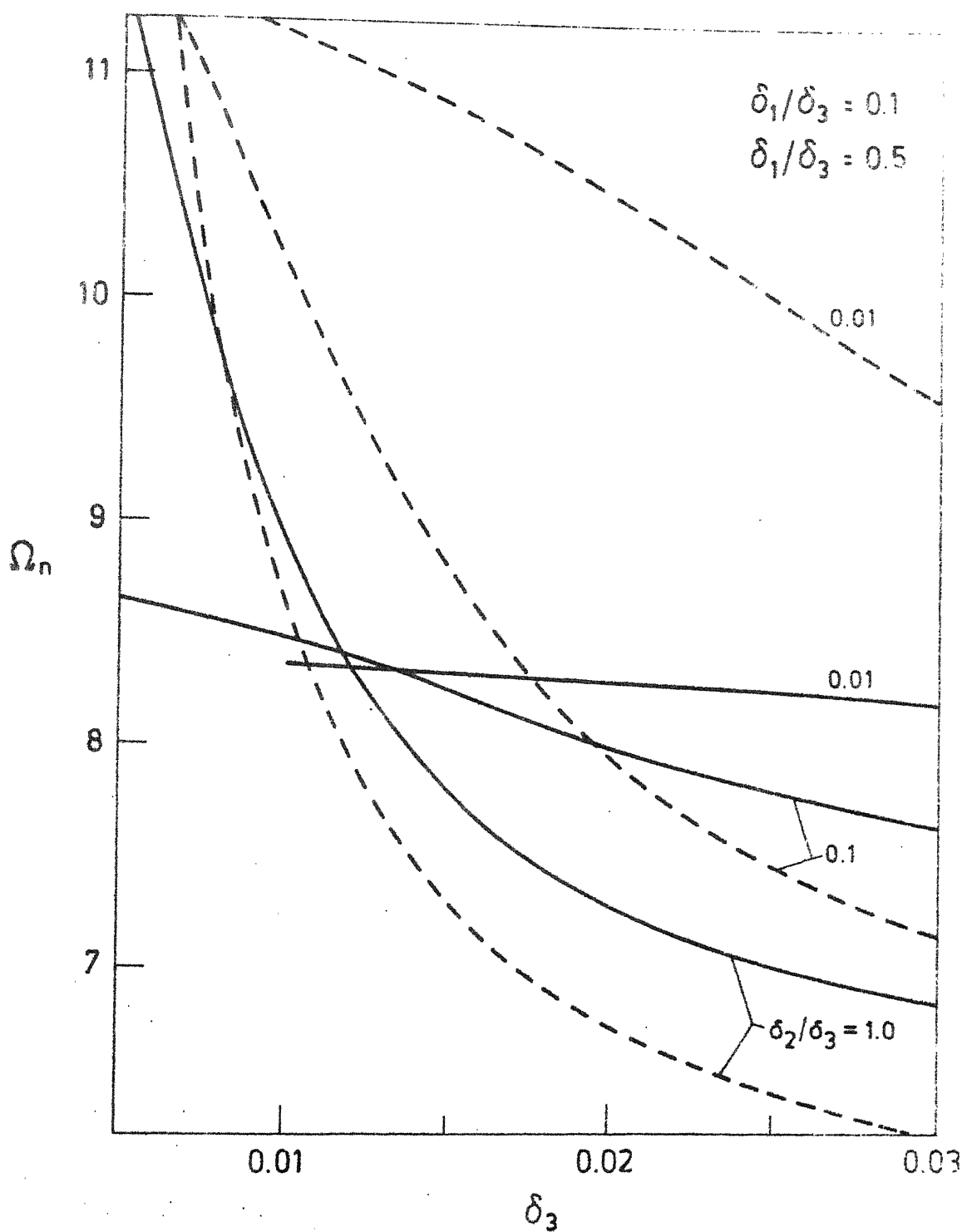


FIG. 3.11. VARIATION OF RESONANT FREQUENCY WITH BASE LAYER THICKNESS (MODE 3): TRI-COUPLED SYSTEM  
 $\bar{k}_r = 0$ .

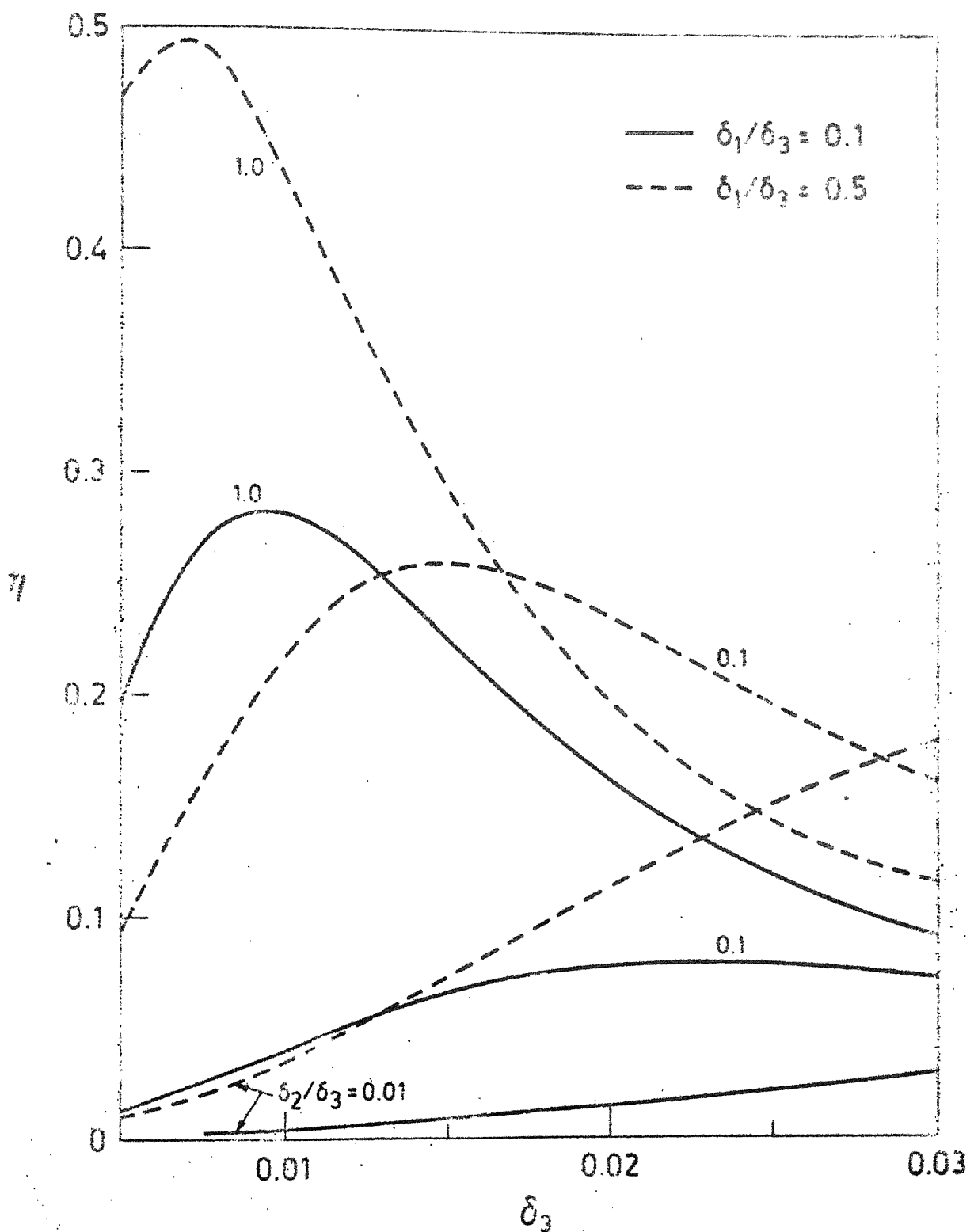


FIG. 3.12. VARIATION OF MODAL LOSS FACTOR WITH BASE LAYER THICKNESS (MODE 1):  
BI-COUPLED SYSTEM,  $\bar{k}_r = 0$ .

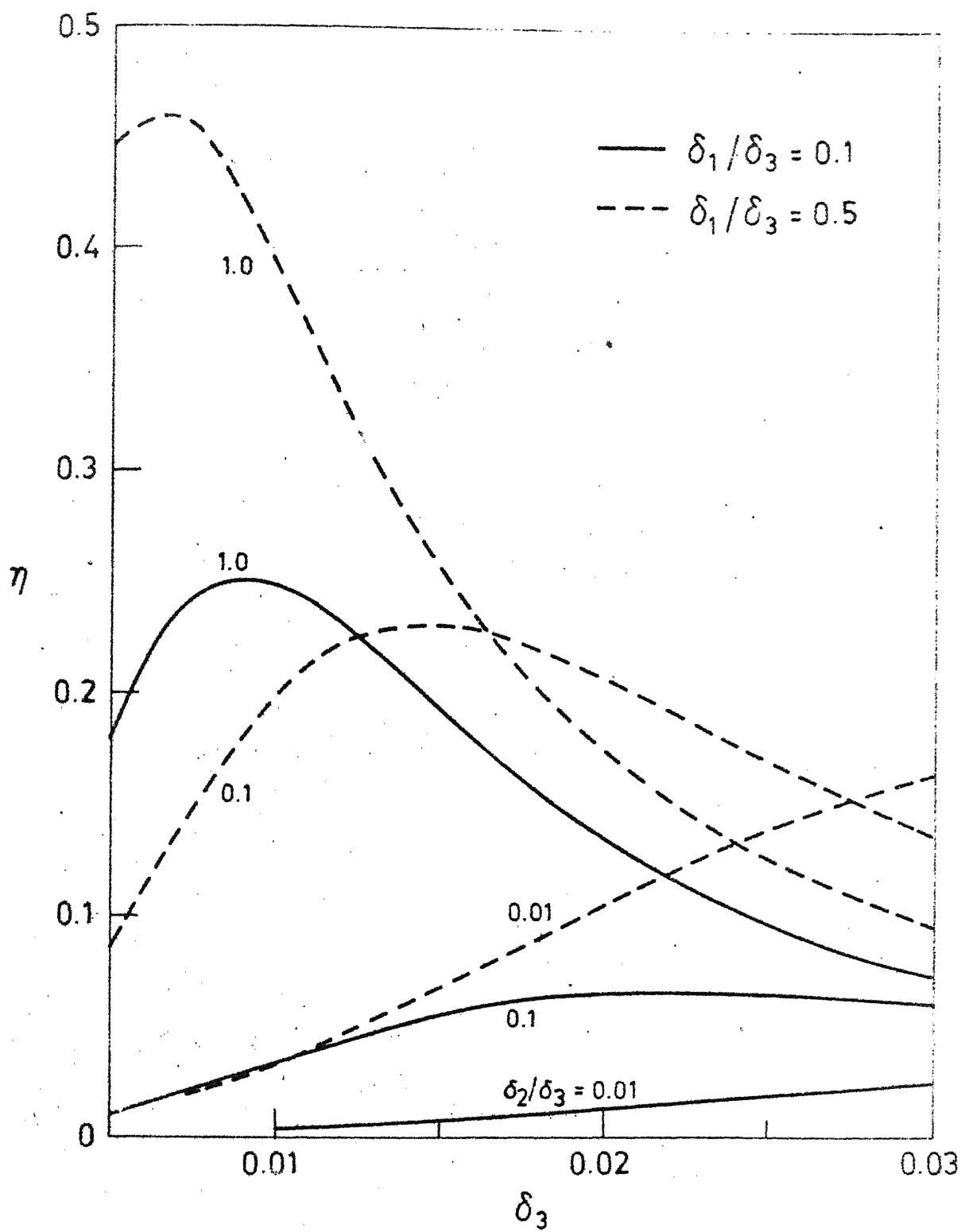


FIG. 3.13. VARIATION OF MODAL LOSS FACTOR WITH BASE LAYER THICKNESS (MODE 1): BI-COUPLED SYSTEM,  $K_r = 2$ .

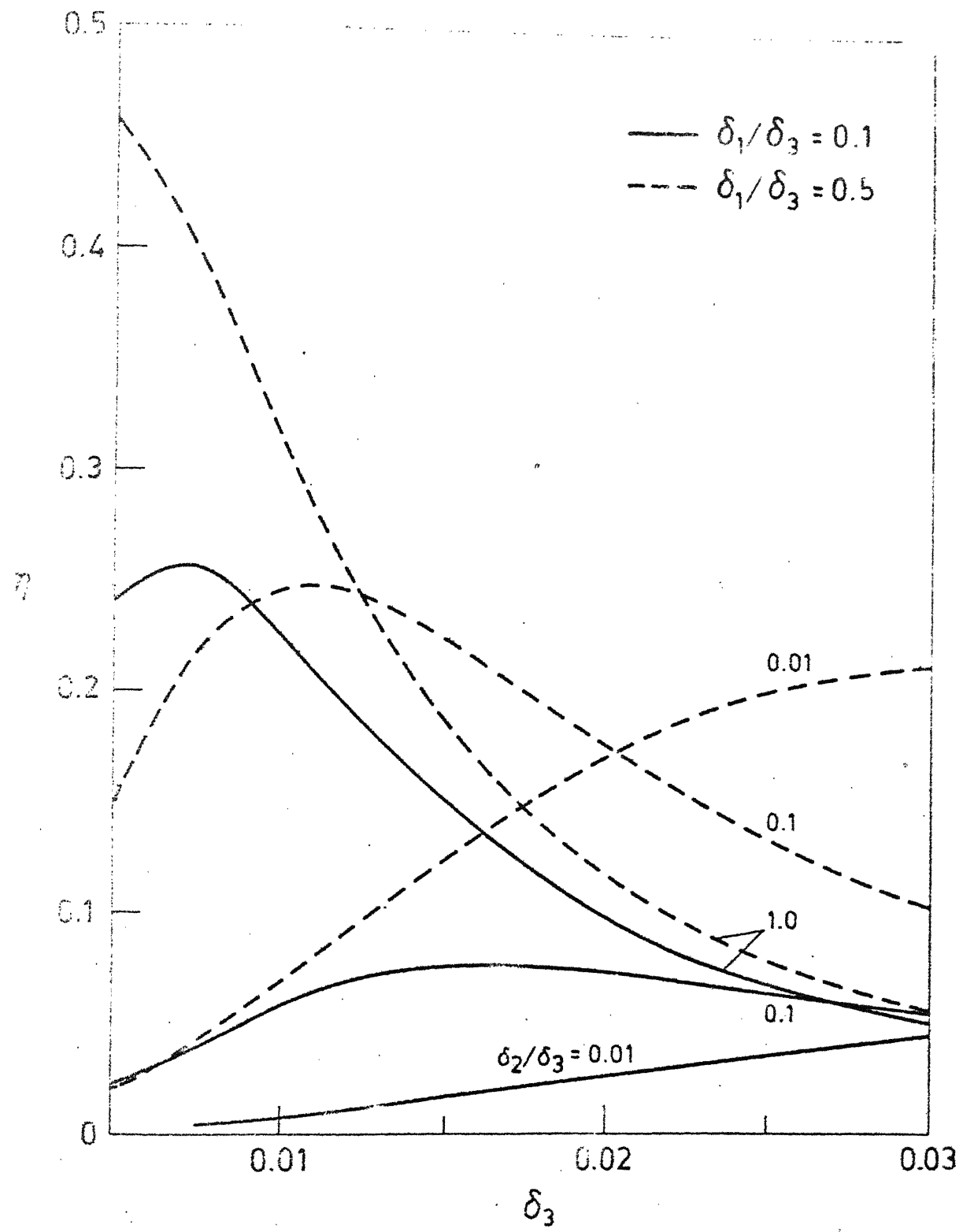


FIG. 3.14. VARIATION OF MODAL LOSS FACTOR WITH BASE LAYER THICKNESS (MODE 2): BI-COUPLED SYSTEM,  $\bar{K}_T = 0$ .

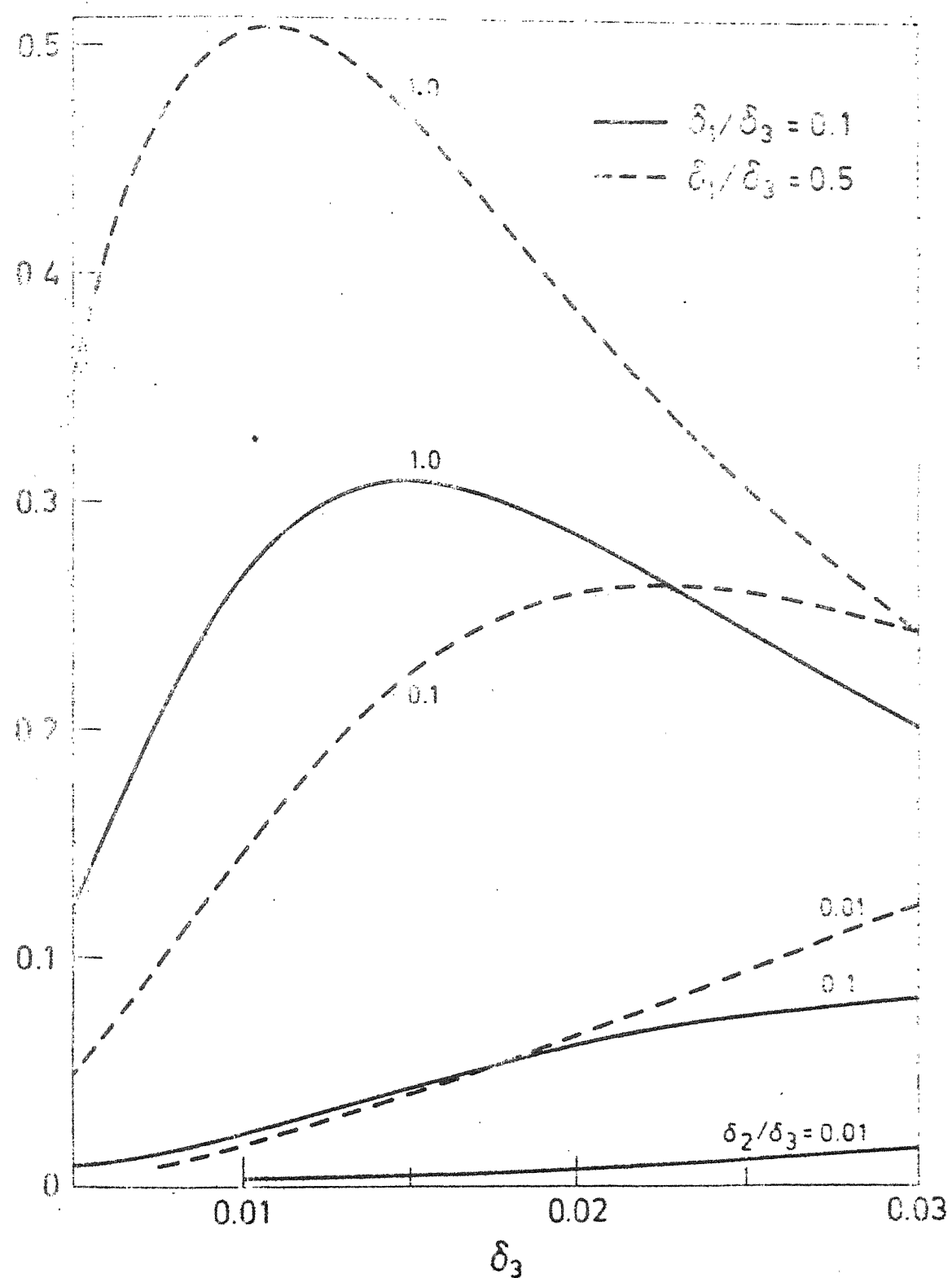


FIG. 3.15. VARIATION OF MODAL LOSS FACTOR WITH BASE LAYER THICKNESS (MODE 2):  
TRI-COUPLED SYSTEM,  $\bar{k}_r=0$ .

two flexural modes. The values of different relevant parameters are also indicated in the figures. Results are presented with the assumption that the core loss factor ( $\beta$ ) is frequency independent. However, variations of  $\beta$  with frequency can be easily incorporated in the computational procedure.

The variations of the resonant frequency in all the figures (Figs. 3.8 - 3.11) are very similar in nature. At low values of  $\delta_1/\delta_3$  and  $\delta_2/\delta_3$ , rate of decrease of  $\Omega_n$  with  $\delta_3$  is very small, whereas with higher values of these parameters, resonant frequencies decrease steeply as  $\delta_3$  increases. The reason for this behaviour is that for the data considered, the effective stiffness of the structure does not change at the same rate as the inertia.

The resonant frequencies were seen to increase with increasing value of  $\beta$ . However, this effect is marginal and depends on the thicknesses of the core and the constraining layer. The presence of rotational stiffness at the supports ( $\bar{k}_r$ ) was also found to increase  $\Omega_n$  as expected.

From Figs. 3.12 - 3.15, it can be seen that there exists an optimum value of  $\delta_3$  at which  $\eta$  is maximum. Now onwards these optimum values are referred to as  $\delta_3^*$  and  $\eta^*$ , respectively. The values of  $\delta_3^*$  and  $\eta^*$  are found to be very sensitive to both  $\delta_1/\delta_3$  and  $\delta_2/\delta_3$ .

For low values of the core thickness, the optimum value  $\delta_3^*$  turns out to be very large. As expected, with a thicker core i.e., with decreasing value of  $\delta_3^*$ , the value of  $\eta^*$  increases. However, for a given value of  $\delta_3^*$ , the core layer and the constraining layer thicknesses have to be chosen suitably so as to yield a maximum possible loss factor. This is obvious, because for a given value of  $\delta_1/\delta_3$ , the loss factor curves for various values of  $\delta_2/\delta_3$  intersect each other at different points. Furthermore, the curves for different combinations of  $\delta_2/\delta_3$  and  $\delta_1/\delta_3$  are also seen to intersect. All these imply that both the core and the constraining layer thicknesses govern the modal loss factors of the composite ring in a complicated manner.

The introduction of rotational stiffness at the supports decreases the loss factor (Fig. 3.13) as observed in the case of a two layered ring. Comparing Figs. 3.12 and 3.14, it is apparent that at higher modes, the optimum value  $\delta_3^*$  shifts to lower values. For the tri-coupled system, the nature of variation of loss factors in the third mode remains same as those in the first mode of the bi-coupled system and hence, not shown separately. This is so because these modes are comparable and is explained in connection with the elastic ring. On the other hand, the loss factors in the second mode, shown in Fig. 3.15, have wider peaks. This gives the

designer, the flexibility to choose different thicknesses of the layers, without sacrificing the loss factor in the second mode.

Resonant frequencies and modal loss factors are given in Table 3.2. It can be seen that the third and the fourth resonant frequencies of the tri-coupled system are comparable to the first and the second ones, respectively, of the bi-coupled system. In these modes loss factors are also nearly the same. In the tangential modes the loss factor,  $\eta$ , for the tri-coupled system is equal to that of the core. Whereas for the bi-coupled system  $\eta$  is almost equal to  $\beta$ . This is expected because in these modes, shear strain energies of the corresponding elastic ring (i.e., with  $\beta = 0$ ) are seen to be very high (see Table 3.1). This effect is more pronounced in the tri-coupled system where the supports do not prevent tangential movement of the base layer and thus allowing the core to deform entirely in shear without any other deformation anywhere.

Figures 3.16 and 3.17 show the effect of core shear modulus ( $G/E_3$ ) on the loss factor ( $\eta$ ) and on the resonant frequency ( $\Omega_n$ ) in the first flexural mode. For the tri-coupled system, the curves (Fig. 3.17) are similar to the ones reported for a damped three layered unsupported ring [19]. Here,  $\Omega_n$  increases with increase in  $G/E_3$  whereas the loss factor reaches a maximum for an

TABLE 3.2

RESONANT FREQUENCIES AND LOSS FACTORS OF  
A DAMPED THREE LAYERED RING

$$\delta_1 = 0.015, \quad \delta_2 = \delta_3 = 0.03, \quad \bar{k}_r = 0, \quad G/E_3 = 0.0001,$$

$$\rho_1/\rho_3 = 1, \quad N = 3, \quad \rho_2/\rho_3 = 0.2, \quad \beta = 1.0$$

Mode No.	Phase Constant ( $\mu_{in}$ )	Resonant Frequency ( $\Omega_n$ )	Loss Factor ( $\eta$ )
(i) Bi-coupled System			
1	0	5.567	0.1143
2	$2\pi/3$	8.265	0.0571
3	0	11.850	0.9417
4	$2\pi/3$	14.921	0.0284
(ii) Tri-coupled System			
2	$2\pi/3$	1.458	0.2436
3	0	6.236	0.1019
4	$2\pi/3$	8.327	0.0580
5	0	15.552	1.0000

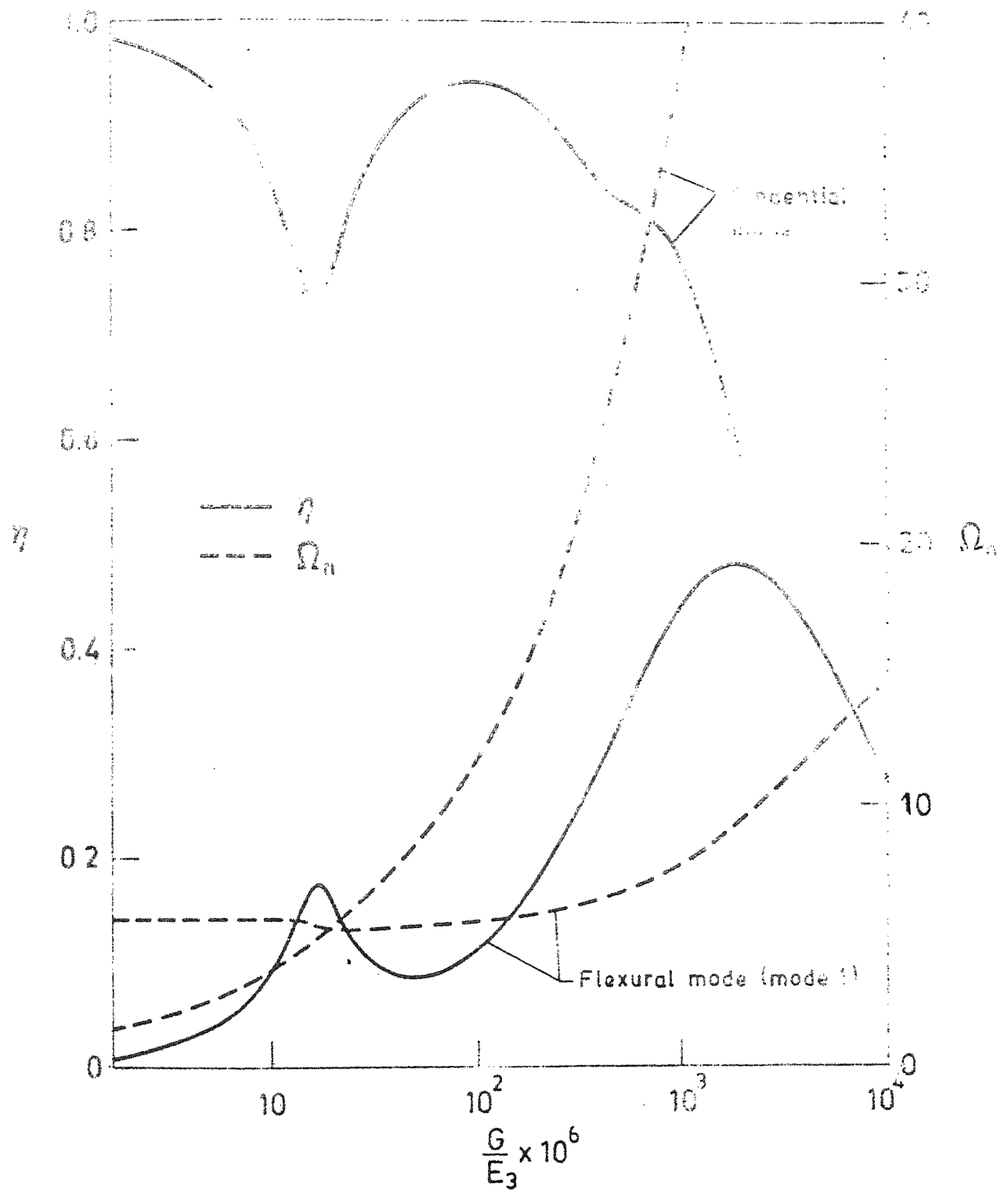


FIG. 3.16. VARIATION OF MODAL LOSS FACTOR AND RESONANT FREQUENCY WITH CORE SHEAR MODULUS:  
BI-COUPLED SYSTEM,  $k_r = 0$ .

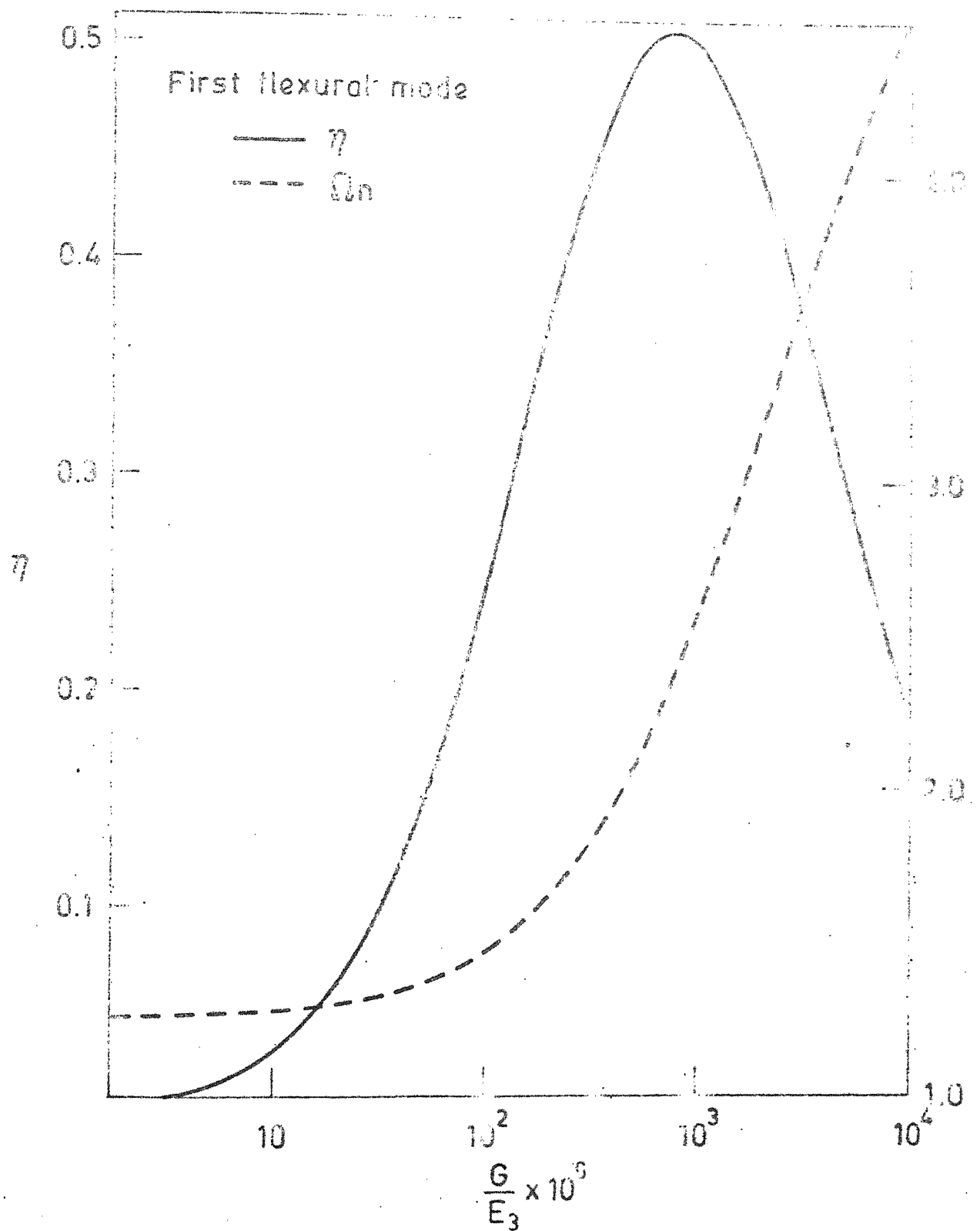


FIG. 3.17. VARIATION OF MODAL LOSS FACTOR AND RESONANT FREQUENCY WITH CORE SHEAR MODULUS :  
TRI-COUPLED SYSTEM,  $k_r = 0$ .

optimum value of  $G/E_3$ . This is due to the fact that at higher values of  $G/E_3$ , shear deformation is less and at lower values of  $G/E_3$ , damping force is less. In both the cases, the resulting dissipation of energy is reduced and maximum energy is dissipated at an intermediate value of  $G/E_3$ .

The loss factor curve for the bi-coupled system shows two peaks (Fig. 3.16). The second peak having a large value of  $\eta$ , occurs at the optimum value of  $G/E_3$  discussed above. In order to explain the presence of the first peak, resonant frequency and loss factor of the tangential mode are also shown in Fig. 3.16. At the value of  $G/E_3$  where the first peak in the flexural mode occurs, it can be seen that the resonant frequencies of flexural and tangential modes coincide resulting in a coupling of these modes. Due to the coupling, modes near this frequency are neither predominantly tangential nor predominantly flexural. As a result, the loss factor in the flexural mode has a peak whereas that in the tangential mode shows a dip. This type of coupling doesn't exist for the tri-coupled system because the flexural mode considered in Fig. 3.17 corresponds to  $\mu_{in} = 2\pi/3$  (mode 2) whereas the first tangential mode corresponds to a different value of  $\mu_{in}$  ( $= 0$ ).

## CHAPTER 4

### IN VACUO RESPONSE OF LAYERED RINGS

#### 4.1 INTRODUCTION

In this chapter the response of two and three layered rings to harmonic pressure loadings is investigated. Stiffened shell structures are very often subjected to exciting forces resulting from boundary layer turbulence, jet noise etc. Such forces can be expressed as an infinite series of circumferential harmonics of integer wave numbers. Here, the response analysis of a ring is presented for a particular wave number of the pressure loading.

The governing differential equations presented in the previous chapters are modified to include the forcing function. The general solution giving the steady-state response in one of the bays (periodic element) of the ring is obtained. The first two types of support conditions discussed in the earlier chapters are investigated.

#### 4.2 RESPONSE ANALYSIS FOR A TWO LAYERED RING

For studying the response behaviour of a two layered ring, a single circumferential pressure wave, harmonic in both space and time, acting radially inward on the outside surface of the ring is considered. The  $l^{th}$  space harmonic of the pressure is expressed as

$$p_o = P_o e^{i(\omega t - l\theta)} \quad (4.1)$$

where  $P_o$  and  $\omega$  are the amplitude and frequency, respectively of the pressure.

The virtual work done by this pressure on one bay of the ring,

$$\delta w = - \int_0^{\lambda} p_o b (R_2 + h_2 + 2h_1) d\theta \delta u \approx - \int_0^{\lambda} p_o b R_2 \delta u d\theta \quad (4.2)$$

as both  $h_1$  and  $h_2$  are very small compared to  $R_2$ .

Using (2.1), (2.2) and (4.2) and applying the generalized Hamilton's principle (i.e.,  $\int_{t_1}^{t_2} (\delta T - \delta \Pi + \delta w) dt = 0$ ), the modified differential equations are obtained as

$$L_1 U + L_2 V_2 = - P_o b R_2 e^{-i l \theta} \quad (4.3a)$$

and

$$L_2 U + L_3 V_2 = 0 \quad (4.3b)$$

where the steady-state responses are given by  $u = U e^{i \omega t}$  and  $v_2 = V_2 e^{i \omega t}$ . The differential operators  $L_1$ ,  $L_2$  and  $L_3$  are defined in section 2.5.

It should be noted that in the present chapter  $\omega^2$  is real as  $\omega$  represents the forcing frequency.

The general solution of (4.3) can be written as

$$\bar{U}(\theta) = \sum_{j=1}^6 C_j e^{s_j \theta} + \bar{U}_P \text{ and } \bar{V}_2(\theta) = \sum_{j=1}^6 B_j e^{s_j \theta} + \bar{V}_{2P} \quad (4.4)$$

where  $\bar{U} = U/R_2$  and  $\bar{V}_2 = V_2/R_2$ .

In (4.4),  $\bar{U}_P$  and  $\bar{V}_{2P}$  represent the particular solutions of (4.3) and are of the form

$$\bar{U}_P = -\gamma_{11} \bar{P}_o e^{-il\theta} \text{ and } V_{2P} = -\gamma_{21} \bar{P}_o e^{-il\theta} \quad (4.5)$$

where the non-dimensional pressure amplitude  $\bar{P}_o = P_o b/D_2$  and the constants  $\gamma_{11}$  and  $\gamma_{21}$  are given by

$$\gamma_{11} = [ - (1 + \frac{K_1^* d_3^2}{K_2 d_1^2}) l^2 + \Omega^2 \frac{D_2}{K_2} (1 + \frac{m_1 d_3^2}{m_2 d_1^2}) ] / I_D f(l) \quad (4.6a)$$

and

$$\gamma_{21} = [ \frac{K_1^* d_2 d_3}{K_2 d_1^2} l^2 + (1 + \frac{K_1^* d_3}{K_2 d_1} - \frac{m_1 D_2}{m_2 K_2} \frac{d_2 d_3}{d_1^2}) ] il/I_D f(l) \quad (4.6b)$$

with  $I_D = [ \frac{D_2^*}{D_2} (1 + \frac{K_1^* d_3^2}{K_2 d_1^2}) + \frac{K_1^* d_2^2}{D_2 d_1^2} ]$  (4.7)

and  $f(l) = -l^6 + a_1 l^4 - a_2 l^2 + a_3$  (4.8)

The coefficients  $a_1$ ,  $a_2$  and  $a_3$  appearing in (4.8) are defined in Appendix C (see equation (C.1)).

All the unknown coefficients (C's and B's) in (4.4) are not independant and their ratios ( $B_j/C_j = T_j$ ) are defined by (C.2). The six independent coefficients can be obtained by satisfying the zero-displacement conditions at the supports alongwith the wave boundary conditions which are discussed in a later section.

#### 4.3 RESPONSE ANALYSIS FOR A THREE LAYERED RING

The response analysis of a three layered ring is carried out on lines similar to those presented for a two layered ring in section 4.2.

As before, considering one bay of the ring, the virtual work done by the pressure  $p_0$  can be written as

$$\delta W = - \int_0^\lambda p_0 b R_3 \delta u d\theta \quad (4.9)$$

Now, applying the generalized Hamilton's principle, the modified differential equations are obtained as

$$L_1 U + L_2 V_1 + L_3 V_3 = - \frac{P_0}{D_3} b R_3 e^{-i l \theta} \quad (4.10a)$$

$$L_2 U + L_4 V_1 + L_5 V_3 = 0 \quad (4.10b)$$

$$L_3 U + L_5 V_1 + L_6 V_3 = 0 \quad (4.10c)$$

where  $U$ ,  $V_1$  and  $V_3$  are the steady-state harmonic amplitudes and  $L_1$ ,  $L_2$ , ...  $L_6$  are defined in section 3.5.

The general solution of (4.10) can be written as

$$\bar{U}(\theta) = \sum_{j=1}^8 C_j e^{s_j \theta} + \bar{U}_P, \quad \bar{V}_1(\theta) = \sum_{j=1}^8 B_j e^{s_j \theta} + \bar{V}_{1P}$$

$$\text{and } \bar{V}_3(\theta) = \sum_{j=1}^8 \bar{B}_j e^{s_j \theta} + \bar{V}_{3P} \quad (4.11)$$

where  $\bar{U} = U/R_3$ ,  $\bar{V}_1 = V_1/R_3$  and  $\bar{V}_3 = V_3/R_3$ .

The particular solutions  $\bar{U}_P$ ,  $\bar{V}_{1P}$  and  $\bar{V}_{3P}$  are of the form

$$\bar{U}_P = -\gamma_{11} \bar{P}_0 e^{-il\theta}, \quad \bar{V}_{1P} = -\gamma_{21} \bar{P}_0 e^{-il\theta} \text{ and } \bar{V}_{3P} = -\gamma_{31} \bar{P}_0 e^{-il\theta} \quad (4.12)$$

where

$$\gamma_{11} = [I_6 I_9 l^4 - (I_6 I_{10} + I_7 I_9) l^2 + (I_7 I_{10} - I_8^2)] / I_1 I_6 I_9 f(l) \quad (4.13a)$$

$$\gamma_{21} = [-I_4 I_9 l^2 - (I_5 I_8 - I_4 I_{10})] il / I_1 I_6 I_9 f(l) \quad (4.13b)$$

and

$$\gamma_{31} = [-I_5 I_6 l^2 - (I_4 I_8 - I_5 I_7)] il / I_1 I_6 I_9 f(l) \quad (4.13c)$$

with

$$f(l) = l^8 - a_1 l^6 + a_2 l^4 - a_3 l^2 + a_4 \quad (4.14)$$

The coefficients C's and the constants I's appearing above are defined by (E.1) and (E.2), respectively.

Among the unknown constants ( $C_j$ 's,  $B_j$ 's and  $\bar{B}_j$ 's) appearing in (4.11), only eight constants are independent. The ratios  $\bar{B}_j/C_j$  ( $= \bar{T}_j$ ) and  $B_j/C_j$  ( $= T_j$ ) are defined by (E.3) and (E.4), respectively. The response can be obtained by applying the necessary conditions explained in the previous section.

#### 4.4 SUPPORT CONDITIONS

For a pressure loading ( $P_0 e^{-il\theta} e^{i\omega t}$ ) with an integer wave number,  $l$ , the phase difference between pressures at two points distance  $\lambda$  radians apart is  $l\lambda$  [44]. This phase difference may be regarded as the propagation constant of the loading. At steady state, the flexural wave motion excited by this loading has this propagation constant imposed upon it. The forced

response quantities at corresponding points in adjacent bays then have the same amplitude but they differ in phase by  $l\lambda$ . In otherwords, the new wave conditions to be satisfied by the coupling co-ordinates and the associated coupling forces are

$$q_{j\lambda} = e^{-il\lambda} q_{j0} \text{ and } Q_{j\lambda} = e^{-il\lambda} Q_{j0} \quad (4.15)$$

where the suffix  $j$  represents a particular coupling co-ordinate/force.

By applying zero-displacement conditions and the wave conditions (Eqs. (4.15)) on displacements and forces at the supports, a set of linear equations can be obtained. Unlike in Chapters 2 and 3, these equations are non-homogeneous and can be solved for the unknown constants.

## 4.5 RESULTS AND DISCUSSION

### 4.5.1 Two Layered Ring

Numerical results presented in Figs. 4.1 - 4.6 are obtained with the following data:  $\delta_1 = 0.04$ ,  $\delta_2 = 0.02$ ,  $E_1/E_2 = 0.001$ ,  $\rho_1/\rho_2 = 0.2$ ,  $N = 3$ ,  $\bar{k}_r = 0$ ,  $\bar{P}_o = 1$ ,  $\beta = 0$  and  $1$ ,  $l = 1, 2$  and  $3$ .

Response behaviour of a bay depends not only on the exciting frequency but also on the nature of the distribution of external pressure. Moreover, response at any one point may not necessarily reveal the resonating

characteristics of the structure if that point happens to be a nodal point of the mode being excited. So response of the ring is obtained at two different points for different circumferential pressure harmonics (1). The response expressed in terms of the amplitudes of the radial displacement at  $\theta = \lambda/2$  and at  $\theta = \lambda/4$  are shown in the figures.

For a given value of  $l$ , the structure does not resonate at all natural frequencies (Tables 4.1 and 4.2). It may also be observed that only the modes which have a phase constant ( $\mu_{in}$ ) equal to zero are excited by the wave numbers  $l = 0$  and  $3$ , (Fig. 4.3), whereas the other modes (with  $\mu_{in} \neq 0$ ) are excited with  $l = 1$  and  $2$  (Figs. 4.1 and 4.2). This is because only an identical pressure distribution in all the bays can excite the modes having identical shapes in all the bays. Moreover, the wave numbers generating identical pressure wave in each bay have both symmetric and anti-symmetric components in its complex form. So they can excite both symmetric and anti-symmetric modes in a bay. But the constant pressure ( $l = 0$ ), being only symmetric in each bay, can excite only symmetric modes in a bay. Similar characteristics are also observed with the bi-coupled system as well (Figs. 4.4 - 4.6).

In general, it can be concluded that

TABLE 4.1

PRESSURE HARMONICS EXCITING VARIOUS MODES OF A TWO LAYERED RING: MONO-COUPLED SYSTEM

Mode No.	$\mu_{in}$	$\Omega_n$	Pressure Harmonics ( 1 )				
1	0.0	5.973	-	-	-	-	3
2	$2\pi/3$	8.976	-	1	2	-	
3	$2\pi/3$	16.381	-	1	2	-	
4	0.0	20.130	0	-	-	-	3

TABLE 4.2

PRESSURE HARMONICS EXCITING VARIOUS MODES OF A TWO LAYERED RING: BI-COUPLE SYSTEM

Mode No.	$\mu_{in}$	$\Omega_n$	Pressure Harmonics ( 1 )				
1	0.0	0.000	-	-	-	-	-
2	$2\pi/3$	1.414	-	1	2	-	
3	0.0	6.581	-	-	-	-	3
4	$2\pi/3$	9.031	-	1	2	-	
5	$2\pi/3$	17.500	-	1	2	-	
6	0.0	20.130	0	-	-	-	3

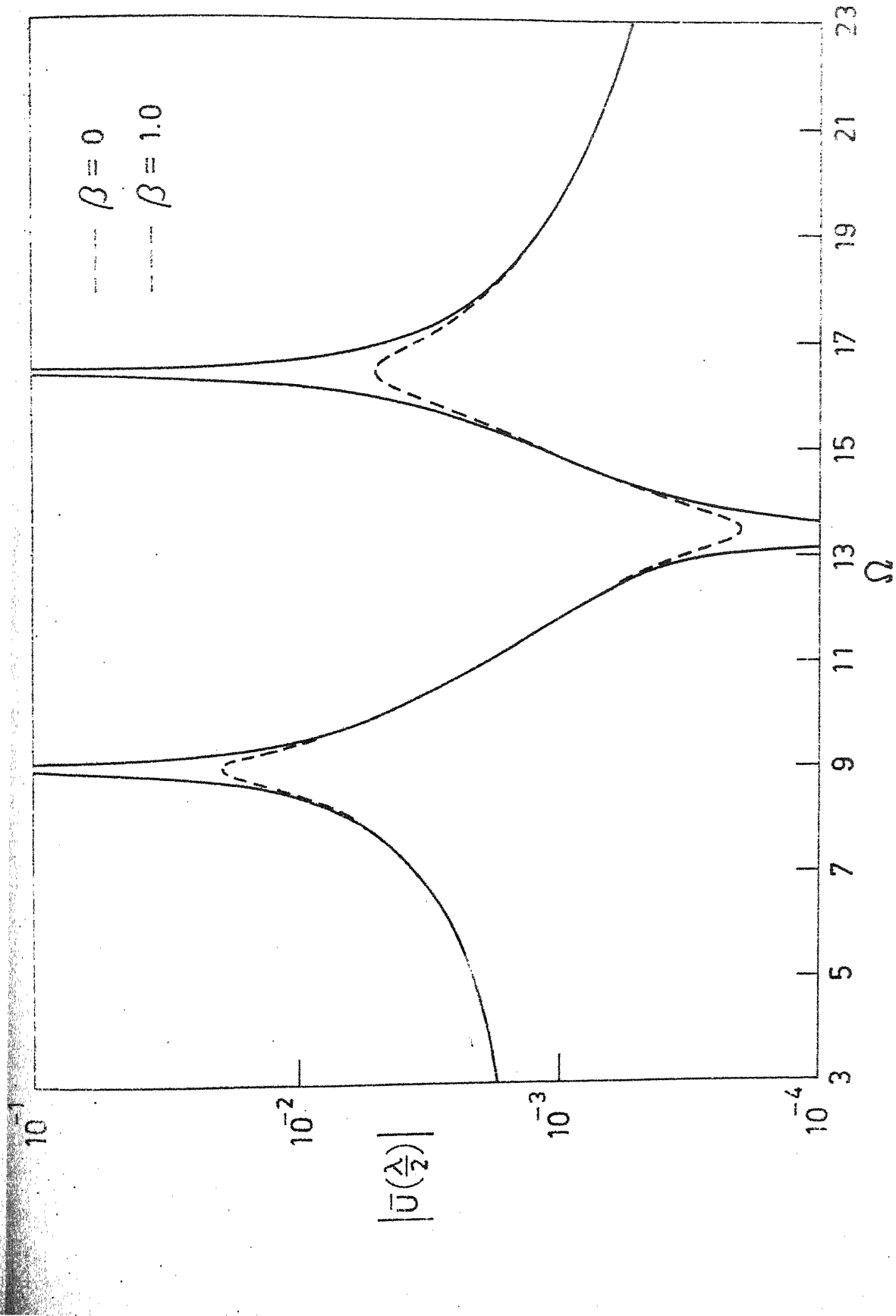


FIG. 4.1. RESPONSE OF TWO LAYERED RING: MONO-COUPLED SYSTEM,  $|U(\lambda/2)|$

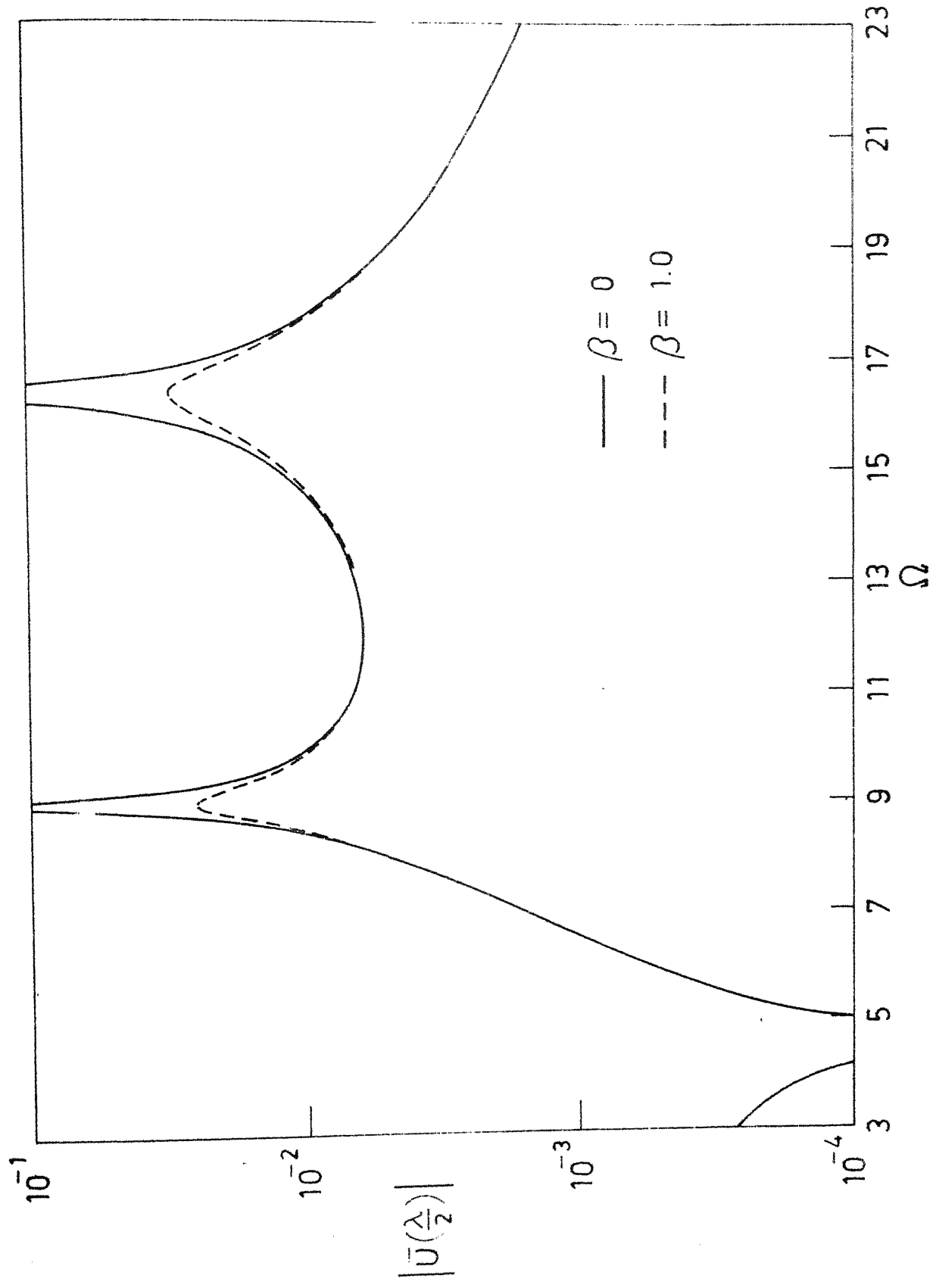


FIG. 4.2. RESPONSE OF TWO LAYERED RING : MONO-COUPLING SYSTEM,  $l=2$ ,  $=$

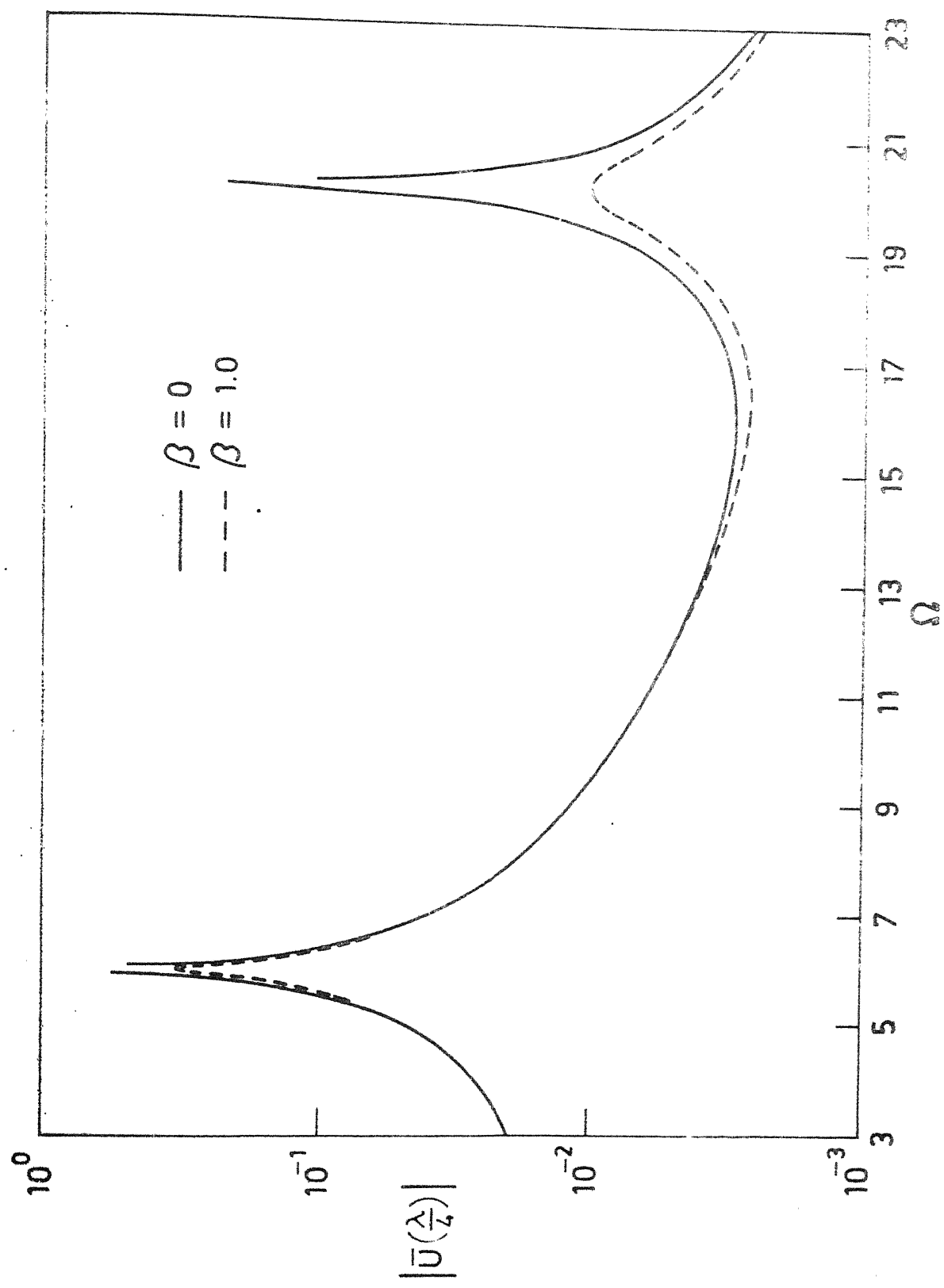


FIG. 4.3. RESPONSE TWO LAYERED RING : MONO-COUPLED SYSTEM,  $\lambda = 3$ .

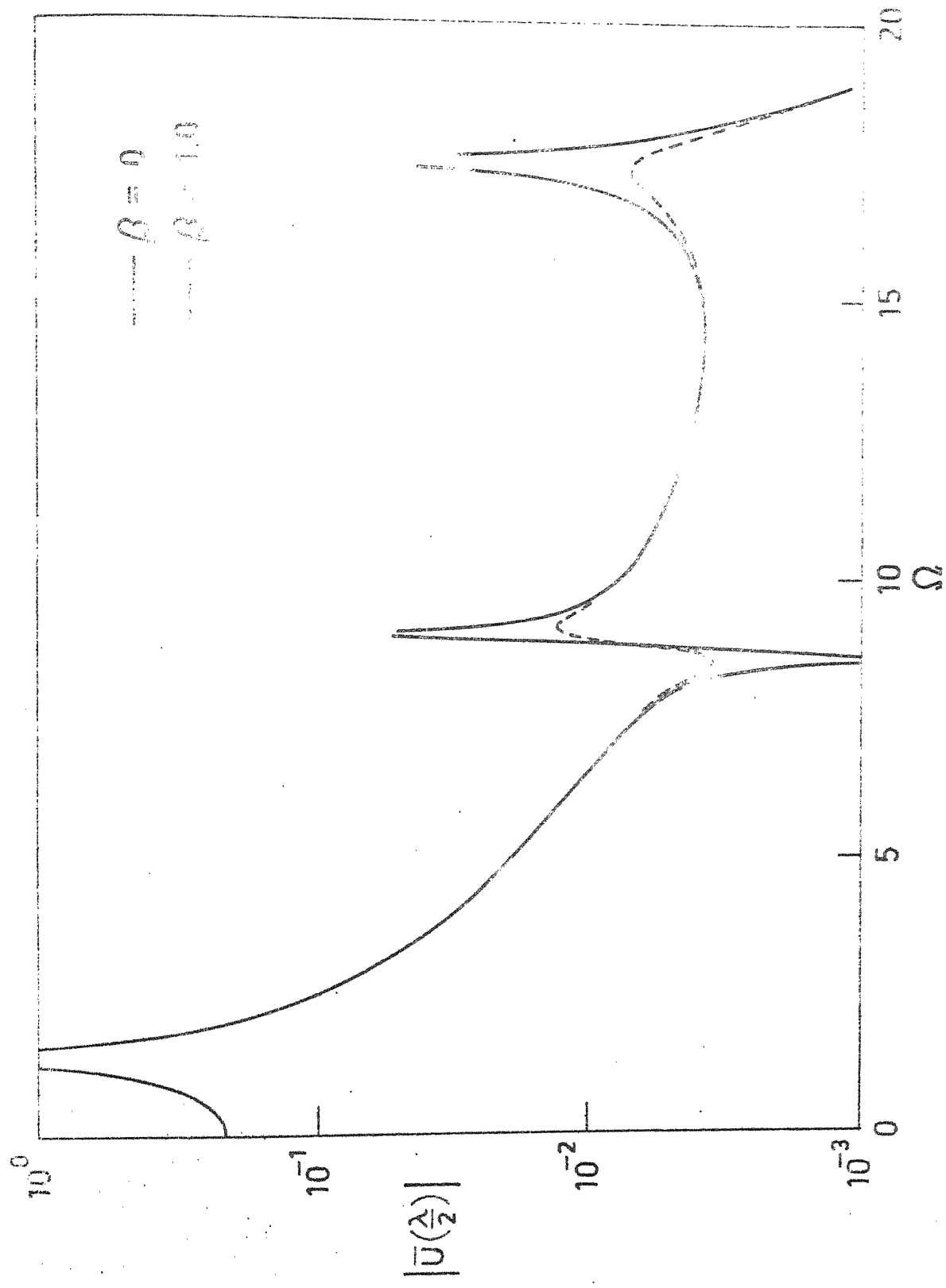


FIG. 4.4. RESPONSE OF TWO LAYERED RING: BI-COUPLED SYSTEM,  $\beta = 0$

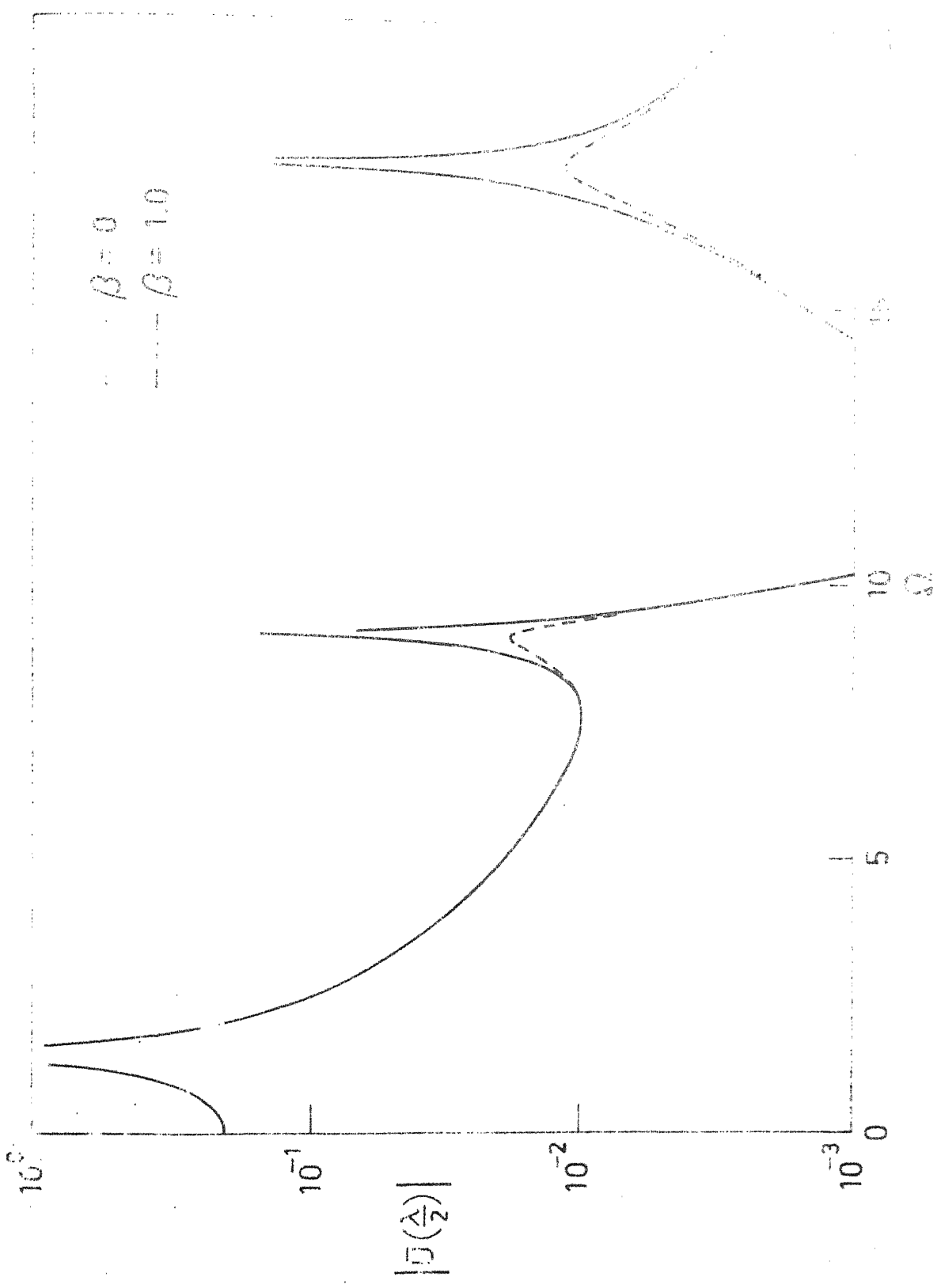


FIG. 4.5. RESPONSE OF TWO LASER MODES

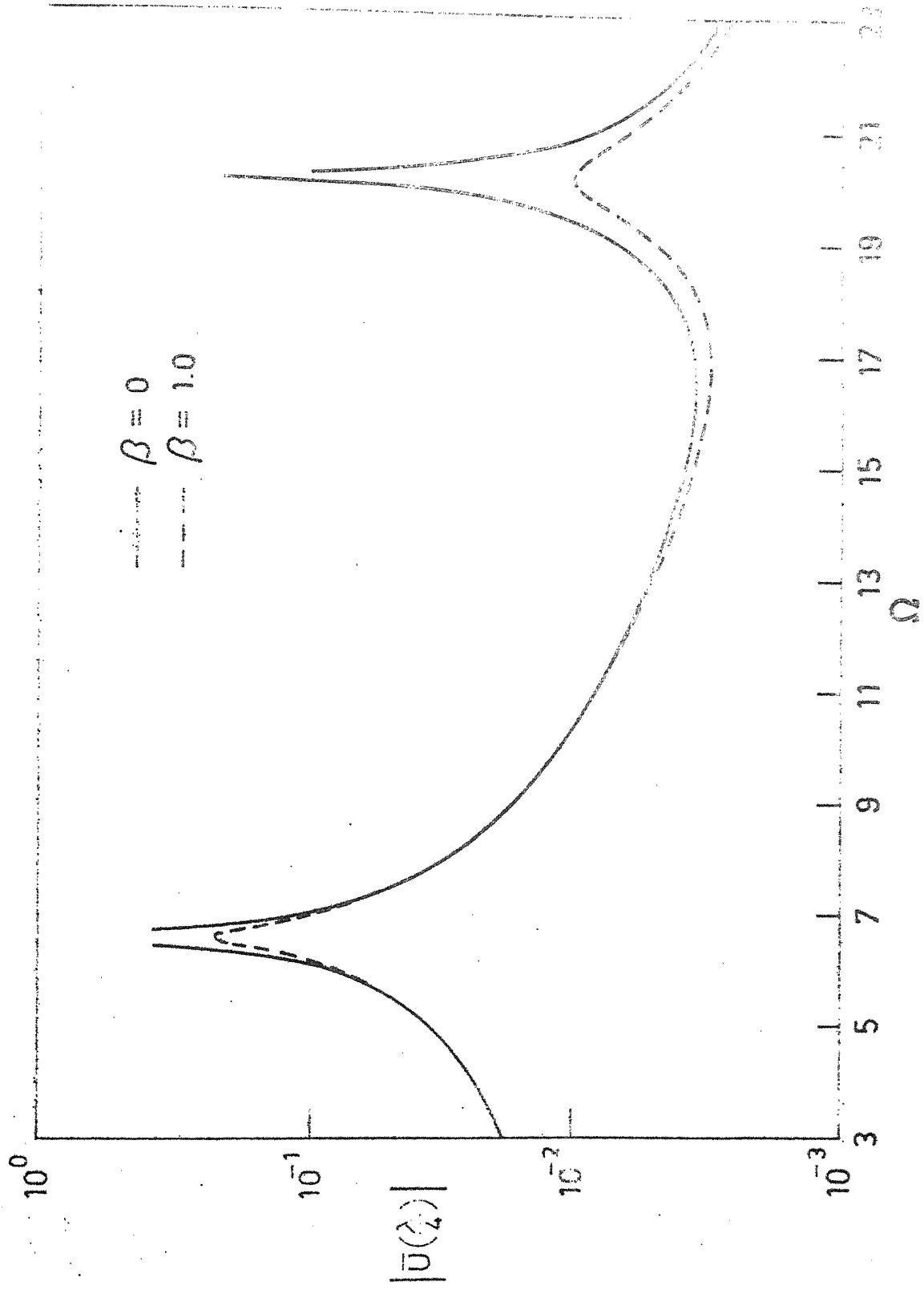


FIG. 4.6. RESPONSE OF TWO LAYERED RING: BI-COUPLED SYSTEM

- i) The harmonics  $l = j N$ ,  $j = 1, 2, 3, \dots$ , can excite the modes having identical shapes in each bay, whereas the other harmonics can excite the remaining degenerate modes.
- ii) The constant pressure (i.e.,  $l = 0$ ) can excite only the symmetric modes with identical shapes in each bay.

For selected values of  $l$ , the response is very small (almost negligible) at certain frequencies (see for example Figs. 4.1 and 4.2). These frequencies are called anti-resonant frequencies [45]. With the introduction of damping in the outer layer, it can be seen that the response is altered only near the resonant and the anti-resonant frequencies. As expected, it is seen that viscoelastic damping reduces the response only near the resonances and is detrimental near the anti-resonances.

#### 4.5.2 Three Layered Ring

Numerical results presented in Figs. 4.7 - 4.12 are obtained with the following data:  $\delta_1 = 0.015$ ,  $\delta_2 = 0.03$ ,  $\delta_3 = 0.03$ ,  $E_1/E_3 = 1$ ,  $\rho_1/\rho_3 = 1$ ,  $G/E_3 = 0.0001$ ,  $\rho_2/\rho_3 = 0.2$ ,  $\bar{k}_r = 0$ ,  $N = 3$ ,  $\beta = 0$  and  $1$ ,  $l = 1, 2$  and  $3$ .

For a three layered ring, variation of the amplitude of the radial displacement at  $\theta = \lambda/2$  and at  $\theta = \lambda/4$  are shown in Figs. 4.7 - 4.12. At all the flexural

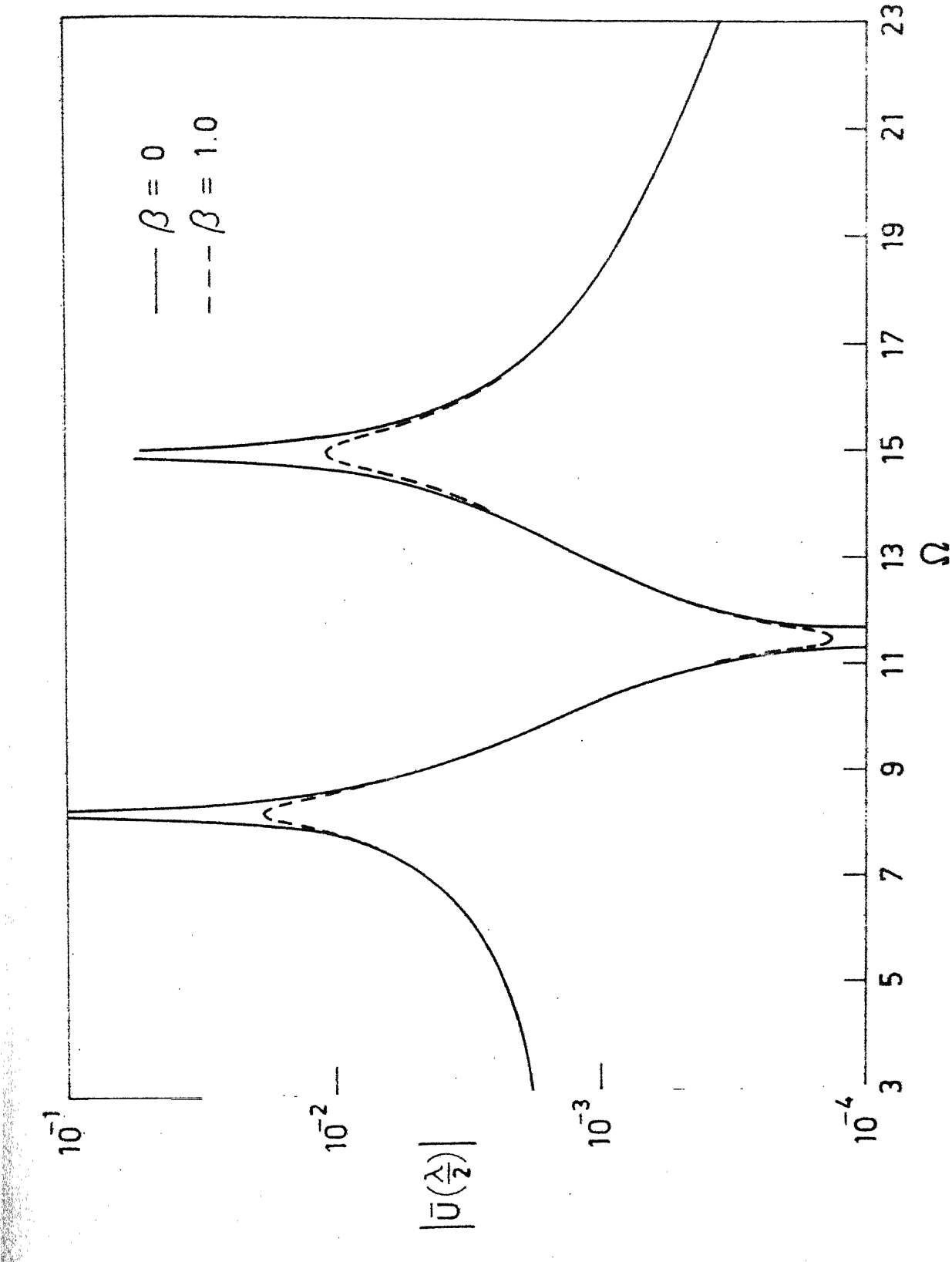


FIG. 4.7. RESPONSE OF THREE LAYERED RING : BI-COUPLED SYSTEM,  $l=1$ .

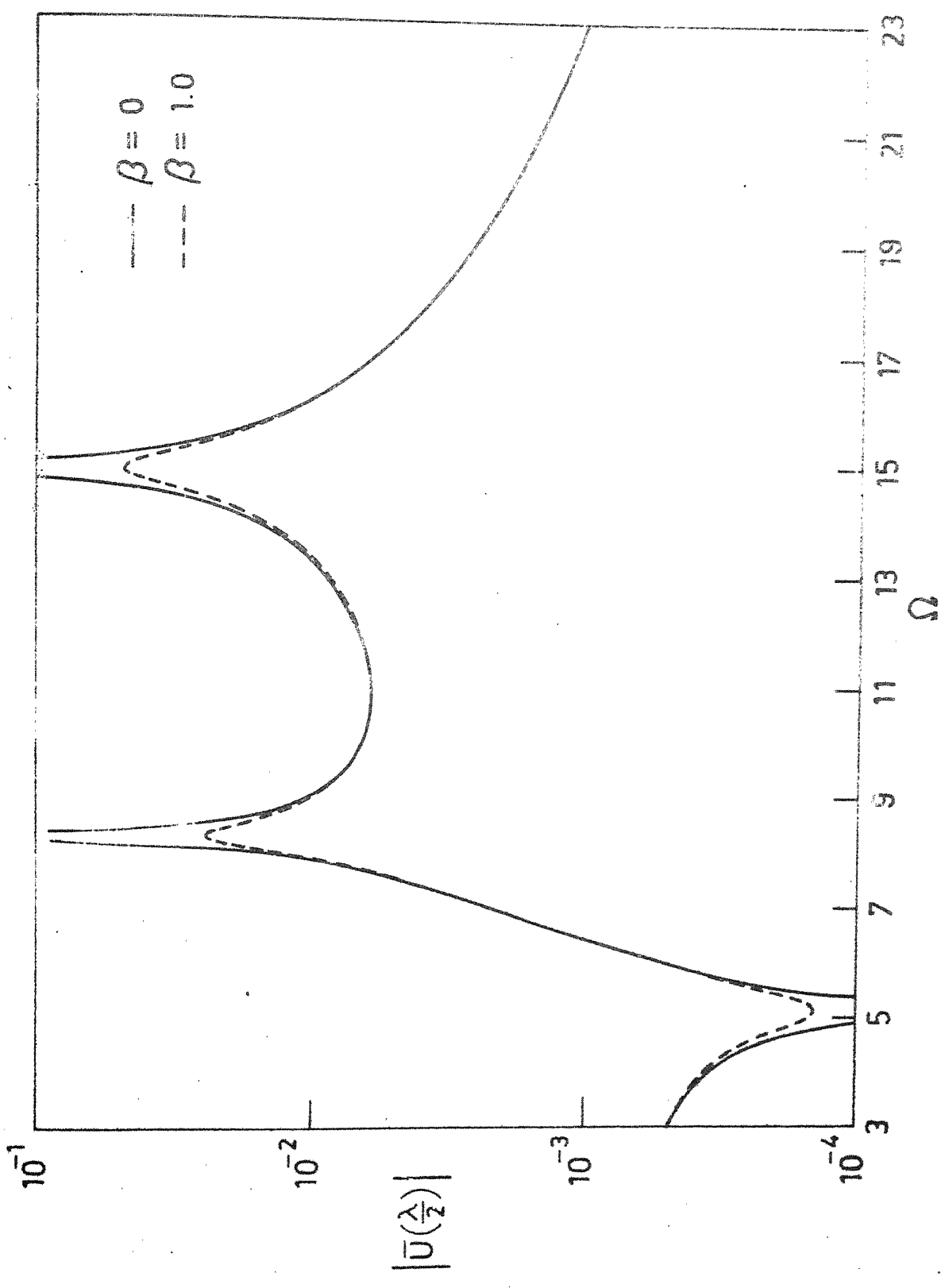


FIG. 4.8. RESPONSE OF THREE LAYERED RING : BI-COUPLED SYSTEM,  $l=2$

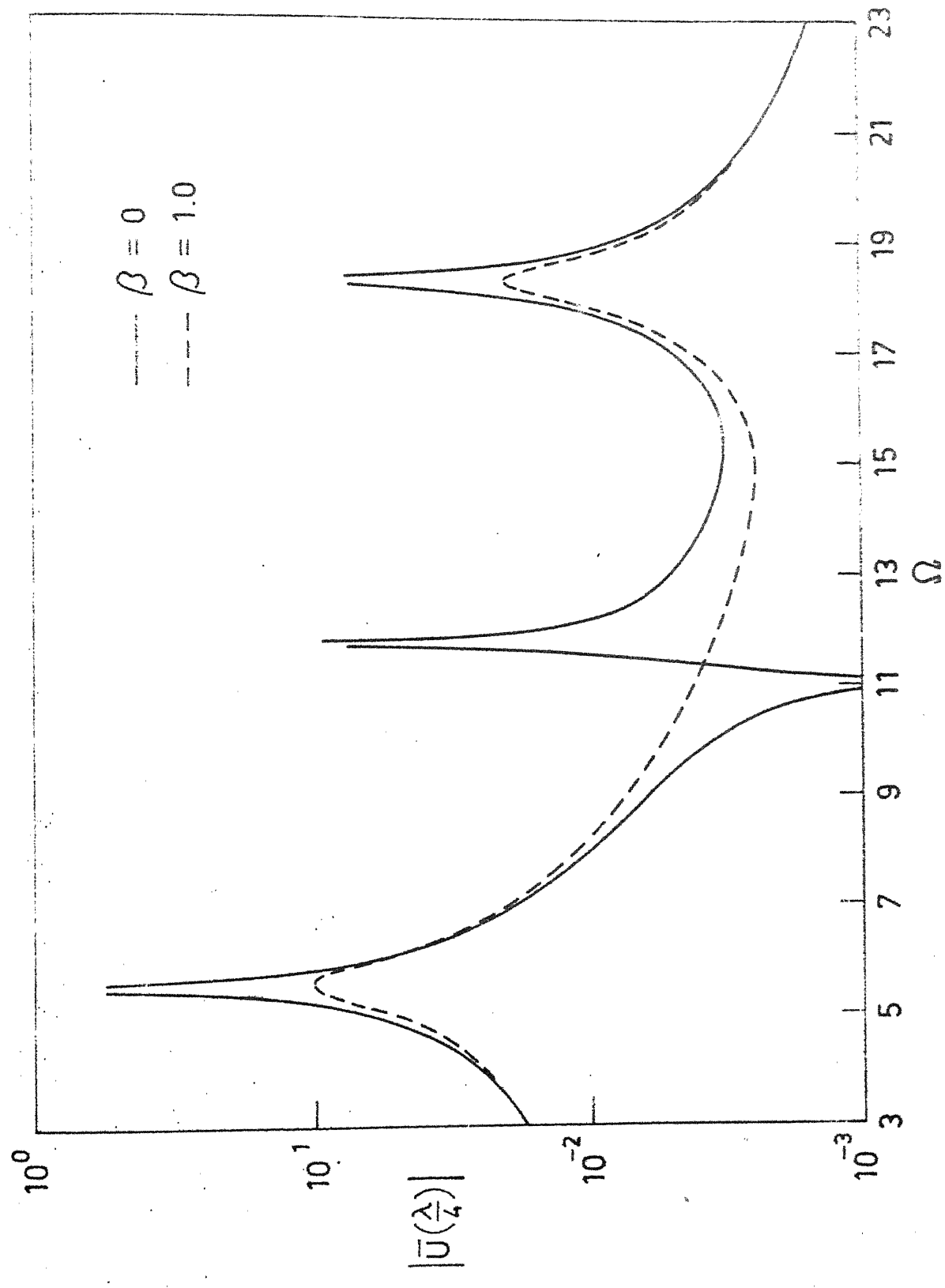
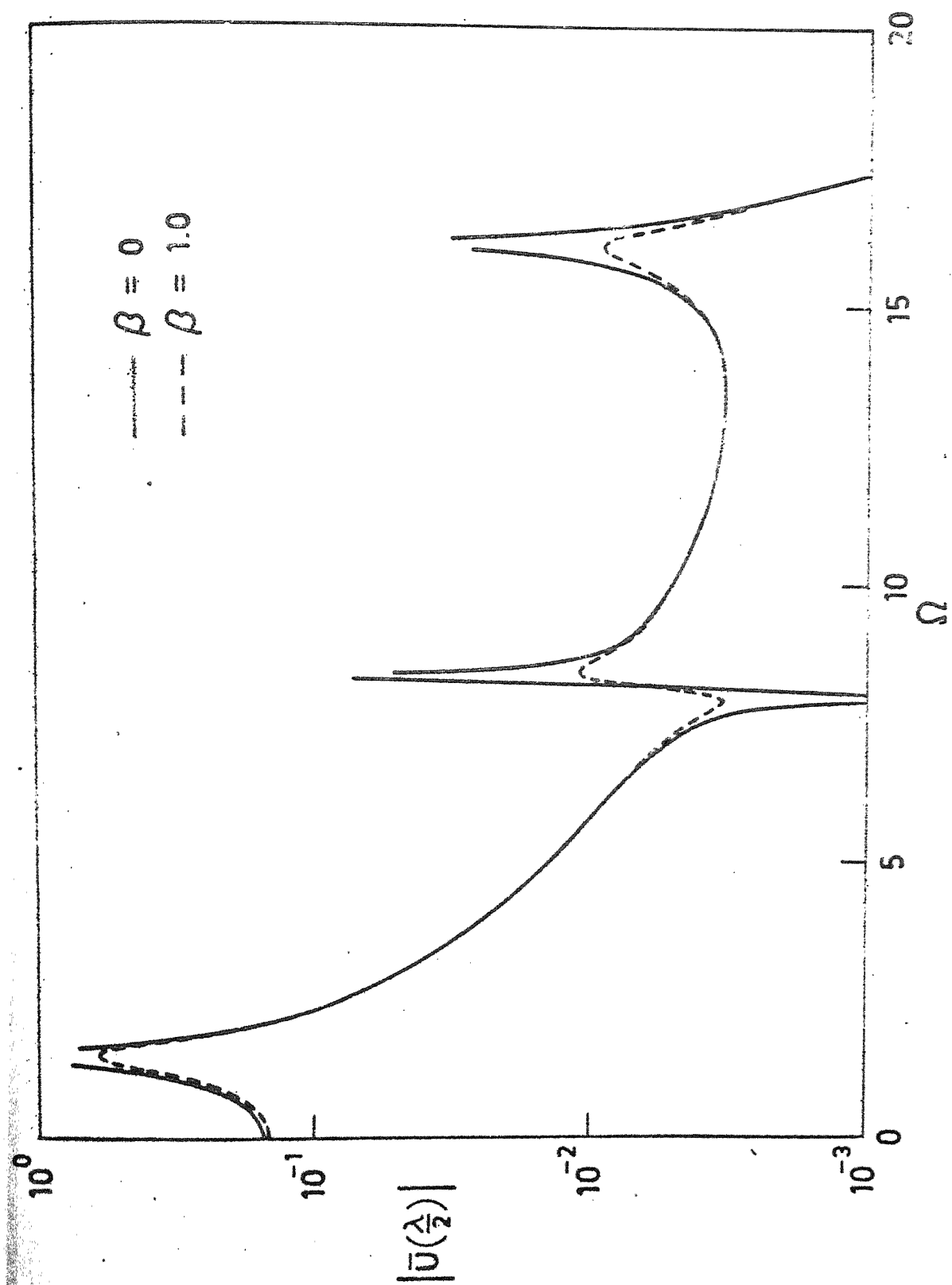


FIG. 4.9. RESPONSE OF THREE LAYERED RING : BI-COUPLED SYSTEM,  $l = 3$ .

FIG. 4.10. FREQUENCY OF THREE LAYERED SYSTEMS:  $\Omega$ -CONFINED,  $\Omega$ -OPEN



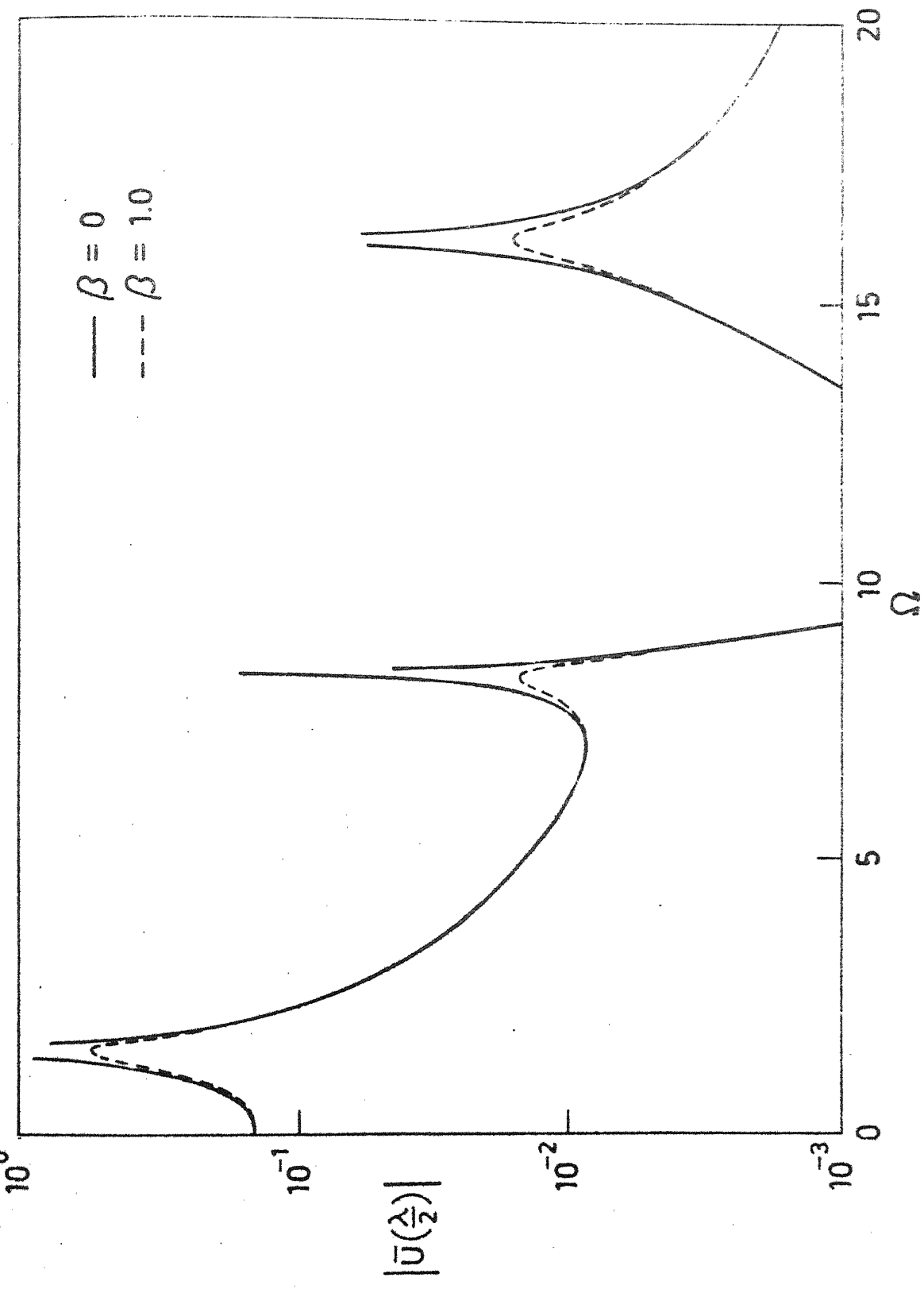


FIG. 4.11. RESPONSE OF THREE LAYERED RING :TRI-COUPLED SYSTEM,  $l = 2$ .

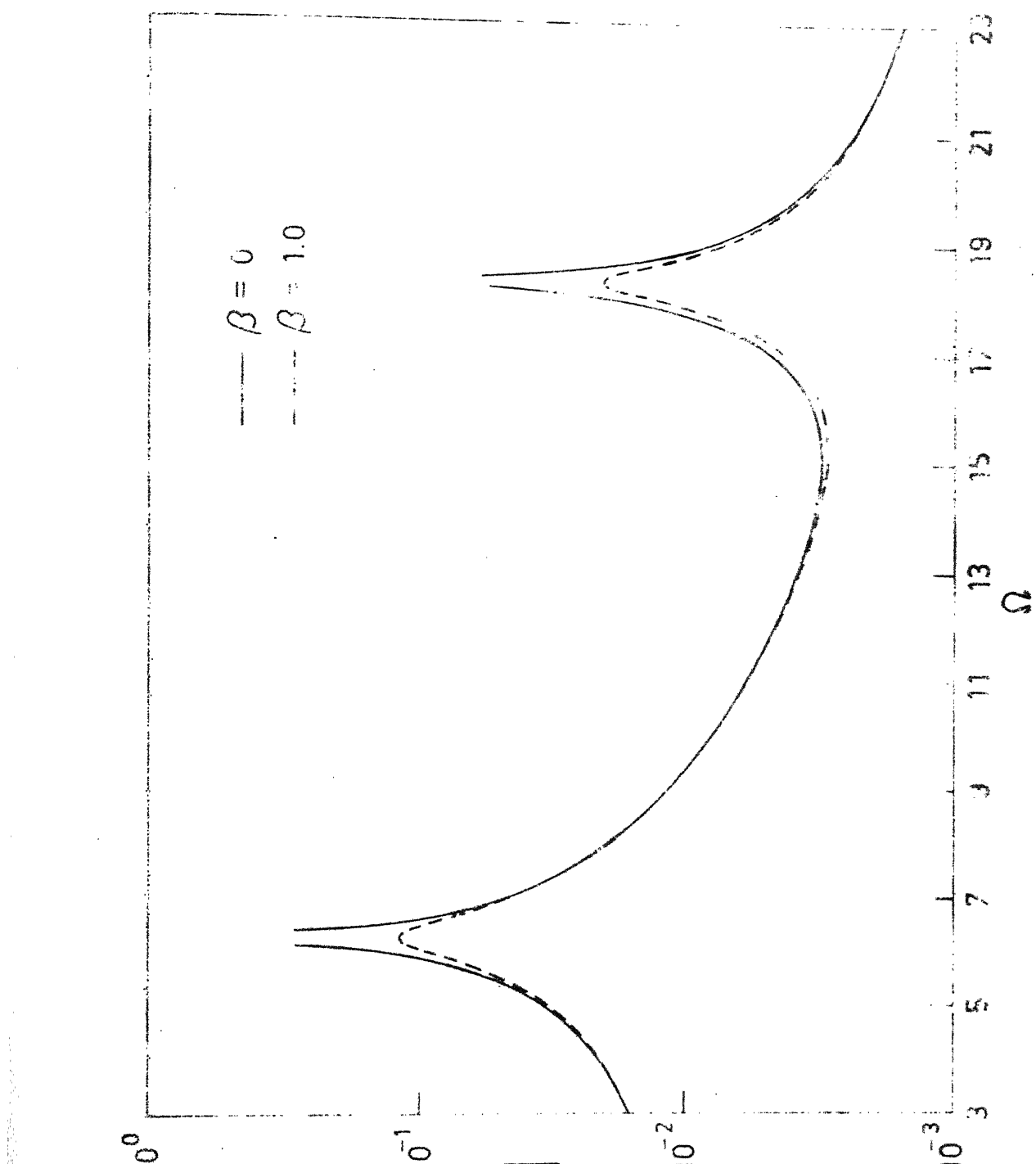


FIG. 4.12. RESPONSE OF THREE LAYERED RING : TRI-COUPLED SYSTEM, I : 3.

modes, the response characteristics are very similar to those for the two layered ring. The natural frequencies, and the pressure harmonics exciting their associated normal modes are shown in Tables 4.3 and 4.4.

With the first type of supports, it can be seen that the pressure harmonic  $l = 3$  excites the 'tangential' mode ( $\Omega_n = 11.768$ ) because this tangential mode is associated with considerable radial displacements (see Figs. 3.4d and 3.5d). When damping is introduced in the core ( $\beta = 1$ ), the peak at this frequency disappears altogether. This is due to high loss factor associated with this mode (Table 3.2). On the other hand, the tangential mode in the tri-coupled system is not excited by the same pressure loading (Fig. 4.12). As discussed in Chapter 3, this mode is a purely tangential one (Fig. 3.7d) without any radial displacement and hence cannot be excited by a radial loading.

Figures 4.13 and 4.14 show the effectiveness of damping treatment with unconstrained and constrained layers. For the sake of comparison, the thicknesses of the core and the base layers in the three layered ring are chosen to be same ( $\delta_2 = 0.02$  and  $\delta_3 = 0.02$ ) as those of the outer and inner layers ( $\delta_1 = 0.02$  and  $\delta_2 = 0.02$ ) in the two layered ring. The thickness of the constraining layer is arbitrarily taken as half of that for the base layer ( $\delta_1 = 0.5 \delta_3$ ). With the both types of

TABLE 4.3

PRESSURE HARMONICS EXCITING VARIOUS MODES OF A THREE  
LAYERED RING: BI-COUPLED SYSTEM

Mode No.	$\mu_{in}$	$\Omega_n$	Pressure Harmonics (1)				
1	0.0	5.522	-	-	-	-	3
2	$2\pi/3$	8.262	-	1	2	-	
3	0.0	11.768	-	-	-	-	3
4	$2\pi/3$	14.920	-	1	2	-	
5	0.0	18.302	0	-	-	-	3

TABLE 4.4

PRESSURE HARMONICS EXCITING VARIOUS MODES OF A THREE  
LAYERED RING: TRI-COUPLED SYSTEM

Mode No.	$\mu_{in}$	$\Omega_n$	Pressure Harmonics (1)				
1	0.0	0.000	-	-	-	-	-
2	$2\pi/3$	1.452	-	1	2	-	
3	0.0	6.230	-	-	-	-	3
4	$2\pi/3$	8.325	-	1	2	-	
5	0.0	15.550	-	-	-	-	3
6	$2\pi/3$	16.114	-	1	2	-	
7	0.0	18.302	0	-	-	-	3

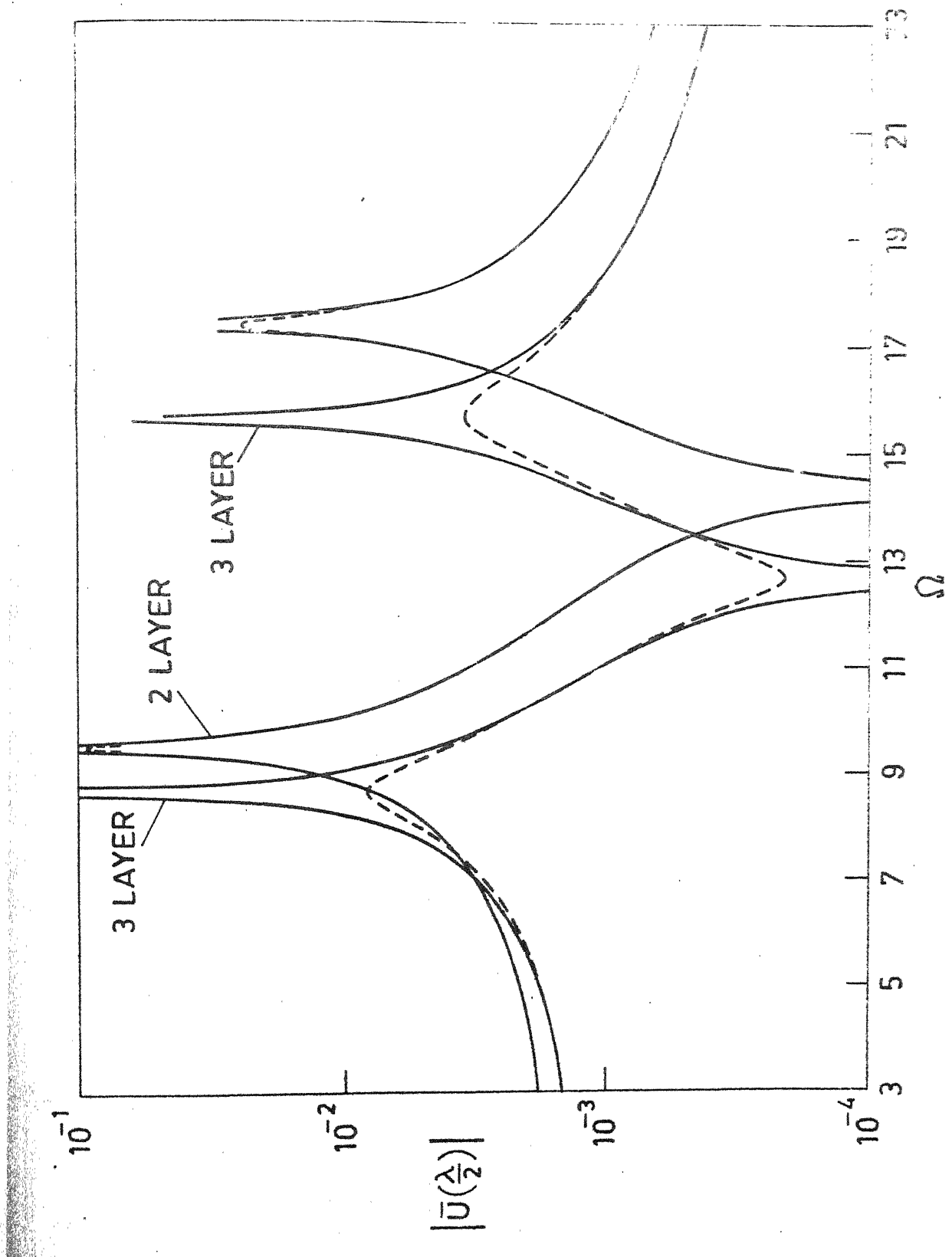


FIG. 4.13. COMPARISON OF RESPONSE FOR TWO (MONO COILED) AND THREE (BI-COUPLED) LAYERED RINGS,  $l = 1$ .

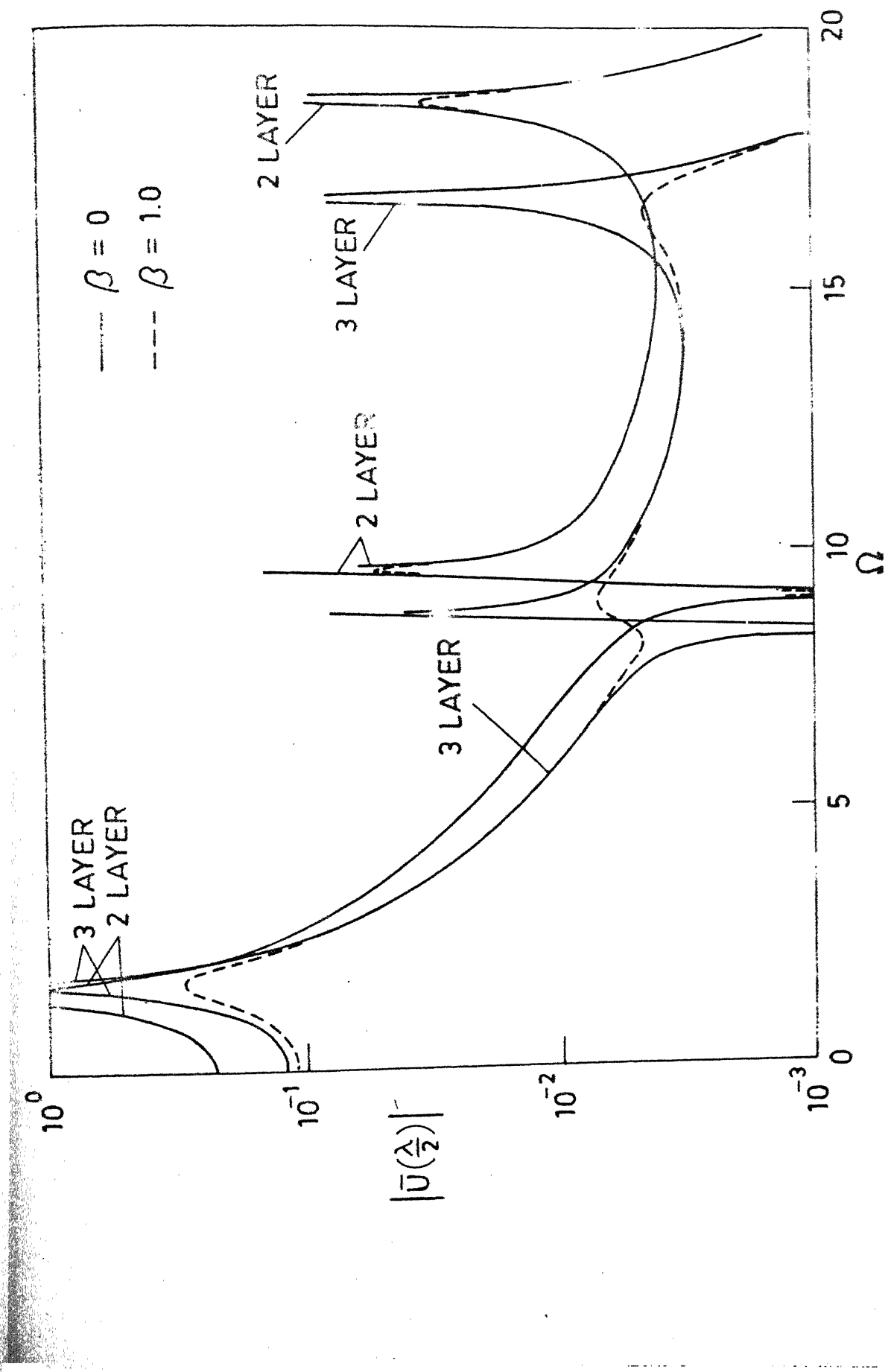


FIG. 4.16. COMPARISON OF RESPONSE FOR TWO ( $E_{12}$ -COUPLED) AND THREE (TRI-COUPLED) LAYERED RINGS,  $I = 1$ .

supports, it can immediately be seen that the constrained layer treatment is more effective in controlling the resonant response.

## CHAPTER 5

# RESPONSE AND SOUND TRANSMISSION CHARACTERISTICS IN AN ACOUSTIC FIELD

### 5.1 INTRODUCTION

In the response analysis presented in the previous chapter, it has been assumed that acoustic effects are small and do not have an appreciable effect on the motion of the structure. However, this assumption is not necessarily true, particularly when the vibrations are in fact induced by acoustic pressures. Furthermore, if the objective is to determine the inward noise transmission characteristics, the interaction of the vibrating surface with the inside fluid medium should be taken into consideration. For example, these effects are important for studying the vibrations and the cabin noise of an aircraft fuselage.

A cylindrical shell subjected to external pressure field undergoes vibration and thereby transmits/radiates pressure. This transmitted/radiated pressure is strongly coupled with the motion of the structure. A simple and relatively idealized model which can be solved exactly is the two dimensional problem of an infinitely long cylinder with circumferential stiffeners [28]. In this chapter, single

and multi-layered rings on radial supports, which are two dimensional approximations of infinitely long axially stiffened cylinders are considered.

In the first part of the work, response analyses of two and three layered rings are carried out considering a particular harmonic (space) of the external pressure and the associated transmitted pressure. Different types of interior region viz., totally resonant, totally absorbent and partially absorbent [34] are investigated. Only the first type of support condition is considered in this analysis. In the later part, an incident plane wave is expressed as a sum of infinite cylindrical harmonics. A particular component of this series and the associated scattered and transmitted pressure fields are considered for the analysis of a single layer ring. This analysis can, of course be extended easily to include multi-layered rings. No numerical results are presented for this case.

## 5.2 INTERNAL ACOUSTIC FIELD

The solution for the internal (transmitted) pressure,  $p_t$ , can be written as [28, 34]

$$p_t = \sum_{n=-\infty}^{\infty} P_{tn} e^{-in\theta} e^{i\omega t} \quad (5.1)$$

where

$$P_{tn} = A_n^t J_{|n|}(k_1 r) \quad \text{if the cylinder has resonant interior.} \quad (5.2)$$

$$P_{tn} = A_n^t H_{|n|}^{(1)}(k_1 r) \quad \text{if the cylinder has non-resonant interior,} \quad (5.3)$$

In (5.2) and (5.3),  $A_n^t$ 's are constants,  $k_1$  is the acoustic wave number of the medium,  $H_{|n|}^{(1)}$  ( $= J + i Y$ ) is the Hankel function of first kind,  $J$  and  $Y$  are the Bessel functions of the first and second kind, respectively. The symbol  $|n|$  indicates the modulus of  $n$ .

The solution given by (5.3) represents an inward-propagating wave that is totally absorbed in the cylinder cavity. To study the partially absorbing cavity, the Hankel function in (5.3) is replaced by a modified function  $\underline{H}_{|n|}^{(1)}$  [34], i.e.,

$$P_{tn} = A_n^t \underline{H}_{|n|}^{(1)}(k_1 r) \quad (5.4)$$

$$\text{where } \underline{H}_{|n|}^{(1)} = J + i \alpha Y \quad (5.5)$$

In (5.5),  $\alpha = 1$  corresponds to a totally absorbing interior and  $\alpha = 0$  to a totally resonant interior. Thus, selection of an appropriate value for  $\alpha$  can bridge the gap between the two extremes. It should be noted that the parameter  $\alpha$  is arbitrarily introduced into (5.5) and is not the same as the classical absorption coefficient used in architectural acoustics. A relation between these is given in reference [34].

### 5.3 RESPONSE ANALYSIS FOR A TWO LAYERED RING

For a two layered ring, taking the internal pressure into account, the modified differential equations can be written as

$$e^{i\omega t} (L_1 \bar{U} + L_2 \bar{V}_2) = (p_t \Big|_{r=R_2} - p_o) b \quad (5.6a)$$

$$\text{and } L_2 \bar{U} + L_3 \bar{V}_2 = 0 \quad (5.6b)$$

where  $p_o$  is given by (4.1).

The general solution of (5.6) is of the form

$$\bar{U}(\theta) = \sum_{j=1}^6 C_j e^{s_j \theta} + \sum_{n=-\infty}^{\infty} \gamma_{1n} (\bar{P}_{tn} \Big|_{r=R_2} - \bar{P}_o \delta_{nl}) e^{-in\theta} \quad (5.7a)$$

$$\bar{V}_2(\theta) = \sum_{j=1}^6 B_j e^{s_j \theta} + \sum_{n=-\infty}^{\infty} \gamma_{2n} (\bar{P}_{tn} \Big|_{r=R_2} - \bar{P}_o \delta_{nl}) e^{-in\theta} \quad (5.7b)$$

where  $\delta_{nl}$  is the Kronecker delta function,

$$\gamma_{1n} = \frac{- (1 + \frac{K_1^*}{K_2} \frac{d_3^2}{d_1^2}) n^2 + \Omega^2 \frac{D_2}{K_2} (1 + \frac{m_1}{m_2} \frac{d_3^2}{d_1^2})}{I_D f(n)} \quad (5.8a)$$

$$\gamma_{2n} = \frac{\text{in} [\frac{K_1^*}{K_2} \frac{d_2 d_3}{d_1^2} n^2 + (\frac{K_1^*}{K_2} \frac{d_3}{d_1} + 1 - \frac{m_1}{m_2} \frac{D_2}{K_2} \frac{d_2 d_3}{d_1^2} \Omega^2)]}{I_D f(n)} \quad (5.8b)$$

$\bar{P}_{tn} = P_{tn} b/D_2$ ,  $\bar{P}_o = P_o b/D_2$ ,  $I_D$  is given by (4.7),

and

$$f(n) = -n^6 + a_1 n^4 - a_2 n^2 + a_3 \quad (5.9)$$

The coefficients  $a_1$ ,  $a_2$  and  $a_3$  are defined by (C.1).

As mentioned in the previous section, the terms containing  $\bar{P}_{tn}$  in (5.7) is unknown and is related to the radial displacement,  $\bar{U}(\theta)$ , by the boundary condition on the internal pressure. Using this condition,  $\bar{P}_{tn}$  can be eliminated from (5.7) and the details are given in a later section.

#### 5.4 RESPONSE ANALYSIS FOR A THREE LAYERED RING

When the acoustic pressure inside the structure is considered, the differential equations (4.10) can be modified as

$$e^{i\omega t} (L_1 \bar{U} + L_2 \bar{V}_1 + L_3 \bar{V}_3) = (p_t|_{r=R_3} - p_o) \frac{b}{D_3} \quad (5.10a)$$

$$L_2 \bar{U} + L_4 \bar{V}_1 + L_5 \bar{V}_3 = 0 \quad (5.10b)$$

$$L_3 \bar{U} + L_5 \bar{V}_1 + L_6 \bar{V}_3 = 0 \quad (5.10c)$$

The general solution of (5.10) can be written as

$$\bar{U}(\theta) = \sum_{j=1}^8 C_j e^{s_j \theta} + \sum_{n=-\infty}^{\infty} \gamma_{1n} (\bar{P}_{tn}|_{r=R_3} - \bar{P}_o \delta_{nl}) e^{-in\theta} \quad (5.11a)$$

$$\bar{V}_1(\theta) = \sum_{j=1}^8 B_j e^{s_j \theta} + \sum_{n=-\infty}^{\infty} \gamma_{2n} (\bar{P}_{tn}|_{r=R_3} - \bar{P}_o \delta_{nl}) e^{-in\theta} \quad (5.11b)$$

and

$$\bar{V}_3(\theta) = \sum_{j=1}^8 \bar{B}_j e^{s_j \theta} + \sum_{n=-\infty}^{\infty} \gamma_{3n} (\bar{P}_{tn} \Big|_{r=R_2} - \bar{P}_o \delta_{nl}) e^{-in\theta} \quad (6.11c)$$

where

$$\begin{aligned} \gamma_{1n} &= \{I_6 I_9 n^4 - (I_6 I_{10} + I_7 I_9) n^2 \\ &\quad + (I_7 I_{10} + I_8^2)\} / f(n) \end{aligned} \quad (5.12a)$$

$$\gamma_{2n} = \{-I_4 I_9 n^2 - (I_5 I_8 - I_4 I_{10})\} in / f(n) \quad (5.12b)$$

$$\gamma_{3n} = \{-I_5 I_6 n^2 - (I_4 I_8 - I_5 I_7)\} in / f(n) \quad (5.12c)$$

$$f(n) = n^8 - a_1 n^6 + a_2 n^4 - a_3 n^2 + a_4 \quad (5.13)$$

$$\bar{P}_{tn} = P_{tn} b/D_3 \text{ and } \bar{P}_o = P_o b/D_3 .$$

The quantities I's and a's appearing above are defined in Appendix E.

Here also, the amplitudes ( $\bar{P}_{tn}$ ) of the internal pressure are related to the radial displacement,  $\bar{U}(\theta)$ , by the boundary condition which is given in the following section.

## 5.5 BOUNDARY CONDITION ON INTERNAL PRESSURE

The analysis presented here remains same for both the two and the three layered rings except that the corresponding displacement solution and the non-dimensional quantities are to be used.

The boundary condition on internal pressure is given by [24]

$$\frac{\partial p_t}{\partial r} \Big|_{r=R_b} = \rho_1^a \frac{\partial^2 u}{\partial t^2} \quad (5.14)$$

where  $\rho_1^a$  is the density of the acoustic medium and  $R_b$  is the mid-plane radius of the base layer.

From (5.4) and (5.14) we get

$$\sum_{n=-\infty}^{\infty} P_{tn} \Big|_{r=R_b} k_1 \frac{\underline{H}^{(1)}(k_1 R_b)}{\underline{H}^{(1)}(k_1 R_b)} e^{-in\theta} = \rho_1^a \omega^2 U \quad (5.15)$$

where prime denotes derivative with respect to the argument. Hereafter, the arguments and the subscripts of  $\underline{H}^{(1)}$  and  $\underline{H}^{(1)'}(k_1 R_b)$  are consistently dropped.

After non-dimensionalization, (5.15) transforms to

$$\sum_{n=-\infty}^{\infty} \bar{P}_{tn} \Big|_{r=R_b} \frac{\underline{H}^{(1)'}}{\underline{H}^{(1)}} e^{-in\theta} = \bar{\rho}_1^a \Omega \bar{c}_1 \bar{U} \quad (5.16)$$

In (5.16), the non-dimensional density,  $\bar{\rho}_1^a$ , and the velocity,  $\bar{c}_1$ , are defined for the two and the three layered rings separately. They are given later in this section.

When external pressure  $p_o$  is of the form  $P_o e^{-il\theta} e^{i\omega t}$ , the forced flexural wave motion in the structure is spatially periodic over the wave length  $2\pi/l$  and so can be analysed into spatial-harmonic wave components [ 37, 39 ]. The total wave motion so represented must have the same amplitude at any two points

distance  $\lambda$  radians apart, but the two motions must differ in phase by  $l\lambda$ . These conditions will be satisfied by a series of harmonic waves which have phase differences  $l\lambda + 2j\pi$  with  $j = 0, 1, 2, \dots$  over the interval  $\lambda$ . Hence, the radial displacement,  $\bar{U}$  can be expanded into a Fourier series as

$$\bar{U} = \sum_{n=-\infty}^{\infty} [\bar{U}_{1n} + \gamma_{1n} (\bar{P}_{tn} \Big|_{r=R_b} - \bar{P}_o \delta_{nl})] e^{-in\theta} \quad (5.17)$$

where

$$\bar{U}_{1n} = \frac{1}{\lambda} \int_0^\lambda \left( \sum_j c_j e^{sj\theta} \right) e^{in\theta} d\theta, \quad n=1, l \pm N, \dots \quad (5.18)$$

and  $\bar{U}_{1n} = 0$  Otherwise

Substituting (5.17) in (5.15) and solving for  $\bar{P}_{tn}$ ,

$$\bar{P}_{tn} \Big|_{r=R_b} = X_n \left( \bar{U}_{1n} - \gamma_{1n} \bar{P}_o \delta_{nl} \right) \quad (5.19)$$

$\frac{H(1)}{H}, \rho_1^a \bar{c}_1 \Omega$  for  $n=1, l \pm N,$   
 $l \pm 2N, \dots$

$$\text{where } X_n = \frac{1}{(1 - \frac{H}{H(1)} \cdot \rho_1^a \bar{c}_1 \Omega \gamma_{1n})} \quad (5.20)$$

$\frac{H}{H}$  and  $\bar{P}_{tn} \Big|_{r=R_b} = 0$  otherwise

Now, knowing the pressure amplitudes, the displacement solution for the two and the three layered rings can be written as follows:

(i) two layered ring

$$\bar{U}(\theta) = \sum_{j=1}^6 c_j \left( e^{sj\theta} + \sum_{n=1, l \pm N, \dots}^{\infty} z_{nj} e^{-in\theta} \right) - \bar{P}_o \gamma_{11} \bar{f}_1 e^{-il\theta} \quad (5.21a)$$

$$\bar{V}_2(\theta) = \sum_{j=1}^6 (B_j e^{s_j \theta} + C_j \sum_{n=1, n \neq N}^{\infty} z_{nj} e^{-in\theta}) - \bar{P}_o \gamma_{21} \bar{f}_1 e^{-il\theta} \quad (5.21b)$$

where  $z_{nj} = \gamma_{1n} X_n z_{nj}$ ,  $\bar{z}_{nj} = \gamma_{2n} X_n z_{nj}$   
and  $\bar{f}_1 = (1 + \gamma_{11} X_1)$  with  $z_{nj} = \frac{(e^{(s_j + il)\lambda} - 1)}{(s_j + in)\lambda}$ .

For the inside medium, the non-dimensional density and the sound velocity are defined as

$$\bar{\rho}_1 = \rho_1^a b R_2^2 / m_2 \text{ and } \bar{c}_1 = \frac{\omega}{k_1 R_2} \sqrt{\frac{m_2}{D_2}}$$

(ii) three layered ring

$$\bar{U}(\theta) = \sum_{j=1}^8 C_j (e^{s_j \theta} + \sum_{n=1, n \neq N}^{\infty} z_{nj} e^{-in\theta}) - \bar{P}_o \gamma_{11} \bar{f}_1 e^{-il\theta} \quad (5.22a)$$

$$\bar{V}_1(\theta) = \sum_{j=1}^8 (\bar{B}_j e^{s_j \theta} + C_j \sum_{n=1, n \neq N}^{\infty} \bar{z}_{nj} e^{-in\theta}) - \bar{P}_o \gamma_{21} \bar{f}_1 \bar{e}^{-il\theta} \quad (5.22b)$$

and  $\bar{V}_3(\theta) = \sum_{j=1}^8 (\bar{B}_j e^{s_j \theta} + C_j \sum_{n=1, n \neq N}^{\infty} \bar{z}_{nj} e^{-in\theta}) - \bar{P}_o \gamma_{31} \bar{f}_1 \bar{e}^{-il\theta} \quad (5.22c)$

where  $z_{nj} = \gamma_{1n} X_n z_{nj}$

$$\bar{z}_{nj} = \gamma_{2n} x_n z_{nj}$$

$$\bar{z}_{nj} = \gamma_{3n} x_n z_{nj}$$

$$\text{and } \bar{f}_1 = (1 + \gamma_{11} x_1) \text{ with } z_{nj} = \frac{ie^{(s_j + il)\lambda}}{(s_j + in)\lambda} - 1 .$$

For the inside medium, the non-dimensional density and the sound velocity are defined as

$$\bar{\rho}_1^a = \rho_1^a b R_3^2 / m_3 \text{ and } \bar{c}_1 = \frac{\omega}{k_1 R_3} \sqrt{\frac{m_3}{D_3}} .$$

Using the above displacement solutions of the corresponding structure and applying the necessary support conditions, the response can be obtained as discussed in Chapter 4. In order to compute the response, a finite number of terms in the series for the internal pressure are to be chosen.

Here, it should be noted that for computing the response, the number of linear equations to be solved does not depend on the number of terms chosen in the infinite series (Eq. 5.1). However, in reference [37] this is not so though the basic principle involved is same as that of the present work.

From the radial displacement, the sound power transmitted (SP) inside can be obtained as [36]

$$SP = \left[ \operatorname{Re} \frac{i\Omega}{2} \sum_{n=1,1+N,\dots}^{\infty} \bar{P}_{tn} \bar{U}_n^* \right] \text{ or } SP = \frac{\bar{\rho}_a \Omega^2 \bar{c}_1}{2} \sum_{n=1,1+N,\dots}^{\infty} \operatorname{Re} \left[ i \frac{\bar{H}^{(1)}}{\bar{H}^{(1)*}} \right] |\bar{U}_n|^2 \quad (5.23)$$

where  $\bar{U}_n = \bar{U}_{in} + \gamma_{in} (\bar{P}_{tn} - \bar{P}_o \delta_{nl})$ ,  $\bar{U}_n^*$  is complex conjugate of  $\bar{U}_n$  and  $\operatorname{Re}$  represents the real part.

### 5.6 RESPONSE OF A SINGLE LAYER RING TO A PLANE ACOUSTIC WAVE

A more general problem in which the structure is subjected to an incident, scattered and transmitted acoustic fields is considered here. In a practical case, the incident acoustic field will be a random noise field. However, in the following analysis, the incident field is assumed to be a plane wave which can be expressed in cylindrical co-ordinates as

$$p_i = P_i e^{-i k_2 r \cos \theta} e^{i \omega t} \quad (5.24)$$

$$= P_i \sum_{n=-\infty}^{\infty} A_n^i J_{|n|} (k_2 r) e^{-in\theta} e^{i\omega t} \quad (5.25)$$

where  $k_2$  is the acoustic wave number in the outside medium,  $P_i$  is the amplitude of the plane wave,

$$\left. \begin{aligned} A_n^i &= (-i)^n \\ A_{-n}^i &= A_n^i \end{aligned} \right\} \text{ for } n = 0, 1, 2, \dots \infty \quad (5.26)$$

Considering only a single term (harmonic), say  $n = 1$ , in the series (5.25), outside pressure,  $p_o$ , can be written as

$$p_o = P_{il} e^{i\theta} e^{i\omega t} \quad (5.27)$$

where

$$P_{il} = P_i A_1^i J_{|1|} \quad (5.28)$$

The scattered ( $p_s$ ) and the transmitted ( $p_t$ ) pressures corresponding to this component of the incident pressure are of the form

$$p_s = \sum_{n=-\infty}^{\infty} P_{sn} e^{in\theta} e^{i\omega t} \quad (5.29)$$

$$\text{and } p_t = \sum_{n=-\infty}^{\infty} P_{tn} e^{in\theta} e^{i\omega t} \quad (5.30)$$

$$\text{where } P_{sn} = A_n^s H_{|n|}^{(2)} (k_2 r), \quad P_{tn} = A_n^t H_{|n|}^{(1)} (k_1 r),$$

with  $H^{(2)}$  ( $= J - i Y$ ) as the Hankel function of the second kind and  $H^{(1)}$  ( $= J + i aY$ ) as the modified Hankel function of the first kind defined in earlier sections. In the above equations  $A_n^s$  and  $A_n^t$  are constants. The subscripts 1 and 2 refer to inside and outside mediums, respectively.

Incorporating these pressures in the governing differential equations of a single layer ring, the equations are obtained as

$$e^{i\omega t} (L_1 U + L_2 V_2) = (p_t - p_o - p_s) \Big|_{r=R_2} b R_2 \quad (5.31a)$$

$$\text{and } L_2 U + L_3 V_2 = 0 \quad (5.31b)$$

$$\text{where } L_1 = D_2 \frac{d^4}{d\theta^4} + 2 D_2 \frac{d^2}{d\theta^2} + (D_2 + K_2 - m_2 \omega^2)$$

$$L_2 = K_2 \frac{d}{d\theta} \quad (5.32)$$

$$\text{and } L_3 = K_2 \frac{d^2}{d\theta^2} + m_2 \omega^2$$

Equations (5.32) are obtained from the differential operators of the two layered ring (see section 2.5) with the outer layer thickness ( $\delta_1$ ) as zero.

The general solution of (5.31) can be written as

$$\bar{U}(\theta) = \sum_{j=1}^6 C_j e^{s_j \theta} + \sum_{n=-\infty}^{\infty} \gamma_{1n} (\bar{P}_{tn} - \bar{P}_{in} \delta_{nl} - \bar{P}_{sn}) \Big|_{r=R_2} e^{in\theta} \quad (5.33a)$$

and

$$\bar{V}_2(\theta) = \sum_{j=1}^6 B_j e^{s_j \theta} + \sum_{n=-\infty}^{\infty} \gamma_{2n} (\bar{P}_{tn} - \bar{P}_{in} \delta_{nl} - \bar{P}_{sn}) \Big|_{r=R_2} e^{in\theta} \quad (5.33b)$$

$$\text{where } \bar{P}_{tn} = P_{tn} b/D_2, \quad \bar{P}_{in} = P_{in} b/D_2,$$

$$\bar{P}_{sn} = P_{sn} b/D_2$$

$$\gamma_{1n} = (\omega^2 \delta_2^2/3 - n^2)/f(n) \quad \text{and} \quad \gamma_{2n} = in / f(n) \quad (5.34)$$

$$\text{In (5.34): } f(n) = -n^6 + a_1 n^4 - a_2 n^2 + a_3$$

with

$$a_1 = 2 + \frac{\delta^2}{3} \Omega^2, \quad a_2 = 1 - \Omega^2 (1 - \frac{2}{3} \frac{\delta^2}{\Omega^2}),$$

$$a_3 = \Omega^2 \left\{ 1 + \frac{\delta^2}{3} (1 - \Omega^2) \right\}$$

The pressure amplitudes  $\bar{P}_{tn}$  and  $\bar{P}_{sn}$  appearing on the right hand side of (5.33) are not known and are dependent on  $\bar{U}(\theta)$ . These can be determined using the boundary conditions on internal and external pressures which are given by

$$(i) \quad \left. \frac{\partial p_t}{\partial r} \right|_{r=R_2} = - \rho_1^a \frac{\partial^2 u}{\partial t^2} \quad (5.35)$$

$$\text{and (ii)} \quad \left. \frac{\partial(p_o + p_s)}{\partial r} \right|_{r=R_2} = - \rho_2^a \frac{\partial^2 u}{\partial t^2} \quad (5.36)$$

where  $\rho_1^a$  and  $\rho_2^a$  are the densities of inside and outside acoustic mediums, respectively.

Following the procedure outlined in the previous section, (5.35) and (5.36), transform to

$$\bar{U} = f_1 \sum_{n=-\infty}^{\infty} \bar{P}_{tn} \frac{H^{(1)}}{H^{(1)}} e^{-in\theta} \quad (5.37)$$

$$\text{and } \bar{U} = f_2 \left\{ \bar{P}_{il} \frac{J'}{J} e^{il\theta} + \sum_{n=-\infty}^{\infty} \bar{P}_{sn} \frac{H^{(2)}}{H^{(2)}} e^{-in\theta} \right\} \quad (5.38)$$

respectively,

$$\text{where } f_1 = 1 / \bar{\rho}_1^a \Omega \bar{c}_1 \quad \text{and} \quad f_2 = 1 / \bar{\rho}_2^a \Omega \bar{c}_2$$

$$\text{with } \bar{\rho}_1^a \left( = \frac{\rho_1^a b R_2^2}{m_2} \right), \quad \bar{\rho}_2^a \left( = \frac{\rho_2^a b R_2^2}{m_2} \right) \text{ as the}$$

non-dimensional densities of the inside and outside media, respectively and  $\bar{c}_1 (= \frac{\omega}{k_1 R_2} \sqrt{\frac{m_2}{D_2}})$ ,  $\bar{c}_2 (= \frac{\omega}{k_2 R_2} \sqrt{\frac{m_2}{D_2}})$  as the non-dimensional sound velocities in those media.

It should be understood that argument for  $J$ ,  $J'$ ,  $H^{(2)}$  and  $H^{(2)'}$  is  $k_2 R_2$  and that for  $H^{(1)}$  and  $H^{(1)'} = k_1 R_2$ . Here also, prime denotes derivative with respect to the argument.

In the above equations, expressing  $\bar{U}$  in terms of space harmonics (see section 5.5) and eliminating  $\bar{P}_{tn}$  and  $\bar{P}_{sn}$  from (5.33), displacement solutions of the structure can be obtained as

$$\begin{aligned}\bar{U}(\theta) &= \sum_{j=1}^6 c_j (e^{s_j \theta} - \sum_{\substack{n=1 \\ n \neq l, l \pm N}}^{\infty} z_{nj} e^{in \theta}) \\ &\quad - \bar{P}_{il} \gamma_{1l} \bar{f}_1 e^{il \theta} \quad (5.39a)\end{aligned}$$

$$\begin{aligned}\text{and } \bar{V}_2(\theta) &= \sum_{j=1}^6 (B_j e^{s_j \theta} - c_j \sum_{\substack{n=1 \\ n \neq l, l \pm N}}^{\infty} \bar{z}_{nj} e^{in \theta}) \\ &\quad - \bar{P}_{il} \gamma_{2l} \bar{f}_1 e^{il \theta} \quad (5.39b)\end{aligned}$$

where  $z_{nj} = \gamma_{1n} z_{nj}$ ,  $\bar{z}_{nj} = \gamma_{2n} z_{nj}$ ,

$$\begin{aligned}z_{nj} &= \frac{x_n \{ e^{(s_j + il)\lambda} - 1 \}}{\{ \frac{H^{(2)'}}{H^{(2)}} f_2 + \gamma_{1n} x_n \} (s_j + in)\lambda} \\ \bar{f}_1 &= \{ \frac{\bar{x}_1 (H^{(2)'} / H^{(2)}) - x_1 (J' / J)}{(H^{(2)'} / H^{(2)}) f_2 + \gamma_{1l} x_1} \}\end{aligned}$$

with

$$X_n = \left( 1 - \frac{f_2}{f_1} \frac{\frac{H^{(1)}}{H^{(1)}}, \frac{H^{(2)}}{H^{(2)}}}{\frac{H}{H}} \right) \text{ and}$$

$$\bar{X}_1 = \left( 1 - \frac{f_2}{f_1} \frac{\frac{H^{(1)}}{H^{(1)}}, \frac{J'}{J}}{\frac{H}{H}} \right).$$

## 5.7 RESULTS AND DISCUSSION

### 5.7.1 Two Layered Ring

Numerical results presented in Figs. 5.1 - 5.5 are obtained with the following data :  $\delta_1 = 0.04$ ,  $\delta_2 = 0.02$ ,  $E_1/E_3 = 0.001$ ,  $\rho_1/\rho_2 = 0.2$ ,  $N = 3$ ,  $\bar{k}_r = 0$ ,  $\bar{P}_o = 1$ ,  $\bar{\rho}_1^a = 0.05$ ,  $\bar{c}_1 = 5.0$ ,  $\beta = 0$  and 1,  $l = 1, 2$  and 3.

Figures 5.1 and 5.2 show the response curves for an undamped ring with first and third harmonics ( $l = 1$  and 3). The effect of damping on response is same as explained in the previous chapter and hence not shown. It can be seen that when the interior is considered to be totally resonant ( $\alpha = 0.0$ ) resonances in addition to the ones shown for in vacuo response (Figs. 4.1 and 4.3) are present. This is due to coupling between the vibration of the structure and the wave motion within the structure. The frequencies corresponding to the additional peaks can be identified to be the cavity resonances which are given by the roots of the equation  $J'_n(k_1 R_2) = 0$  [28, 34]. The other peaks corresponding

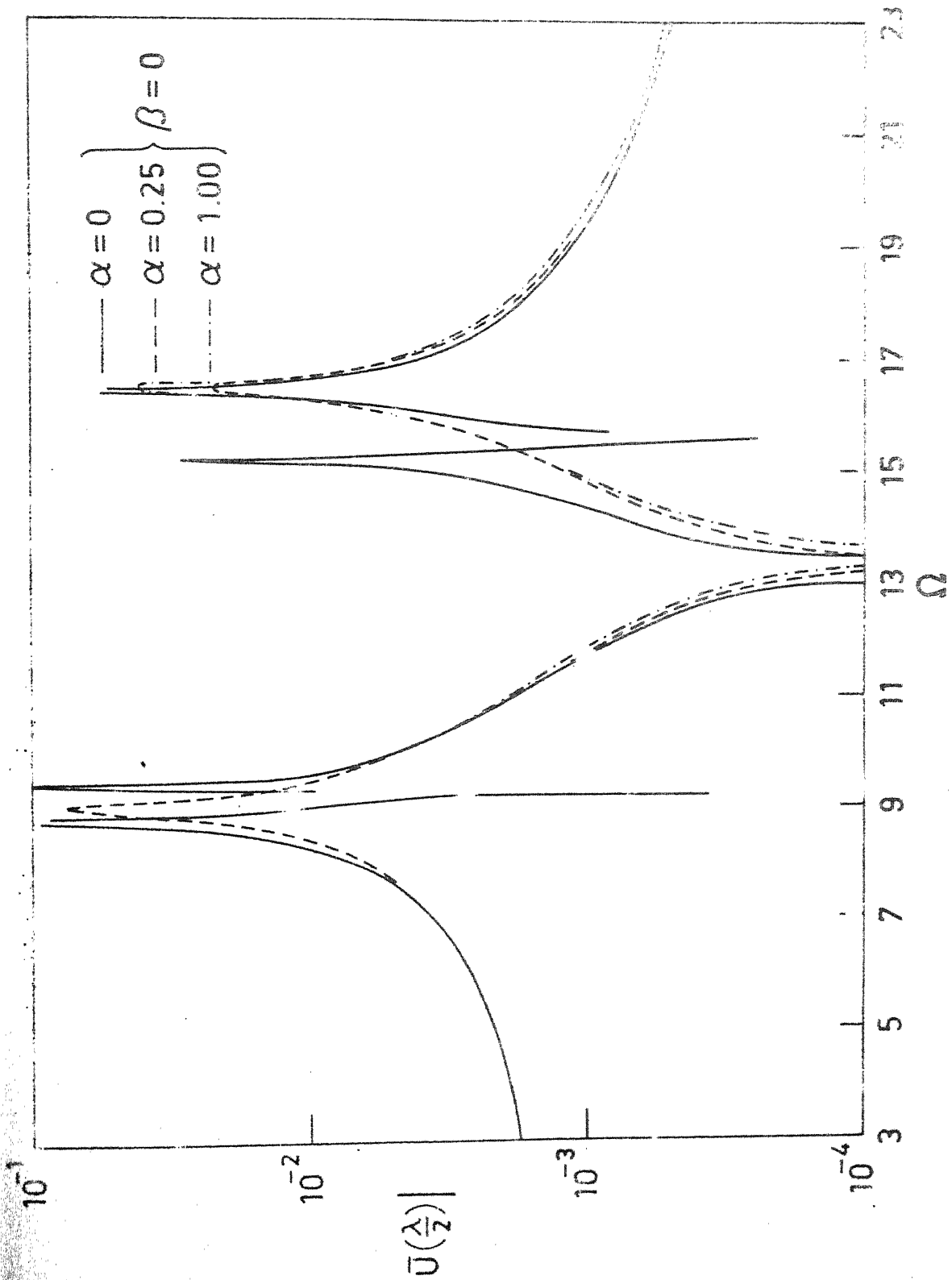


FIG. 5.1. RESPONSE OF TWO LAYERED RINGS, I = 1

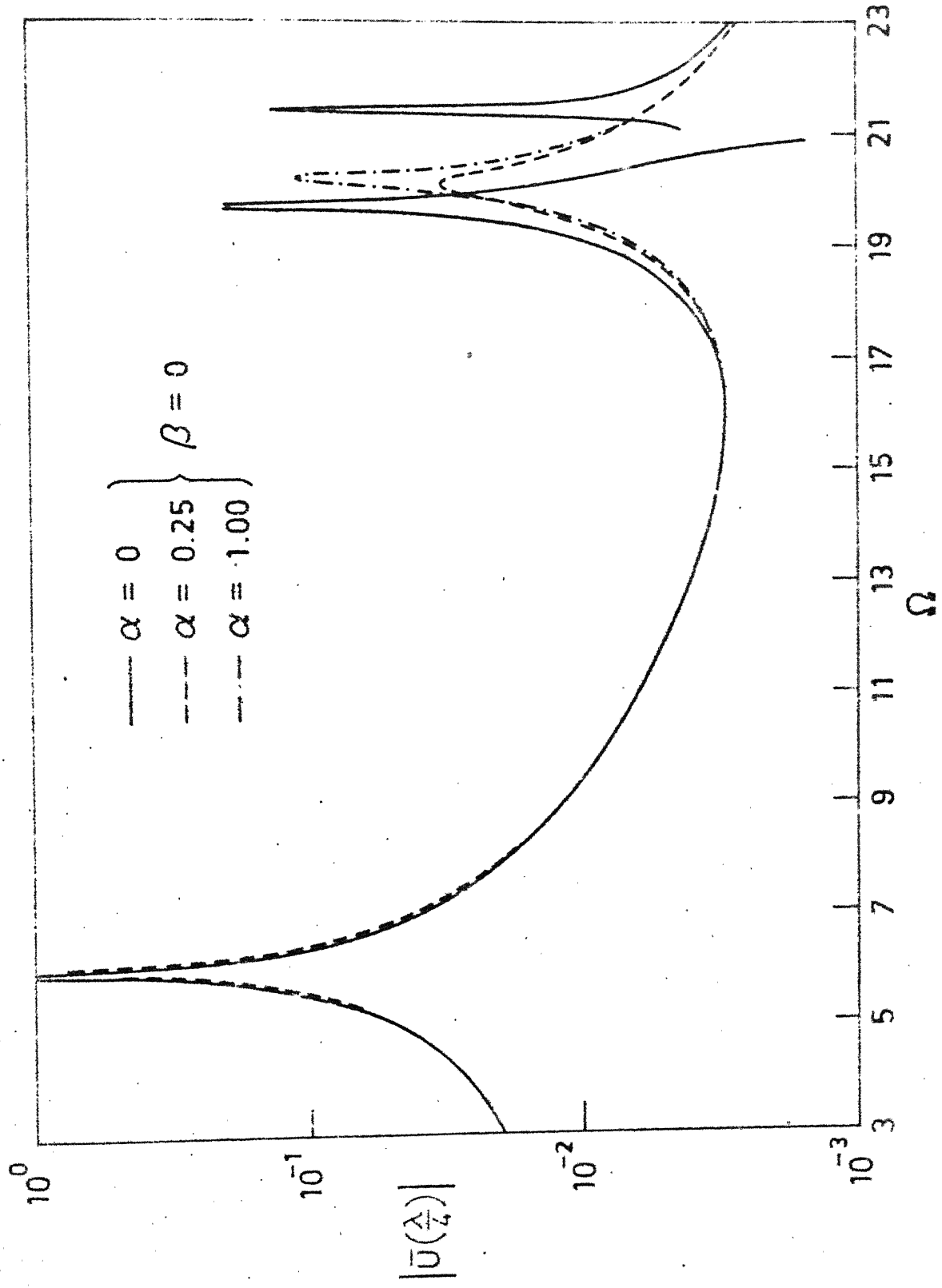


FIG. 5.2 RESPONSE OF TWO LAYERED RING,  $I = 3$ .

to the natural modes of the structure are occurring at lower values of frequencies compared to the natural frequencies. This difference is very marginal if a cavity resonant frequency is close to that natural frequency and is negligible otherwise. However, with an absorbing interior ( $\alpha \neq 0$ ), the cavity resonances disappear and only the natural modes are excited exactly at the natural frequencies of the structure. When compared to partially absorbing interior ( $\alpha = 0.25$ ), totally absorbing interior is seen to result in higher peaks. Away from the peaks, the responses with  $\alpha = 1$  and  $0.25$  are nearly the same.

From (5.23) it is obvious that for a resonant interior ( $\alpha = 0$ ), the sound power transmitted (SP) is zero. With  $\alpha = 0.25$  and  $1.0$ , the variation of SP with frequency is shown in Figs. 5.3 - 5.5 for different pressure harmonics ( $l = 1, 2$  and  $3$ ). It may be observed that SP is maximum at the resonance frequencies where the in vacuo response is also maximum. When the interior is totally absorbent it is less than that with a partially absorbing one ( $\alpha = 0.25$ ). With the introduction of damping ( $\beta = 1$ ) in the structure, SP is reduced considerably only at the peaks as expected.

### 5.7.2 Three Layered Ring

Numerical results presented in Figs. 5.6 - 5.10 are obtained with the following data:  $\delta_1 = 0.015$ ,

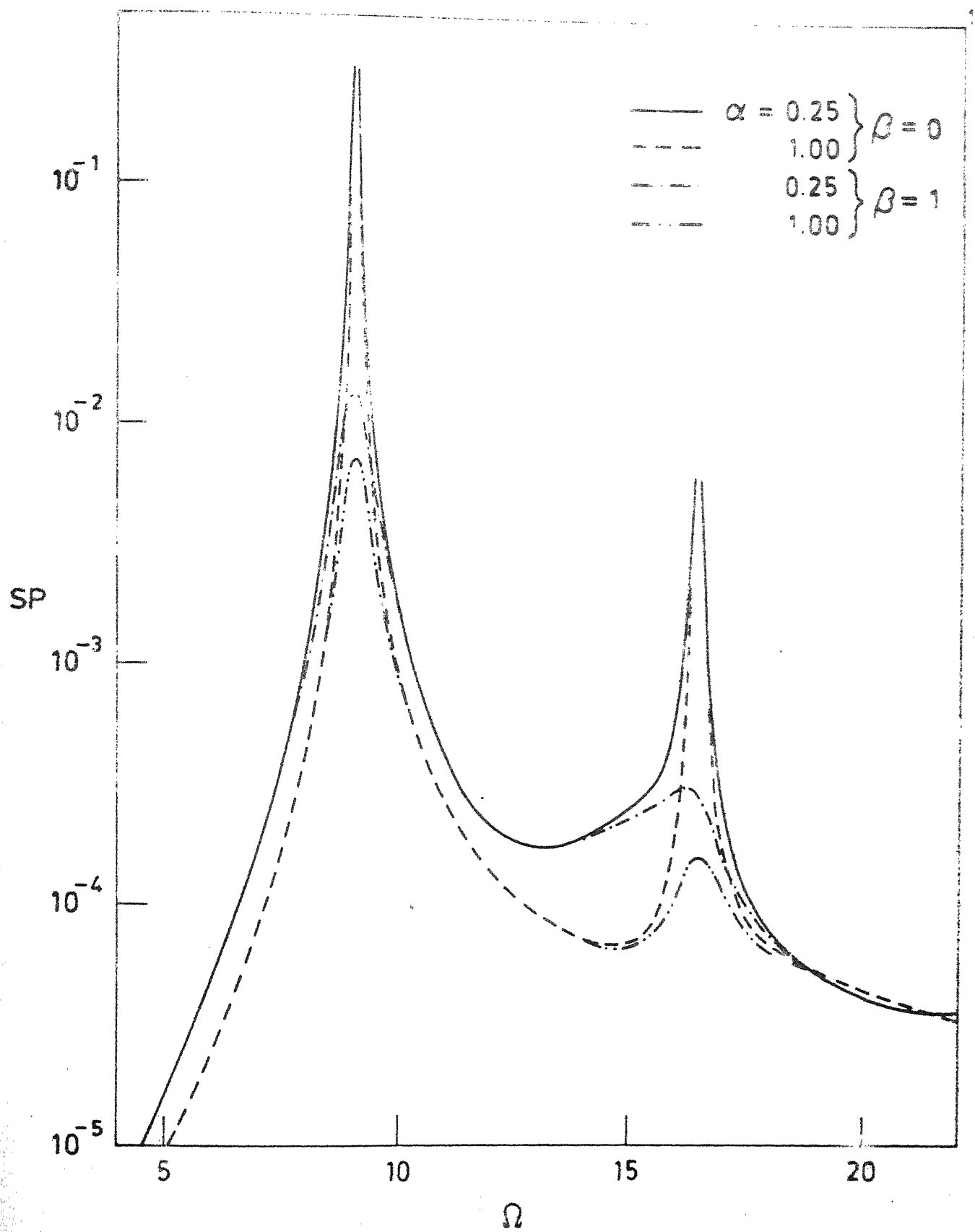


FIG. 5.3. VARIATION OF SOUND POWER WITH FREQUENCY,  
TWO LAYERED RING,  $I=1$ .

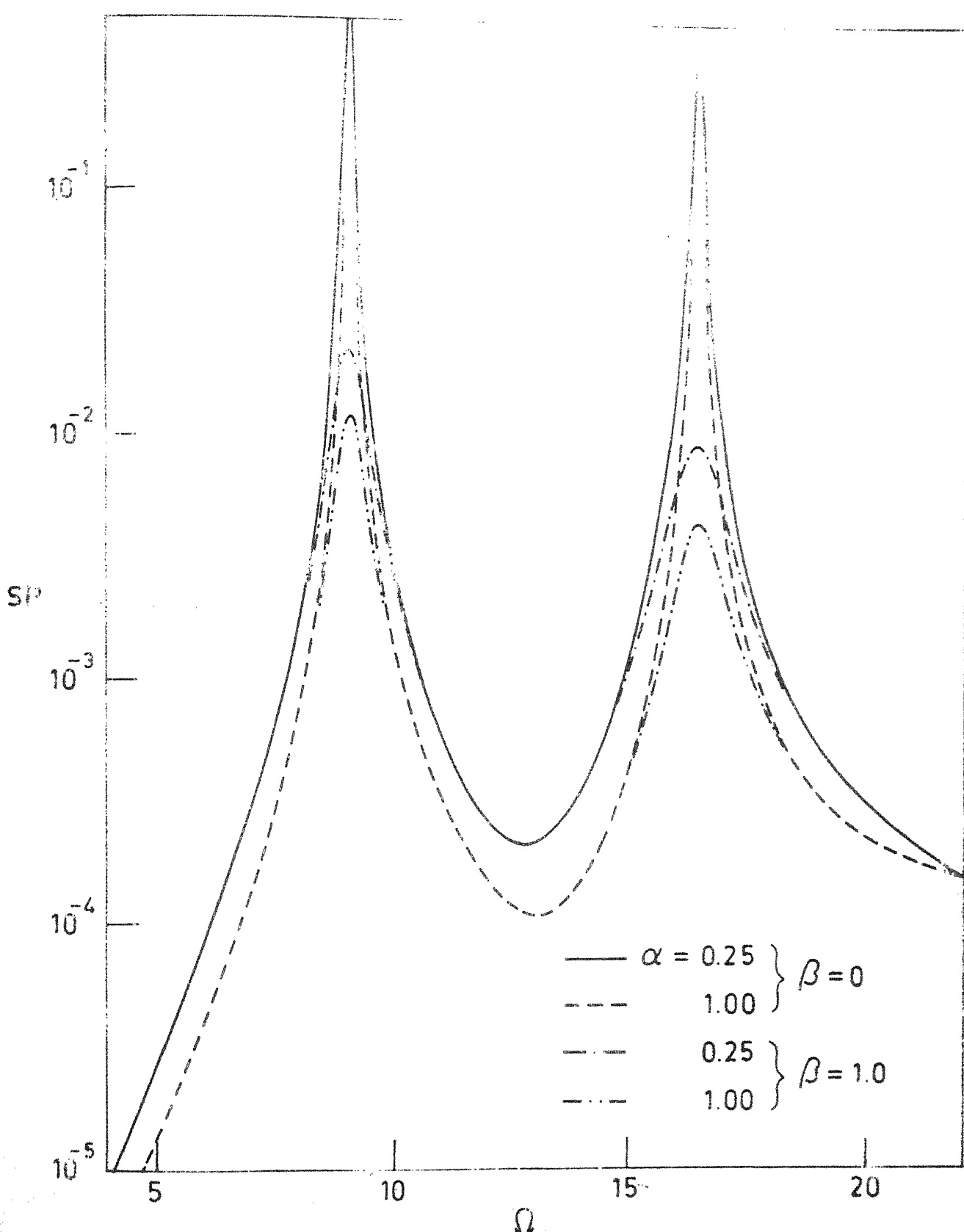


FIG. 5.4. VARIATION OF SOUND POWER WITH FREQUENCY,  
TWO LAYERED RING,  $l=2$ .

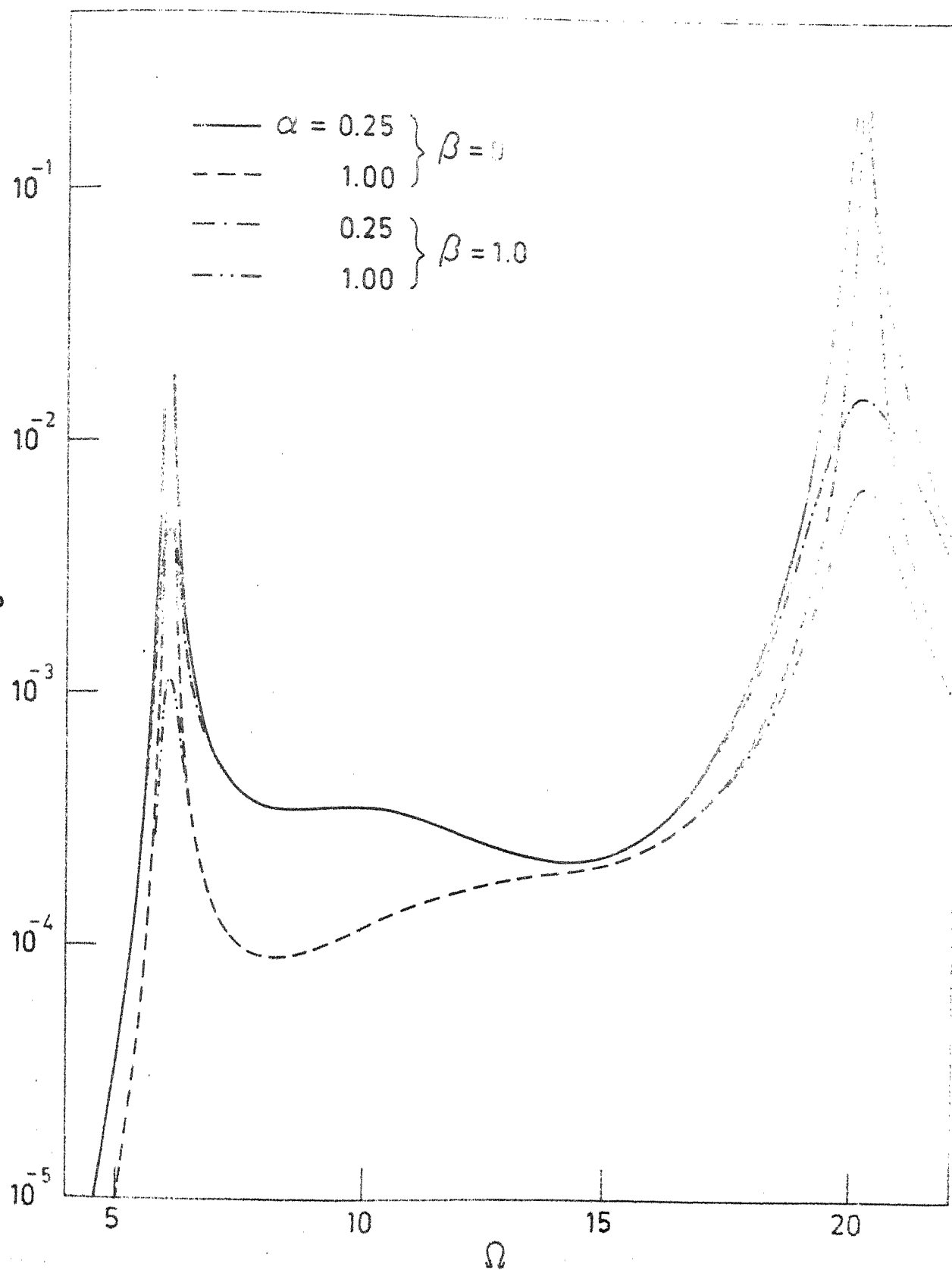


FIG. 5.5. VARIATION OF SOUND POWER WITH FREQUENCY;  
TWO LAYERED RING,  $l = 3$ .

$\delta_2 = 0.03, \delta_3 = 0.03, E_1/E_3 = 1, \rho_1/\rho_3 = 1,$   
 $G/E_3 = 10^{-4}, \rho_2/\rho_3 = 0.2, k_r = 0, N = 3,$   
 $\bar{P}_o = 1, \bar{\rho}_1^a = 0.05, \bar{c}_1 = 5.0, \beta = 0 \text{ and } 1, l = 1, 2$   
and 3.

Figures 5.6 and 5.7 show the response of the three layered ring for pressure harmonics  $l = 1$  and 3. Here also, the curves show characteristics similar to the two layered ring case. In Fig. 5.7, the resonant peak corresponding to the tangential mode (defined in Chapter 3) is present irrespective of the characteristic of the interior. SP for the harmonics  $l = 1, 2$  and 3 is shown in Figs. 5.8 - 5.10. These curves also are very similar to the corresponding ones in the two layer case.

Figure 5.11 shows the effectiveness of damping treatment with unconstrained and constrained layers. For the sake of comparison the thicknesses of core and base layers in the three layered ring are taken to be same as those of the outer and inner layers in the two layered ring (data is same as that for Fig. 4.12). The constrained layer treatment is seen to be more effective in reducing the sound power transmitted at the resonances.

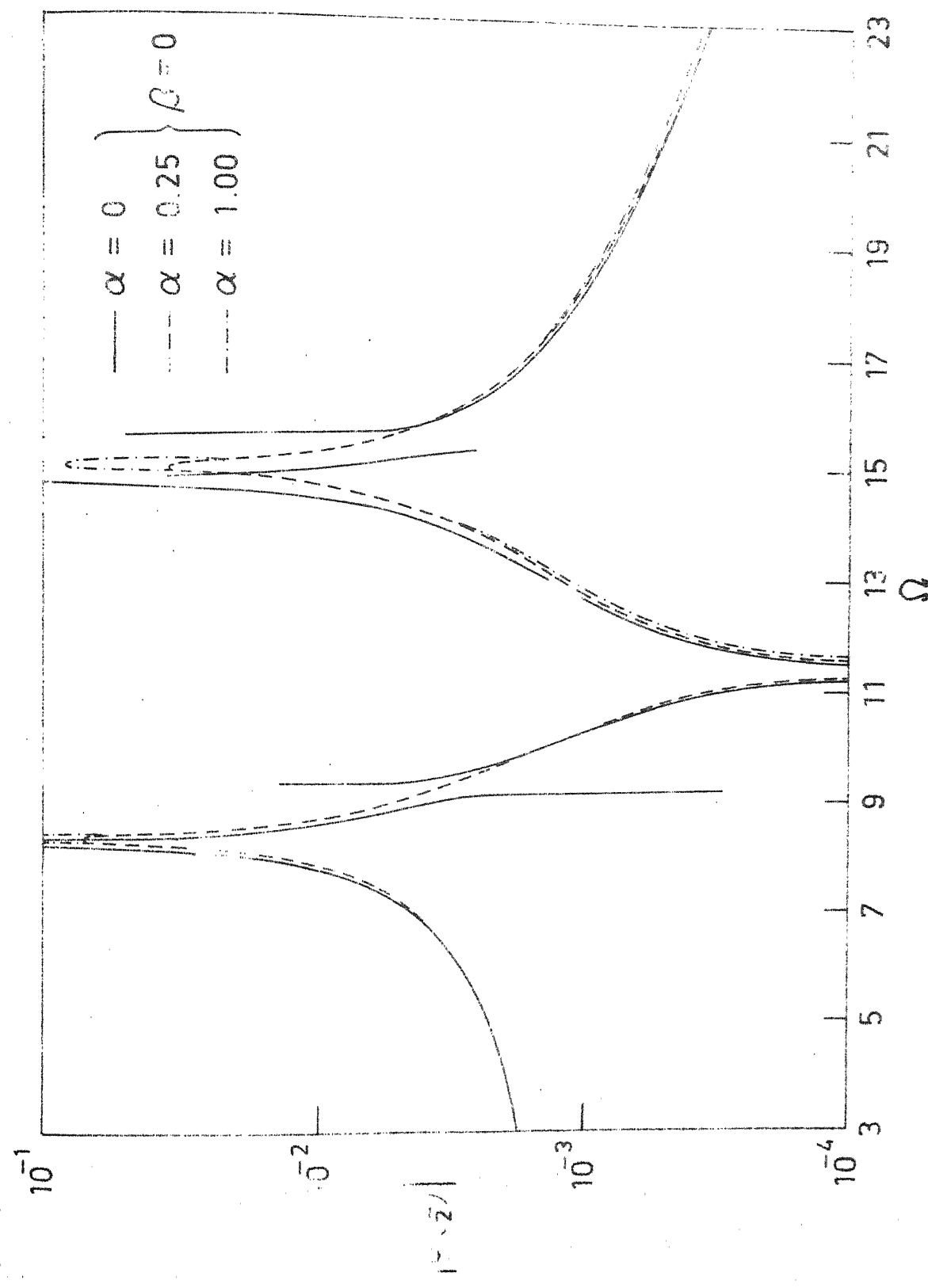


FIG. 5.6. RESPONSE OF THREE LAYERED RING,  $l=1$ .

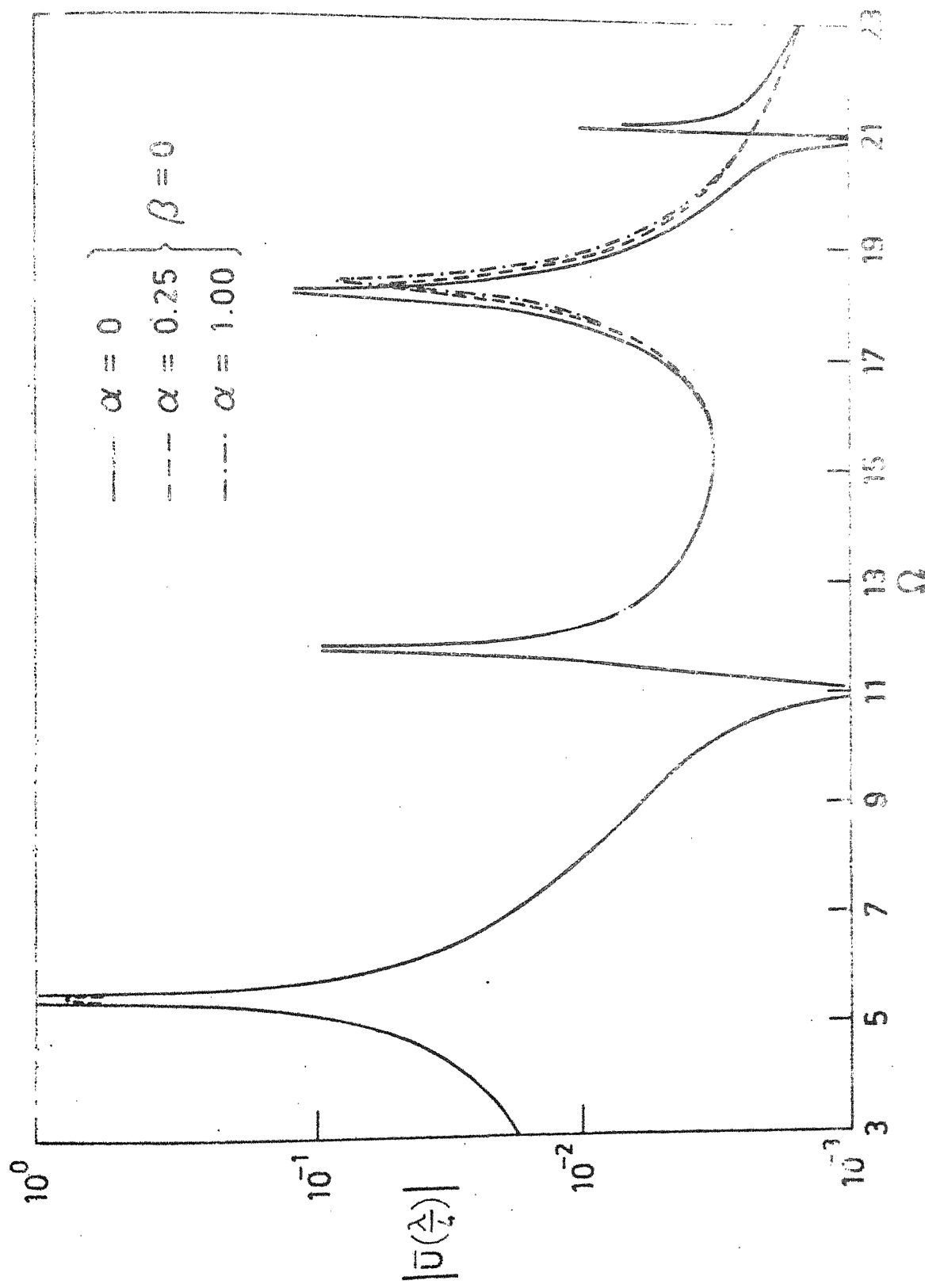


FIG. 5.7. RESPONSE OF THREE LAYERED ZING.

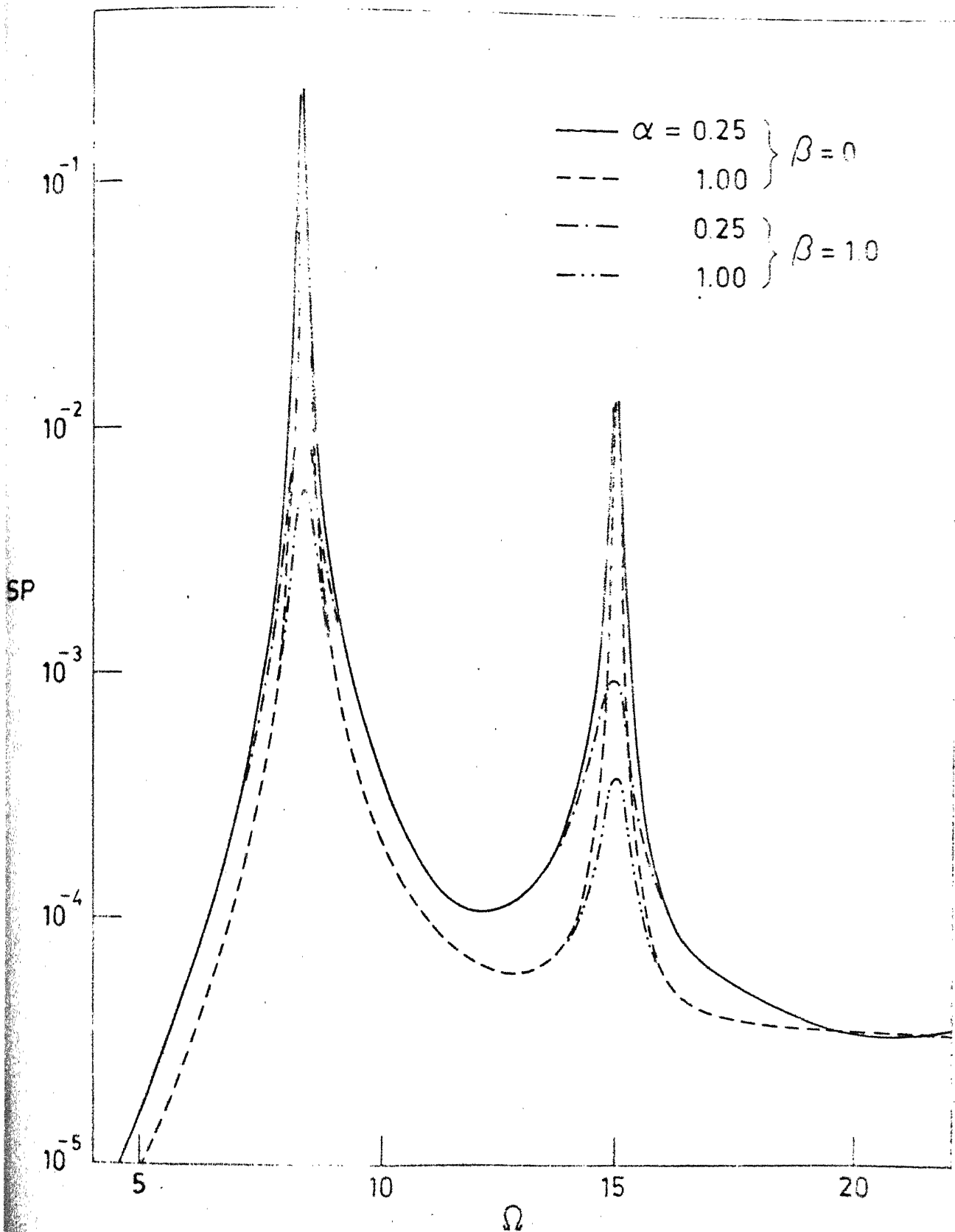


FIG. 5.8. VARIATION OF SOUND POWER WITH FREQUENCY,  
THREE LAYERED RING,  $l=1$ .

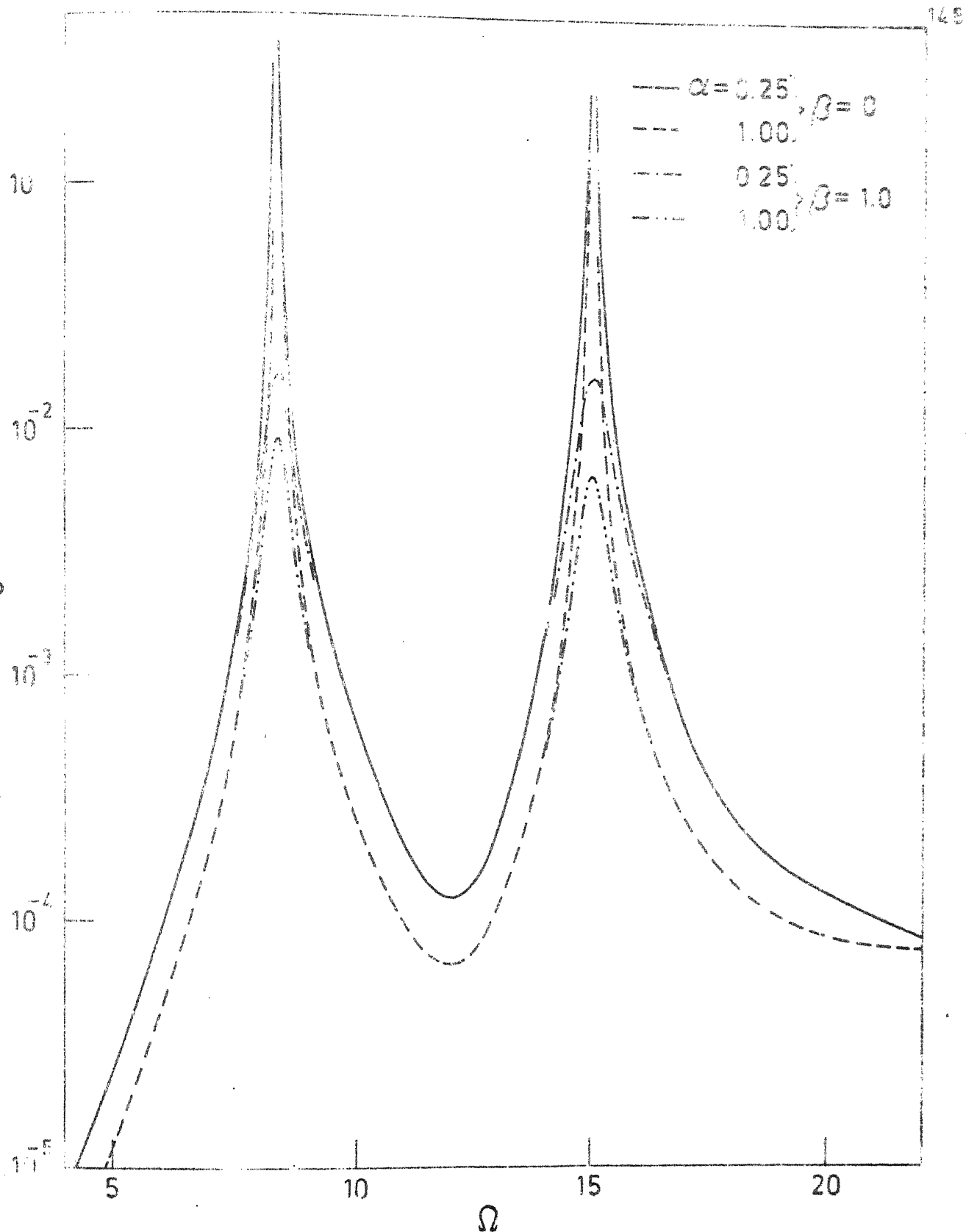


FIG. 5.9. VARIATION OF SOUND POWER WITH FREQUENCY,  
THREE LAYERED RING,  $l = 2$ .

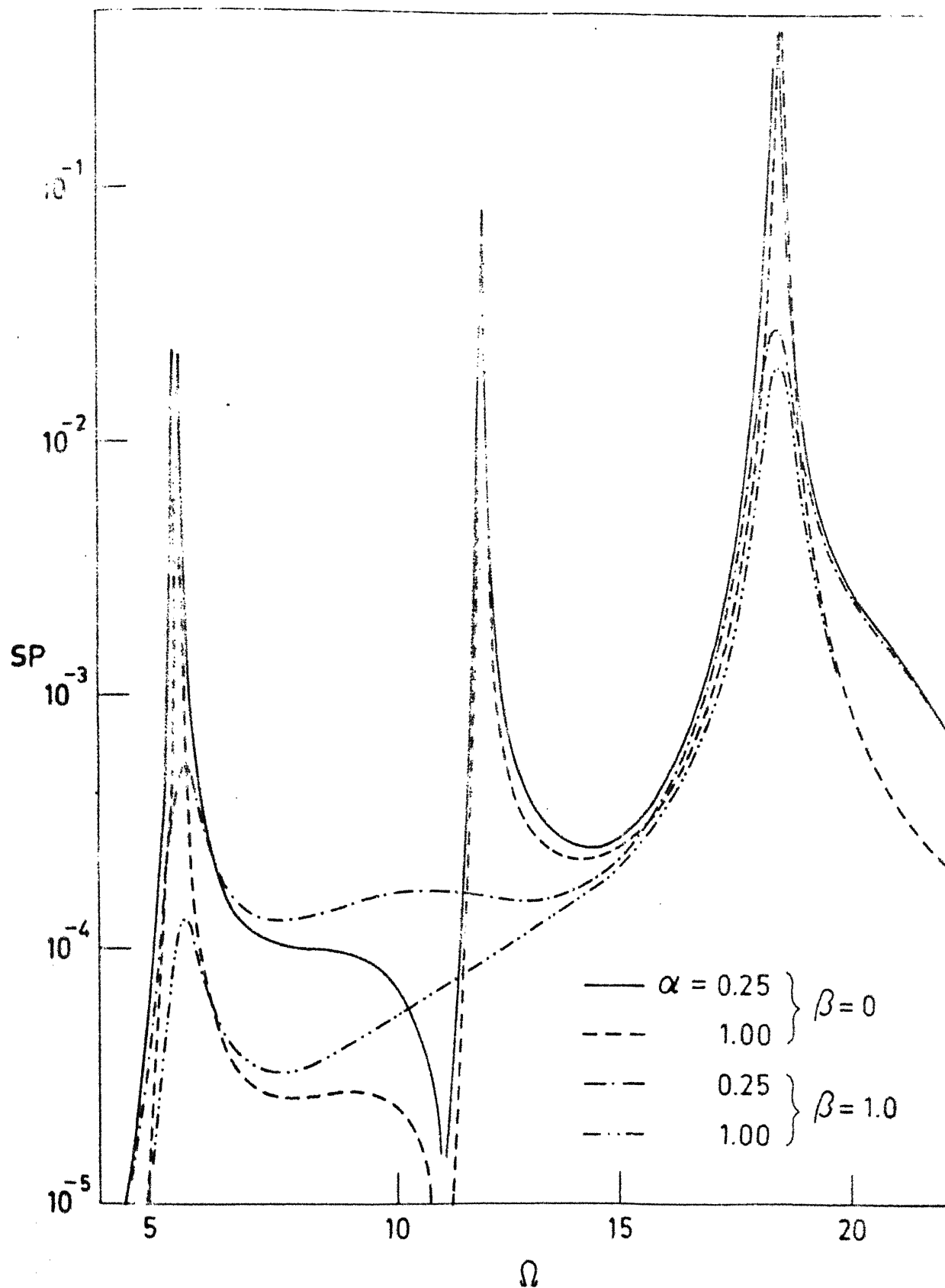


FIG. 5.10. VARIATION OF SOUND POWER WITH FREQUENCY  
THREE LAYERED RING,  $I=3$ .

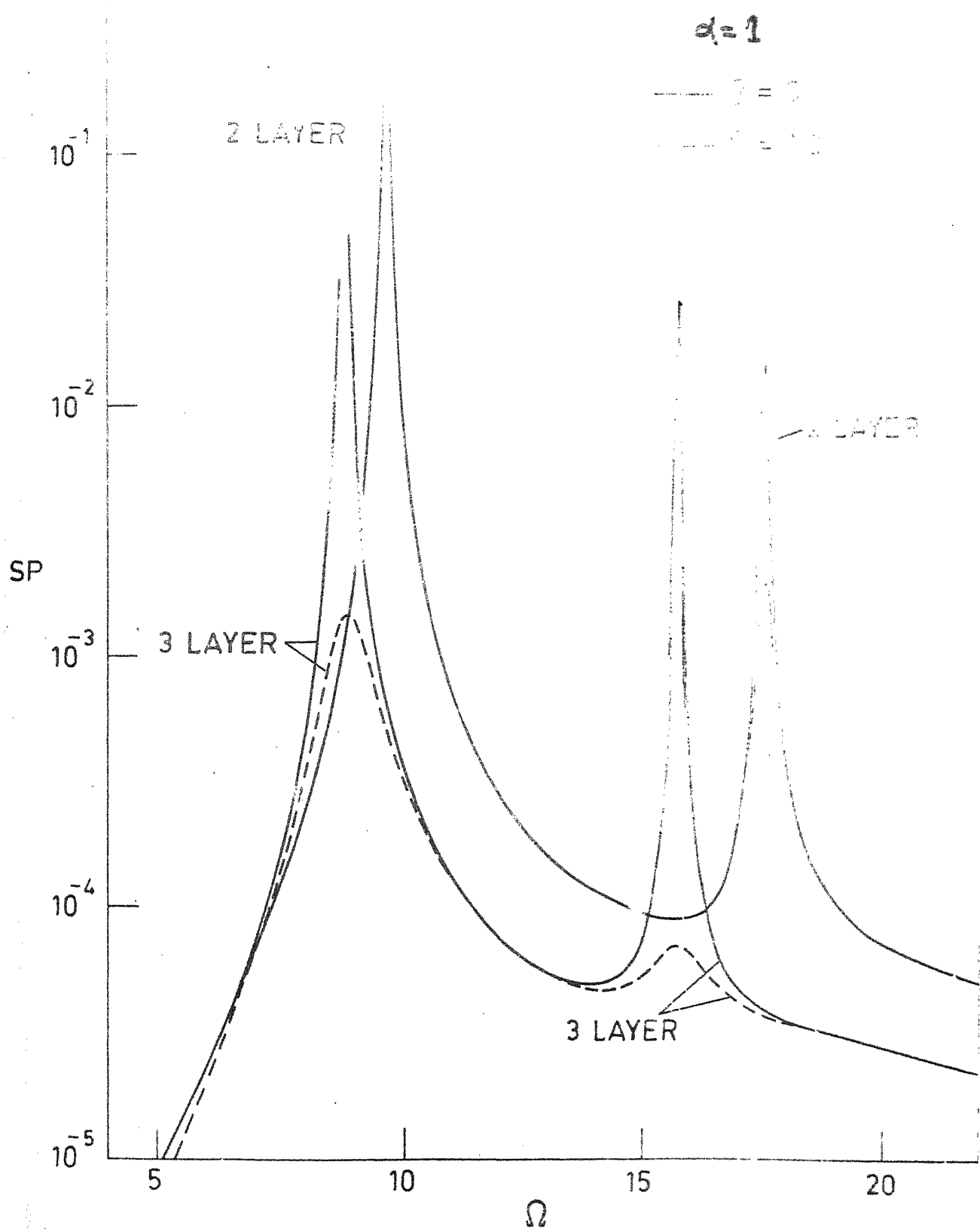


FIG. 5.11. COMPARISON OF SOUND POWER IN TWO (MONO-COUPLED) AND THREE (BI-COUPLED) LAYERED RINGS,  $\Gamma = 1$ .

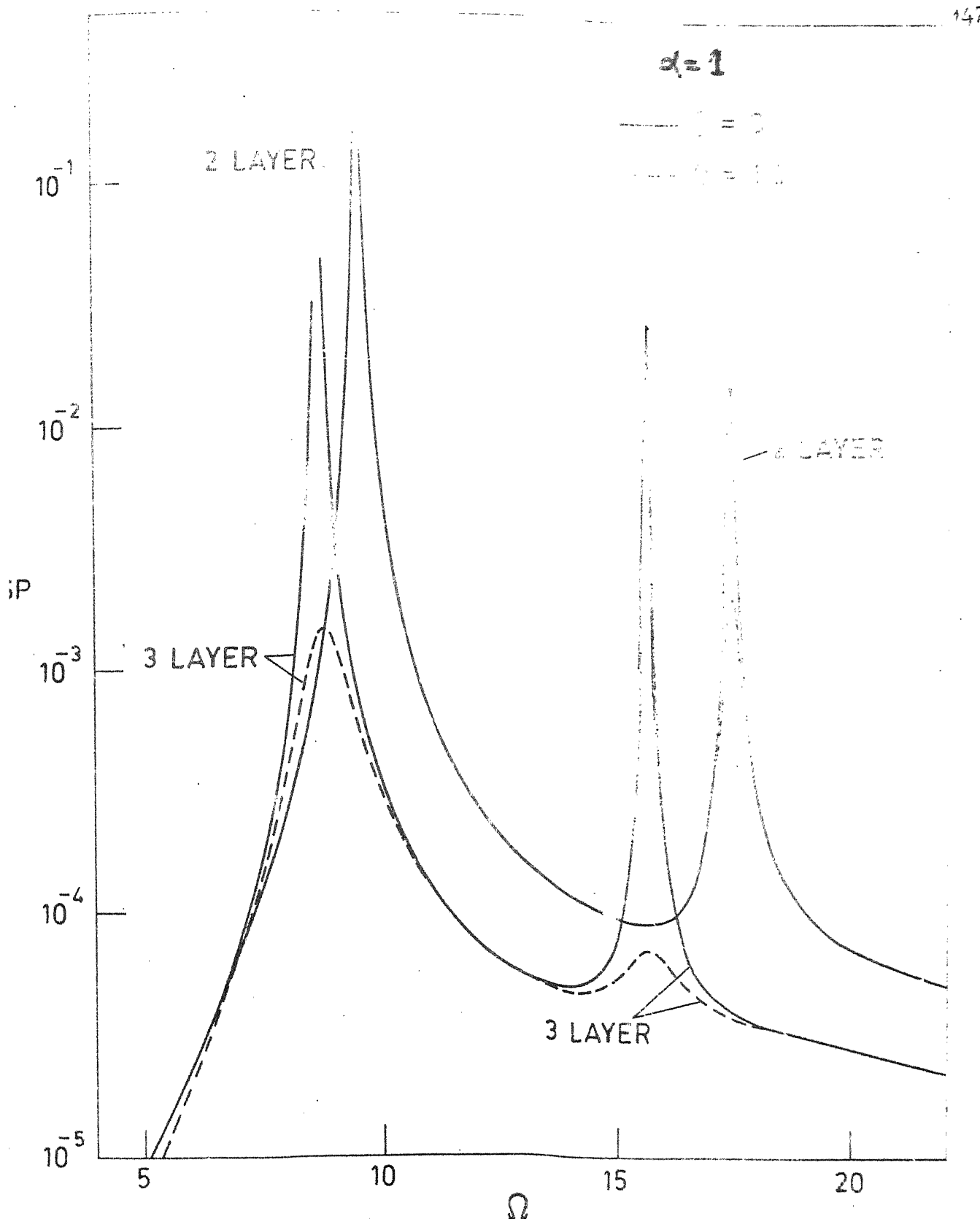


FIG. 5.11. COMPARISON OF SOUND POWER IN TWO (MONO-COUPLED) AND THREE (BI-COUPLED) LAYERED RINGS  
I - 1

## CHAPTER 6

### CONCLUSIONS

This thesis presents a theoretical analysis of free and forced vibrations of layered rings on periodic radial supports. Differential equations and boundary conditions are set up for a single bay of two and three layered rings through a variational approach. These are more accurate than those reported in earlier works. Determination of non-degenerate normal modes of endless periodic structures are posed as an eigen-value problem. For both two and three layered rings, propagation constant curves of an elastic ring are seen to reveal some important characteristics of the damped structures. Natural frequencies of an elastic ring which can be obtained from these curves, provide the first step for computation of the resonant frequencies and the associated modal loss factors. Specific conclusions obtained from parametric investigation of rings on three radial supports are listed below.

#### Free Vibration of a Two Layered Ring:

- i) The basic nature of the propagation constant curves and mode shapes remain same as those of a single layer ring.
- ii) When the rotational stiffness is present at the supports, the first mode has a predominant rigid-body rotation with a low natural frequency.

The associated modal loss factor is also small (compared to those at other modes) due to less bending deformation.

- iii) In the absence of rotational stiffness, the modal loss factor for mono-coupled and bi-coupled systems is independent of the modes as observed in the case of beams. But this is not so with the tri-coupled system. For all the systems, however, the loss factor decreases with the introduction of rotational stiffness and the amount of decrease is different for different modes.
- iv) The resonant frequency of the damped ring is nearly independent of loss factor of the visco-elastic layer ( $\beta$ ), whereas the modal loss factor has a linear dependence on  $\beta$ .

#### Free Vibration of a Three Layered Ring:

- 9) With an elastic core capable of transmitting only shear, the additional propagation constant curve can be associated with the extra degree of freedom, i.e., the tangential displacement of the outer layer. The Mode, associated with the natural frequency obtained from this curve, has predominant tangential motion. At the corresponding resonant frequency of the damped ring, the loss factor is also high as the

shear deformation is large. This mode, in the tri-coupled system, has a purely tangential motion with no radial displacement associated with it.

- ii) There exists a combination of thicknesses of the layers which gives rise to maximum modal loss factor. For a given value of the base layer thickness, the core and the constraining layer thicknesses can be chosen suitably to yield a maximum possible loss factor.
- iii) The introduction of rotational stiffness at the supports decreases the loss factor as observed in the case of a two layered ring.
- iv) When the core shear modulus and the thicknesses are such that the 'tangential mode' frequency is very near to a flexural mode (with  $\mu_{in} = 0$ ) frequency there will be an increase in the flexural mode loss factor and a decrease in the 'tangential mode' loss factor.
- v) There exists an optimum value of core shear modulus which gives rise to the maximum composite modal loss factor.
- vi) With the increase in the core loss factor, resonant frequencies increase marginally and the amount of increase depends upon the thicknesses of the layers.

## Response and Sound Transmission:

- i) The pressure harmonics with  $l = jN$ ,  
 $j = 1, 2, 3, \dots$  can excite all the modes having identical shapes in each bay, whereas the other harmonics can excite the remaining degenerate modes. The constant pressure loading (i.e.,  $l = 0$ ) can excite only the symmetric modes with identical shapes in each bay.
- ii) The tangential mode, present in the case of a three layered ring, also responds to pressure harmonics  $l = j N$ ,  $j = 1, 2, \dots$  for a bi-coupled system. Moreover, damping in the core is very effective in controlling the resonant peak corresponding to this mode. For the tri-coupled systems, however, the 'pure' tangential modes are not excited by the radial loading.
- iii) As expected, the viscoelastic damping treatment reduces the response considerably only near the resonances and is detrimental near the anti-resonances. When compared to unconstrained damping treatment, constrained treatment is more effective in controlling the resonant response.
- iv) When the effect of acoustic pressure inside the structure is considered, the response shows additional peaks in addition to those at natural frequencies. These additional peaks, called

'cavity resonances', are present only for a totally resonant interior. The totally absorbent interior results in higher peaks compared to those with partially absorbing one. Away from the peaks, the response is almost independant of the type of the interior region.

- v) Only for a non-resonant interior, the sound power transmitted inside the structure is non-zero and the maximum occurs at resonant frequencies. The maximum sound power is transmitted for a partially absorbent interior (i.e. with  $\alpha < 1$ ). The viscoelastic damping in the structure reduces the sound power considerably only at the peaks.
- vi) As observed in the case of response, constrained damping treatment is more effective in reducing the sound power transmitted at the resonant frequencies.
- vii) When the acoustic coupling is considered, the method given in reference [37] to find the response is modified. In the present work, the number of linear equations to be solved is equal to the number of support conditions, whereas in reference [37], it is equal to the number of terms chosen in the space harmonic series.

## REFERENCES

1. Heckl, M., "Investigations on the Vibrations of Grillages and Other Simple Beam Structures", Journal of Acoustical Society of America, Vol. 36, pp. 1335-1343, 1964.
2. Mead, D.J., "Free Wave Propagation in Periodically Supported, Infinite Beams", Journal of Sound and Vibration, Vol. 11, pp. 181-197, 1970.
3. Mead, D.J., "A General Theory of Harmonic Wave Propagation in Linear Periodic Systems with Multiple Coupling", Journal of Sound and Vibration, Vol. 27, pp. 235-260, 1973.
4. Mead, D.J., "Wave Propagation and Natural Modes in Periodic Systems: I. Mono-Coupled Systems", Journal of Sound and Vibration, Vol. 40, pp. 1-18, 1975.
5. Mead, D.J., "Wave Propagation and Natural Modes in Periodic Systems: II. Multi-Coupled Systems, with and Without Damping", Journal of Sound and Vibration, Vol. 40, pp. 19-39, 1975.
6. Sengupta, G., "Natural Flexural Waves and the Normal Modes of Periodically Supported Beams and Plates", Journal of Sound and Vibration, Vol. 13, pp. 89-101, 1970.
7. Mallik, A.K. and Mead, D.J., "Free Vibration of Thin Circular Rings on Periodic Radial Supports", Journal of Sound and Vibration, Vol. 54, pp. 13-27, 1977.
8. Rao, S.S. and Sundararajan, V., "In-plane Flexular Vibration of Circular Rings", Journal of Applied Mechanics, Design Data and Methods, Trans. ASME, Vol. 36, pp. 620-625, 1969.
9. Sahay, K.B. and Sundararajan, V., "Vibration of a Stiffened Ring Considered as a Cyclic Structure", Journal of Sound and Vibration, Vol. 22, pp. 467-473, 1972.
10. McDaniel, T.J., "Dynamics of Circular Periodic Structures", Journal of Aircraft, Vol. 8, pp. 143-149, 1971.

11. Murthy, V.R. and Nigam, N.C., "Dynamic Characteristics of Stiffened Rings by Transfer Matrix Approach", *Journal of Sound and Vibration*, Vol. 39, pp. 237-245, 1975.
12. Singh, K. and Dhoopar, B.L., "Free Vibration of Circular Rings on Radial Supports", *Journal of Sound and Vibration*, Vol. 65, pp. 297-301, 1979.
13. Almy, C.R. and Nelson, F.C., "Damping of a Circular Ring Segment by constrained Viscoelastic Layer", *Shock and Vibration Bulletin*, Vol. 42, pp. 121-124, 1972.
14. Lu, Y.P., Douglas, B.E. and Thomas, E.V., "Mechanical Impedance of Damped Three-Layered Sandwich Rings", *AIAA Journal*, Vol. 11, pp. 300-304, 1973.
15. DiTaranto, R.A., Lu, Y.P. and Douglas, B.E., "Forced Response of a Discontinuously Constrained Damped Ring", *Journal of the Acoustical Society of America*, Vol. 54, pp. 74-79, 1973.
16. Lu, Y.P., "An Analytical Formulation of the Forced Responses of Damped Rings", *Journal of Sound and Vibration*, Vol. 48, pp. 27-33, 1976.
17. Lu, Y.P., "A Note on the Forced Responses of Damped Rings", *Journal of the Acoustical Society of America*, Vol. 65, pp. 1329-1331, 1979.
18. DiTaranto, R.A., "Free and Forced Response of a Laminated Ring", *Journal of the Acoustical Society of America*, Vol. 53, pp. 748-757, 1973.
19. Nelson, F.C. and Sullivan, D.F., "The Forced Vibration of Three-Layer Damped Circular Ring", *American Society of Mechanical Engineers, Paper No. 77-DET-154*, 1977.
20. Sagartz, M.J., "Response of a Thre-Layered Ring to an Axisymmetric Impulse", *AIAA Journal*, Vol. 12, pp. 390-392, 1974.
21. Sagartz, M.J., "Transient Response of Thre-Layered Rings", *Journal of Applied Mechanics, Trans. ASME*, Vol. 99, pp. 299-303, 1977.
22. Forrestal, M.J. and Overmier, D.K., "An Experiment on an Impulse Loaded Ring", *AIAA Journal*, Vol. 12, pp. 722-724, 1974.

23. Cremer, L., Heckl, M. and Ungar, E.E., Structure-Borne Sound, Springer Verlag, Heidelberg, New York, 1973.
24. Junger, M.C. and Feit, D., Sound, Structures, and their Interaction, The MIT Press, Cambridge, Massachusetts, and London, England, 1972.
25. Lyon, R.H. and Smith, P.W., Sound and Structural Vibration, NASA, CR-160, 1965.
26. Lyon, R.H., Statistical Energy Analysis of Dynamical Systems: Theory and Application, The MIT Press, Cambridge, Massachusetts; and London, England, 1975.
27. Shanbag, R.L., "Sound Transmission Through Sandwich Structures", Ph.D. Thesis, Indian Institute of Technology, Kanpur, 1980.
28. Foxwell, J.H. and Franklin, R.E., "The Vibration of a Thin-Walled Stiffened Cylinder in an Acoustic Field", The Aeronautical Quarterly, Vol. 10, pp. 47-64, 1959.
29. Smith, Jr. P.W., "Sound Transmission Through Thin Cylindrical Shells", Journal of the Acoustical Society of America, Vol. 29, pp. 721-729, 1957.
30. Koval, L.R., "On Sound Transmission into a Thin Cylindrical Shell Under 'Flight Conditions'", Journal of Sound and Vibration, Vol. 48, pp. 265-275, 1976.
31. Koval, L.R., "On Sound Transmission into a Heavily-Damped Cylinder", Journal of Sound and Vibration, Vol. 57, pp. 155-156, 1978.
32. Koval, L.R., "Effect of Stiffening on Sound Transmission into a Cylindrical Shell in Flight", AIAA Journal, Vol. 15, pp. 899-900, 1977.
33. Koval, L.R., "Effect of Longitudinal Stringers on Sound Transmission into a Thin Cylindrical Shell", Sound Transmission into a Thin Cylindrical Shell, Journal of Aircraft, Vol. 15, pp. 816-821, 1978.
34. Koval, L.R., "Effect of Cavity Resonances on Sound Transmission into a Thin Cylindrical Shell", Journal of Sound and Vibration, Vol. 59, pp. 23-33, 1978.

- 35. Pujara, K.K., "Vibrations of and Sound Radiation from Some Periodic Structures Under Convected Loadings", Ph.D. Thesis, University of Southampton, England, 1970.
- 36. Mead, D.J. and Mallik, A.K., "An Approximate Theory for the Sound Radiated from a Periodic Line-Supported Plate", Journal of Sound and Vibration, Vol. 61, pp. 315-326, 1978.
- 37. Mead, D.J. and Pujara, K.K., "Space Harmonic Analysis of Periodically Supported Beams: Response to Convected Random Loading", Journal of Sound and Vibration, Vol. 44, pp. 525-541, 1971.
- 38. Mead, D.J. and Mallik, A.K., "An Approximate Method of Predicting the Response of Periodically Supported Beams Subjected to Random Convected Loading", Journal of Sound and Vibration, Vol. 47, pp. 457-471, 1976.
- 39. Mead, D.J., "The Existence of Normal Modes of Linear Systems with Arbitrary Damping", Proceedings of the Symposium on Structural Dynamics, Paper C5, Loughborough University of Technology, 1970.
- 40. Mead, D.J., "Loss Factors and Resonant Frequencies of Periodic Damped Sandwich Plates", Journal of Engineering for Industry, Trans. ASME, Vol. 98, pp. 75-80, 1976.
- 41. Lang, T.E., "Vibration of Thin Circular Rings", Jet Propulsion Laboratory Technical Report No. 32-261, 1962.
- 42. Mead, D.J., "The Damping Properties of Elastically Supported Sandwich Plates", Journal of Sound and Vibration, Vol. 24, pp. 275-295, 1972.
- 43. Narayanan, S., Verma, J.P. and Mallik, A.K., "Free Vibration of Thin-Walled Open Section Beams with Unconstrained Damping Treatment", Journal of Applied Mechanics, Trans. ASME, Vol. 103, pp. 169-173, 1981.
- 44. Mead, D.J., "Vibration Response and Wave Propagation in Periodic Structures", Journal of Engineering for Industry, Trans. ASME, Vol. 93, pp. 783-792, 1971.
- 45. Snowdon, J.C., Vibration and Shock in Damped Mechanical Systems, John Wiley and Sons, Inc., New York, 1968.

## APPENDIX A

### STRAIN ENERGY OF A SINGLE LAYER RING ELEMENT

In two dimensional polar coordinates, circumferential strain-displacement relation is given by

$$\epsilon_{\theta} = \frac{u}{r} + \frac{1}{r} \frac{\partial v_{\theta}}{\partial \theta} \quad (\text{A.1})$$

where  $u$  and  $v_{\theta}$  are respectively radial and tangential displacements at radius,  $r$ .

By virtue of assumption (i) in section 2.2, the radial strain is zero. Moreover, neglecting the effect of Poisson's ratio, circumferential stress ( $\sigma_{\theta}$ ) - displacement relation can be written as

$$\sigma_{\theta} = E \epsilon_{\theta} = E \left[ \frac{u}{r} + \frac{1}{r} \frac{\partial v_{\theta}}{\partial \theta} \right] \quad (\text{A.2})$$

where  $E$  is the Young's modulus of the material.

Using assumption (ii) of section 2.2, the tangential displacement at any radius, ( $v_{\theta}$ ) can be written in terms of tangential displacement,  $v$ , at the mid-plane of the layer, mid-plane radius,  $R$ , and radial displacement,  $u$ , as

$$v_{\theta} = \frac{(R+z)}{R} v - \frac{z}{R} \frac{\partial u}{\partial \theta} \quad (\text{A.3})$$

$$\text{Now, } \sigma_{\theta} = E \left[ \frac{u}{(R+z)} + \frac{1}{R} \frac{\partial v}{\partial \theta} - \frac{z}{R(R+z)} \frac{\partial^2 u}{\partial \theta^2} \right] \quad (\text{A.4})$$

where  $z$  is the radial distance of any plane from the mid-plane.

This expression for  $\sigma_\theta$  is the same as that given in reference [14].

STRAIN energy,  $\Pi$  of a layer of width  $b$  and thickness  $2h$  can be written as

$$\Pi = \iiint \frac{\sigma_\theta^2}{2E} dv = \frac{E b}{2} \iint_{\theta-h}^{th} \left[ \frac{u}{(R+z)} - \frac{1}{R} \frac{\partial v}{\partial \theta} - \frac{z}{R(R+z)} \frac{\partial^2 u}{\partial \theta^2} \right] dz d\theta \quad (A.5)$$

Carrying out the integration with respect to  $z$  and making the approximation  $\ln \frac{R+h}{R-h} = 2(\frac{h}{R} + \frac{1}{3} \frac{h^3}{R^3})$ ,  $\Pi$  is finally obtained as

$$\Pi = \frac{1}{2} \frac{E A}{2} \int (u + \frac{\partial v}{\partial \theta})^2 d\theta + \frac{1}{2} (\frac{2 E b h^3}{3 R^3}) \int (u + \frac{\partial^2 u}{\partial \theta^2})^2 d\theta \quad (A.6)$$

where  $A$  is the cross sectional area of the layer.

Equation (A.6) is identical with the one used by Ditaranto [18].

## APPENDIX B

### RECEP TANCE METHOD FOR A TWO LAYERED RING

#### B.1 MONO-COUPLED SYSTEM

For a mono-coupled system, the coupling co-ordinate,  $q_1$  and the coupling force,  $Q_1$ , at the ends  $\theta = 0$  and  $\theta = \lambda$  can be related in the form

$$\{q\} = [\alpha] \{Q\} \quad (B.1)$$

where  $\{q\} = [q_{10}, q_{1\lambda}]^T$  and  $\{Q\} = [Q_{10}, Q_{1\lambda}]^T$

with  $q_{10} = q_1 \Big|_{\theta=0}$ ,  $q_{1\lambda} = q_1 \Big|_{\theta=\lambda}$ ,  $Q_{10} = Q_1 \Big|_{\theta=0}$ ,  $Q_{1\lambda} = Q_1 \Big|_{\theta=\lambda}$

and  $\alpha$ 's are called the dynamic receptances. The receptance  $\alpha_{mn}$  is the value of the  $m^{th}$  component of vector  $\{q\}$  due to a unit value of the  $n^{th}$  component of the vector  $\{Q\}$ . These can be evaluated by considering the forced harmonic vibration of one periodic element.

According to the theory of wave propagation described in section 2.4.1, the coupling co-ordinates and the coupling forces at  $\theta = 0$  (with their directions shown in Fig. 2.2b) are related to those at  $\theta = \lambda$  as

$$q_{1\lambda} = e^\mu q_{10} \quad \text{and} \quad Q_{1\lambda} = e^\mu Q_{10} \quad (B.2)$$

Using (B.2) in (B.1), the condition for non-trivial solution of  $Q$ 's is obtained as

$$\alpha_{12} e^{2\mu} + (\alpha_{11} - \alpha_{22}) e^\mu - \alpha_{21} = 0 \quad (B.3)$$

Moreover, due to symmetry and reciprocity, the receptance

relations for the periodic element shown in Fig. 2.2a are given by

$$\alpha_{11} = -\alpha_{22} \quad \text{and} \quad \alpha_{12} = -\alpha_{21} \quad (\text{B.4})$$

which simplifies (B.3) to the following form:

$$\alpha_{21} e^{2\mu} + 2 \alpha_{22} e^{\mu} + \alpha_{21} = 0 \quad (\text{B.5})$$

The complex roots ( $\mu$ 's) of (B.5) are readily given by

$$\cosh \mu = - \frac{\alpha_{22}}{\alpha_{21}} \quad (\text{B.6})$$

## B.2 BI-COUPLED SYSTEM

When there are two coupling co-ordinates in the periodic structure, the coupling-co-ordinate ( $q_1$  and  $q_2$ ) and the coupling forces ( $Q_1$  and  $Q_2$ ) relation can be put in the matrix form

$$\{ \underline{q} \} = [\alpha] \{ \underline{Q} \} \quad (\text{B.7})$$

$$\text{where } \{ \underline{q} \} = \begin{bmatrix} q_{10}, q_{1\lambda}, q_{20}, q_{2\lambda} \end{bmatrix}^T \quad \{ \underline{Q} \} = \begin{bmatrix} Q_{10}, Q_{1\lambda}, Q_{20}, Q_{2\lambda} \end{bmatrix}^T$$

and  $\alpha$  is a  $(4 \times 4)$  dynamic receptance matrix.

For the bi-coupled system under consideration the symmetry and the reciprocity relations are given by

$$\begin{aligned} \alpha_{11} &= -\alpha_{22}; & \alpha_{23} &= -\alpha_{32}; & \alpha_{14} &= -\alpha_{23} \\ \alpha_{12} &= -\alpha_{21}; & \alpha_{24} &= \alpha_{42}; & \alpha_{13} &= -\alpha_{24} \\ \alpha_{14} &= -\alpha_{41}; & \alpha_{32} &= -\alpha_{41}; & \alpha_{33} &= -\alpha_{44} \\ \alpha_{13} &= \alpha_{31}; & \alpha_{34} &= -\alpha_{43}; & \alpha_{31} &= -\alpha_{42} \end{aligned} \quad (\text{B.8})$$

and the wave conditions are given by

$$q_{j\lambda} = e^\mu q_{jo} \quad (j = 1, 2) \quad (B.9)$$

and  $Q_{j\lambda} = e^\mu Q_{jo} \quad (j = 1, 2)$

Using (B.8) and (B.9) in (B.7), the condition for the non-trivial solution of  $Q$ 's can be derived as

$$z_1 \cosh^2 \mu + z_2 \cosh \mu + z_3 = 0 \quad (B.10)$$

$$\text{where } z_1 = (\alpha_{12}\alpha_{34} - \alpha_{14}^2),$$

$$z_2 = (\alpha_{11}\alpha_{34} + \alpha_{12}\alpha_{33} - 2\alpha_{13}\alpha_{14}) \text{ and}$$

$$z_3 = (\alpha_{11}\alpha_{33} - \alpha_{13}^2).$$

Solution of (B.10) yields

$$\cosh \mu = - \frac{z_2}{2z_1} \pm \sqrt{\frac{z_2^2 - 4z_1z_3}{2z_1}} \quad (B.11)$$

### B.3 TRI-COUPLED SYSTEM

For tri-coupled system, the coupling co-ordinates are  $q_1$ ,  $q_2$  and  $q_3$ . Proceeding on the similar lines as for the bi-coupled system, a cubic equation in  $\cosh \mu$  is obtained as

$$z_1 \cosh^3 \mu + z_2 \cosh^2 \mu + z_3 \cosh \mu + z_4 = 0 \quad (B.12)$$

where

$$z_1 = (\alpha_{14}^2\alpha_{56} - \alpha_{12}\alpha_{34}\alpha_{56} + 2\alpha_{14}\alpha_{16}\alpha_{36} - \alpha_{12}\alpha_{36}^2 - \alpha_{16}\alpha_{34}^2)$$

$$z_2 = (2\alpha_{13}\alpha_{16}\alpha_{36} - \alpha_{11}\alpha_{36}^2 - \alpha_{33}\alpha_{16}^2 + 2\alpha_{13}\alpha_{14}\alpha_{56} + \alpha_{14}\alpha_{55}^2 - \alpha_{12}\alpha_{34}\alpha_{55}^2 - \alpha_{12}\alpha_{33}\alpha_{56}^2 - \alpha_{11}\alpha_{34}\alpha_{56})$$

$$\begin{aligned} z_3 &= (2\alpha_{13}\alpha_{14}\alpha_{55} + \alpha_{13}^2\alpha_{56} - \alpha_{11}\alpha_{33}\alpha_{56} \\ &\quad - \alpha_{12}\alpha_{33}\alpha_{55} - \alpha_{11}\alpha_{34}\alpha_{55} - 2\alpha_{14}\alpha_{16}\alpha_{36} \\ &\quad + \alpha_{12}\alpha_{36}^2 + \alpha_{16}^2\alpha_{34}) \end{aligned}$$

$$\begin{aligned} z_4 &= (\alpha_{13}^2\alpha_{55} - \alpha_{11}\alpha_{33}\alpha_{55} - 2\alpha_{13}\alpha_{16}\alpha_{36} \\ &\quad + \alpha_{11}\alpha_{36}^2 + \alpha_{16}^2\alpha_{33}) \end{aligned}$$

While deriving (B.12), the following receptance relations of the two layered ring are used.

$$\begin{aligned} \alpha_{11} &= -\alpha_{22}; \quad \alpha_{31} = -\alpha_{42}; \quad \alpha_{51} = \alpha_{62}; \quad \alpha_{13} = \alpha_{31}; \\ \alpha_{12} &= -\alpha_{21}; \quad \alpha_{32} = -\alpha_{41}; \quad \alpha_{52} = \alpha_{61}; \quad \alpha_{14} = \alpha_{32}; \\ \alpha_{13} &= -\alpha_{24}; \quad \alpha_{33} = -\alpha_{44}; \quad \alpha_{53} = \alpha_{64}; \quad \alpha_{23} = \alpha_{41}; \\ \alpha_{14} &= -\alpha_{23}; \quad \alpha_{34} = -\alpha_{43}; \quad \alpha_{54} = \alpha_{63}; \quad \alpha_{24} = \alpha_{42}; \\ \alpha_{15} &= \alpha_{26}; \quad \alpha_{35} = \alpha_{46}; \quad \alpha_{55} = -\alpha_{66}; \quad \alpha_{15} = \alpha_{51} \\ \alpha_{16} &= \alpha_{25}; \quad \alpha_{36} = \alpha_{45}; \quad \alpha_{56} = -\alpha_{65}; \quad \alpha_{16} = -\alpha_{52} \end{aligned}$$

$$\begin{aligned} \alpha_{25} &= -\alpha_{61}; \\ \alpha_{26} &= \alpha_{62}; \\ \alpha_{35} &= \alpha_{53} \\ \alpha_{36} &= -\alpha_{54} \\ \alpha_{45} &= -\alpha_{63} \\ \alpha_{46} &= \alpha_{64} \end{aligned}$$

## APPENDIX C

COEFFICIENTS OF THE AUXILIARY EQUATION (2.10) AND  
THE EXPRESSION FOR  $T_j$

$$\begin{aligned}
 a_1 &= 2 + \Omega^{*2} \left\{ \frac{D^*}{K_2} \left( 1 + \frac{m_1}{m_2} \frac{d_3^2}{d_1^2} \right) + \frac{d_2^2}{d_1^2} \left( \frac{K_1^*}{K_2} + \frac{m_1}{m_2} \right) \right\} / a \\
 a_2 &= 1 + [\Omega^{*2} \left\{ 2 \frac{D^*}{K_2} \left( 1 + \frac{m_1}{m_2} \frac{d_3^2}{d_1^2} \right) - 2 \frac{d_2}{d_1} \left( \frac{K_1^*}{K_2} - \frac{m_1}{m_2} \frac{d_3}{d_1} \right) \right. \\
 &\quad \left. - \frac{m_1}{m_2} \left( 1 + \frac{K_1^*}{K_2} \frac{d_3^2}{d_1^2} \right) \right\} + \Omega^{*2} \frac{m_1}{m_2} \frac{D_2}{K_2} \frac{d_2^2}{d_1^2}] / a \\
 a_3 &= \Omega^{*2} \left( 1 + \frac{m_1}{m_2} \frac{d_3^2}{d_1^2} \right) \left( 1 + \frac{D^*}{K_2} + \frac{K_1^*}{K_2} - \Omega^{*2} \frac{D_2}{K_2} \frac{m_1}{m_2} \right) / a
 \end{aligned} \tag{C.1}$$

where  $a = \frac{D^*}{D_2} \left( 1 + \frac{K_1^*}{K_2} \frac{d_3^2}{d_1^2} \right) + \frac{K_1^*}{D_2} \frac{d_2^2}{d_1^2}$

and  $\Omega^* = \Omega (1 + i\eta)^{\frac{1}{2}}$ . All other symbols are defined in section 2.1.

The expression for  $T_j$  is

$$\begin{aligned}
 T_j &= \{ s_j \left( \frac{K_1^*}{D_2} \frac{d_2 d_3}{d_1^2} s_j^2 - \frac{K_1^*}{D_2} \frac{d_3}{d_1} - \frac{K_2}{D_2} + \Omega^{*2} \frac{m_1}{m_2} \frac{d_2 d_3}{d_1^2} \right) \} / \\
 &\quad \{ \left( \frac{K_1^*}{D_2} \frac{d_3^2}{d_1^2} + \frac{K_2}{D_2} \right) s_j^2 + \Omega^{*2} \left( 1 + \frac{m_1}{m_2} \frac{d_3^2}{d_1^2} \right) \}
 \end{aligned}$$

## APPENDIX D

### RECEP TANCE METHOD FOR A THREE LAYERED RING (TRI - COUPLED SYSTEM)

For tri-coupled system, the receptances are defined by

$$\{ \underline{q} \} = [\alpha] \{ \underline{Q} \} \quad (D.1)$$

where  $\{ q \} = [q_{10}, q_{1\lambda}, q_{20}, q_{2\lambda}, q_{30}, q_{3\lambda}]^T$ ,

$$\{ Q \} = [Q_{10}, Q_{1\lambda}, Q_{20}, Q_{2\lambda}, Q_{30}, Q_{3\lambda}]^T$$

and  $[\alpha]$  is a  $(6 \times 6)$  receptance matrix.

For the co-ordinate system shown in Fig. 2.2b, the wave conditions on  $q_j$ 's and  $Q_j$ 's can be written as

$$q_{j\lambda} = e^\mu q_{j0} \quad (j = 1, 2, 3) \text{ and}$$

$$Q_{j\lambda} = e^\mu Q_{j0} \quad (j = 1, 2, 3) \quad (D.2)$$

the receptance relations of the periodic element of the three layered ring can be written as

$$\alpha_{11} = -\alpha_{22}; \quad \alpha_{31} = -\alpha_{42}; \quad \alpha_{51} = -\alpha_{62}; \quad \alpha_{13} = \alpha_{31}; \quad \alpha_{25} = \alpha_{61}$$

$$\alpha_{12} = -\alpha_{21}; \quad \alpha_{32} = -\alpha_{41}; \quad \alpha_{52} = -\alpha_{61}; \quad \alpha_{14} = \alpha_{32}; \quad \alpha_{25} = \alpha_{62}$$

$$\alpha_{13} = -\alpha_{24}; \quad \alpha_{33} = -\alpha_{44}; \quad \alpha_{53} = -\alpha_{64}; \quad \alpha_{23} = \alpha_{41}; \quad \alpha_{35} = \alpha_{53}$$

$$\alpha_{14} = -\alpha_{23}; \quad \alpha_{34} = -\alpha_{43}; \quad \alpha_{54} = -\alpha_{63}; \quad \alpha_{24} = \alpha_{42}; \quad \alpha_{36} = \alpha_{54}$$

$$\alpha_{15} = -\alpha_{26}; \quad \alpha_{35} = -\alpha_{46}; \quad \alpha_{55} = -\alpha_{66}; \quad \alpha_{15} = \alpha_{51}; \quad \alpha_{45} = \alpha_{63}$$

$$\alpha_{16} = -\alpha_{25}; \quad \alpha_{36} = -\alpha_{45}; \quad \alpha_{56} = -\alpha_{65}; \quad \alpha_{16} = \alpha_{52}; \quad \alpha_{46} = \alpha_{64}$$

(D.3)

Using (D.2) and (D.3) in (D.1) and applying the condition that non-trivial solution of Q's should exist, equation for the propagation constant is obtained as

$$z_1 \cosh^3 \mu + z_2 \cosh^2 \mu + z_3 \cosh \mu + z_4 = 0 \quad (\text{D.4})$$

where

$$z_1 = (\alpha_{12} \alpha_{34} \alpha_{56} + 2\alpha_{14} \alpha_{16} \alpha_{36} - \alpha_{12} \alpha_{36}^2 - \alpha_{56}^2 \alpha_{14}^2 - \alpha_{34}^2 \alpha_{16}^2)$$

$$\begin{aligned} z_2 = & \alpha_{11} \alpha_{34} \alpha_{56} + \alpha_{12} (\alpha_{33} \alpha_{56} + \alpha_{34} \alpha_{55}) 2\alpha_{13} \alpha_{16} \alpha_{36} \\ & + 2\alpha_{14} (\alpha_{15} \alpha_{36} + \alpha_{16} \alpha_{35}) - \alpha_{11} \alpha_{36}^2 - 2\alpha_{12} \alpha_{35} \alpha_{36} \\ & - \alpha_{55} \alpha_{14}^2 - 2\alpha_{13} \alpha_{14} \alpha_{56} - \alpha_{33} \alpha_{16}^2 - 2\alpha_{15} \alpha_{16} \alpha_{34} \end{aligned}$$

$$\begin{aligned} z_3 = & \alpha_{12} \alpha_{33} \alpha_{55} + \alpha_{11} (\alpha_{33} \alpha_{56} + \alpha_{34} \alpha_{55}) + 2\alpha_{14} \alpha_{15} \alpha_{35} \\ & + 2\alpha_{13} (\alpha_{15} \alpha_{36} + \alpha_{16} \alpha_{35}) - \alpha_{12} \alpha_{35}^2 - 2\alpha_{11} \alpha_{35} \alpha_{36} \\ & - \alpha_{56} \alpha_{13}^2 - 2\alpha_{13} \alpha_{14} \alpha_{55} - \alpha_{34} \alpha_{15}^2 - 2\alpha_{15} \alpha_{16} \alpha_{33} \end{aligned}$$

$$z_4 = \alpha_{11} \alpha_{33} \alpha_{55} + 2\alpha_{13} \alpha_{15} \alpha_{35} - \alpha_{11} \alpha_{35}^2 - \alpha_{55} \alpha_{13}^2 - \alpha_{33} \alpha_{15}^2$$

## APPENDIX E

### CONSTANTS AND COEFFICIENTS USED IN CHAPTER 3

$$\begin{aligned}
 I_1 &= \frac{D}{D_3} ; \quad I_2 = \frac{2D}{D_3} - \frac{g^* d_2^2}{D_3} + \frac{\Omega^{*2}}{2} \frac{m_2}{m_3} d_4^2 ; \\
 I_3 &= \frac{D}{D_3} + \frac{K_1}{D_3} + \frac{K_3}{D_3} - \Omega^{*2} \frac{m_2}{m_3} ; \quad I_4 = \frac{K_1}{D_3} - \frac{g^* d_1 d_2}{D_3} + \frac{\Omega^{*2}}{2} \frac{m_2}{m_3} d_1 d_4 \\
 I_5 &= \frac{K_3}{D_3} + \frac{g^*}{D_3} d_2 d_3 + \frac{\Omega^{*2}}{2} \frac{m_2}{m_3} d_3 d_4 ; \quad I_6 = \frac{K_1}{D_3} ; \\
 I_7 &= \Omega^{*2} \left( \frac{m_1}{m_3} + \frac{1}{2} \frac{m_2}{m_3} d_1^2 \right) - \frac{g^*}{D_3} d_1^2 ; \quad I_8 = \left( \frac{g^*}{D_3} + \frac{\Omega^{*2}}{2} \frac{m_2}{m_3} \right) d_1 d_3 \\
 I_9 &= \frac{K_3}{D_3} ; \quad I_{10} = \Omega^{*2} \left( 1 + \frac{1}{2} \frac{m_2}{m_3} d_3^2 \right) - \frac{g^*}{D_3} d_3^2
 \end{aligned} \tag{E.1}$$

where  $g^* = g (1 + i\beta)$  and other symbols are defined in Chapter 3.

The coefficients of the auxiliary equation (3.10) are given by

$$\begin{aligned}
 a_1 &= (I_1 I_6 I_{10} + I_1 I_7 I_9 + I_2 I_6 I_9) / I_1 I_6 I_9 \\
 a_2 &= (I_1 I_7 I_{10} + I_3 I_6 I_9 + I_2 I_6 I_{10} + I_2 I_7 I_9 \\
 &\quad - I_1 I_8^2 - I_4^2 I_9 - I_5^2 I_6) / I_1 I_6 I_9 \\
 a_3 &= (I_2 I_7 I_{10} + I_3 I_6 I_{10} + I_3 I_7 I_9 - I_2 I_8^2 \\
 &\quad - I_4^2 I_{10} - I_5^2 I_7 + 2 I_4 I_5 I_8) / I_1 I_6 I_9 \\
 a_4 &= (I_3 I_7 I_{10} - I_3 I_8^2) / I_1 I_6 I_9
 \end{aligned} \tag{E.2}$$

where I's are given by (E.1).

The expressions for  $\bar{T}_j$  and  $T_j$  can be written as

$$\bar{T}_j = \{-I_5 I_6 s_j^3 + (I_4 I_8 - I_5 I_7) s_j\} / a \quad (\text{E.3})$$

$$\text{and } T_j = \{-I_4 I_9 s_j^3 + (I_5 I_8 - I_4 I_{10}) s_j\} / a \quad (\text{E.4})$$

$$\text{where } a = I_6 I_9 s_j^4 + (I_6 I_{10} + I_7 I_9) s_j^2 + (I_7 I_{10} - I_8^2),$$

I's are again given by (E.1) and other symbols are defined in Chapter 3.